(2)

Quantum 1/f Noise in Solid-State Devices in Particular $Hg_{1-x}Cd_xTe$ n^+-p Diodes

Final Report

A. D. van Rheenen

P. H. Handel

August, 1991

U.S. ARMY RESEARCH OFFICE

DAALO3-89-K-0009

Department of Electrical Engineering
University of Minnesota

Quantum 1/f Noise in Solid-State Devices in Particular $Hg_{1-x}Cd_xTe$ n^+-p Diodes

Final Report

A. D. van Rheenen

P. H. Handel

August, 1991

U.S. ARMY RESEARCH OFFICE

DAALO3-89-K-0009

Department of Electrical Engineering
University of Minnesota

MASTER COPY KEEP THIS COPY FOR REPRODUCTION PURPOSES

REPORT DOCUMENTATION PAGE

Form Approved
OMB No. 0704-0188

1. AGENCY USE ONLY (Leave blank)	2. REPORT DATE	3. REPORT TYPE AND DATES COVERED
	August 1991	

4. TITLE AND SUBTITLE
Quantum 1/f Noise in Solid-State Devices, in Particular $Hg_{1-x}Cd_xTe$ n^+-p Diodes

5. FUNDING NUMBERS
DAAL03-89-K-0009

6. AUTHOR(S)
A. D. van Rheenen
P. H. Handel

7. PERFORMING ORGANIZATION NAME(S) AND ADDRESS(ES)
ORTTA
University of Minnesota
1200 Washington Ave. So.
Minneapolis, MN 55455

8. PERFORMING ORGANIZATION REPORT NUMBER

9. SPONSORING / MONITORING AGENCY NAME(S) AND ADDRESS(ES)
U. S. Army Research Office
P. O. Box 12211
Research Triangle Park, NC 27709-2211

10. SPONSORING / MONITORING AGENCY REPORT NUMBER
ARO 26417.13-EL

11. SUPPLEMENTARY NOTES
The view, opinions and/or findings contained in this report are those of the author(s) and should not be construed as an official Department of the Army position, policy, or decision, unless so designated by other documentation.

12a. DISTRIBUTION / AVAILABILITY STATEMENT
Approved for public release; distribution unlimited.

12b. DISTRIBUTION CODE

13. ABSTRACT *(Maximum 200 words)*

Under the grant measurements of the spectral intensity of the current fluctuations produce by n^+-p HgCdTe diodes, p-i-n HgCdTe diodes, AlGaAs/GaAs laser diodes, InGaAs/InP p-i-n diodes, silicon bipolar transistors, AlGaAs/GaAs heterojunction bipolar transistors, silicon junction field effect transistors, and AlGaAs/GaAs resonant tunneling diodes were taken in the frequency range from 1 Hz to 100 kHz under different bias conditions and in the temperature range from 78-400 k. In addition, progress was made on the theoretical aspects of quantum 1/f noise.

14. SUBJECT TERMS
LOW-FREQUENCY NOISE, SEMICONDUCTORS QUANTUM 1/f NOISE

15. NUMBER OF PAGES
88

16. PRICE CODE

17. SECURITY CLASSIFICATION OF REPORT	18. SECURITY CLASSIFICATION OF THIS PAGE	19. SECURITY CLASSIFICATION OF ABSTRACT	20. LIMITATION OF ABSTRACT
UNCLASSIFIED	UNCLASSIFIED	UNCLASSIFIED	UL

FOREWORD

In this report we will discuss the progress that has been made in the area of understanding and quantifying noise spectra that have a component with a characteristic frequency dependence proportional to 1/f. Fluctuations in the time domain of the voltage across a semiconductor device, or of the current through it, are ever present. With the down scaling of the size of electronic devices the signals are becoming smaller as well. Hence, one of the limiting factors determining the device performance, the noise the device itself produces, becomes important. This becomes apparent first when we consider detectors which we use to distinguish useful signals from "background" signals.

Understanding the noise produced by a device is to be understood as (i) being able to identify the physical mechanism that gives rise to the fluctuations and (ii) to know how a locally generated fluctuation, in let us say the current, will contribute to the noise as it is measured at the terminals of the device. Whereas the first has to do with the basic physical forces that work on a carrier as it traverses a device the second has to do with the operating principles of the device which describe the behavior of average quantities such as constant current, etc. Another way of putting it is considering the basic carrier interactions on a microscopic level and evaluate how these processes contribute to the observations on macroscopic level.

Ideally one would like to have a description of the noise produced by the device as a function of the operating conditions. This would allow one to predict the noisiness of, for instance, a transistor in a particular circuit application. One idea in this direction was formulated first in 1975 by P. H. Handel. Since 1984 A. van der Ziel has been taking noise measurements on devices to either support or refute this theory. Some of the experimental evidence seems to support the theory. In the last two years, 1989 and 1990, more experimental data was gathered and some of the aspects of the theory have been considered. The outcome of these investigations is collected and presented in this report.

Under the grant the principal investigators were A. van der Ziel (deceased, January 1991) and A. D. van Rheenen, both at the University of Minnesota. The theory part was subcontracted with P. H. Handel, University of Missouri-St.Louis.

Table of Contents

I. Experimental Results

1. Introduction 2
2. Results of Research as Published. 4
3. Results not yet published 10
4. References 13
5. Scientific personnel 14
6. Degrees granted 14
Appendix A, List of publications under grant A1
Appendix B, Full text of individual journal publications. . B1
Appendix C, Abstracts of theses C1

II. Theoretical Results

1. Introduction 15
2. Collector quantum 1/f noise in BJTs 16
3. A sufficient criterion for 1/f noise in chaotic non-linear systems 17
4. Application of the sufficient criterion to a chain of atoms with anharmonic coupling 20
5. Quantum 1/f effect in quartz resonators 23
6. Quantum 1/f mobility fluctuations in semiconductors 24
7. References 29
Appendix D, Examples D1
Appendix E, List of publications under grant E1

I. EXPERIMENTAL RESULTS

1. Introduction

In the early history of the study of noise in electronic devices investigators were particularly intrigued by the $1/f$ spectrum and several theories were developed to explain the unique spectral shape. Some of the more obvious difficulties with a pure $1/f$-shaped power spectral density is that integration of the spectrum over all frequencies yields infinities at both integration limits. A realistic physical system is of course properly behaved, with none of these infinities. In practice the noise measurements are band limited: on the high-frequency side of the spectrum by the frequency response of the measuring system and on the low-frequency side by the time the equipment is on.

One attempt to describe the $1/f$ noise was to assume that a number of traps with a distribution of trapping time constants is responsible for the $1/f$ shape. A trapping center that captures and releases again a charge carrier gives rise to a Lorentzian shaped $(1/[1 + \omega^2\tau^2])$ contribution to the noise spectrum. It is possible to simulate $1/f$ behavior of the spectrum over decades of frequency by adding Lorentzians with proper time constants τ. Since the theory for generation-recombination (g-r) noise (the noise related to trapping and de-trapping of carriers) is well known this approach would give a physical interpretation. It also eliminates the mathematical problems mentioned earlier. A sum of Lorentzians will result in a frequency independent part at low frequencies and a part that rolls off as $1/f^2$ at high frequencies. The intermediate region exhibits the $1/f$ spectrum. Integration of this spectrum over the frequency gives a finite result. These attributes give this theory its appeal. The only issue would be to identify traps with exactly the right distribution of time constants, which by the way can be related to a distribution of activation energy levels. The first person to propose such a model was McWorther [1].

In 1969 it was observed by Hooge [2] that the essence of $1/f$ noise in a wide variety of devices could be captured by a single equation relating the power spectral density (S_I) as a function of frequency (f) to the DC operating current (I) and the number of free carriers (N) in the device. It was found that the proportionality constant (now named after Hooge) α_H had a constant value of 2×10^{-3}, independent of the material or size of the device. This relation is expressed as follows:

$$S_I(f) = \frac{\alpha_H I^2}{fN}. \qquad (1)$$

The advantage of the formulation of Eq. 1 is that by assuming that the Hooge parameter is a constant one can predict the noise the

device will produce under certain operating conditions.

With the advances made in the technology, smaller and smaller devices were fabricated and from noise measurements smaller and smaller values for the Hooge parameter were deduced. Possibly the improved processing techniques resulted in cleaner samples resulting in less noisy devices. With the observation that the Hooge parameter was no longer a constant the interpretation of Eq. 1 and of the Hooge parameter changed. Now Eq. 1 would be used to normalize the measured current noise spectrum to find the parameter α_H. This then allows one to compare the noise behavior of different devices with different carrier numbers under different operating conditions. The Hooge parameter would simply be a measure of the noisiness of the device: a small parameter value would indicate a quiet device and a large value would show that the device produces a lot of noise.

It was also observed that the value of α_H depended on the electric field, see Bosman et. al. [3]. This made the case stronger to let the Hooge parameter be an adjustable parameter in stead of a constant. Continuing this line of thought it became apparent that there was a need for a theory describing how the noisiness parameter depends on external parameters such as the temperature, the electric field, etc. An attempt to describe the noisiness from first principles was made by Handel in 1975 [4]. The physical mechanism invoked is the emission of Bremsstrahlung when electrons are accelerated and it was shown that this would result in a $1/f^{1-\varepsilon}$ shaped spectrum with ε a positive number, small compared to 1. This formulation does remove the infinity at $f = 0$ when integrating the spectrum. The magnitude of the noise is expressed in terms of the velocity changes the electron undergoes when it interacts with phonons, impurities, other electrons, etc. This formulation then would enable one to predict the noisiness of the device from knowledge of the dominant scattering mechanism under certain device operating conditions. In principle the theory would be a powerful tool to study and predict the magnitude of the $1/f$ noise. However, this theory has been severely criticized, both on the grounds of the mathematical detail and the underlying physical assumptions.

In order to shed some light on the controversy the Noise group at the University of Minnesota under the guidance of the late Dr. A. van der Ziel set out to measure noise in a variety of devices and compare the resulting values of the noisiness (still called Hooge) parameter with predictions made by Handel's theory. The idea was to either confirm or refute the theory based on these measurements. The body of this report is concerned with the results that were obtained over the period of the grant from January 1, 1989 through March 31, 1991. A large number of different devices were studied: n^+-p and n-i-p $Hg_{1-x}Cd_xTe$ infrared detector diodes, AlGaAs/GaAs laser diodes, InGaAs/InP p-i-n photodiodes, silicon bipolar transistors, AlGaAs/GaAs heterojunction bipolar transistors, silicon Junction Field Effect Transistors, and AlGaAs/GaAs Double Barrier Resonant Tunneling Diodes. Most of the results and interpretation of the data has been published in the open literature. What follows is a recapture of these results in

the form of a section on each subject. At the end the accomplishments on the theory part of the project will be high lighted.

2. Results of research as published.

2.1 Extensions of Handel's 1/*f* noise equations and their semiclassical theory (see p. B2 for full paper)

Handel's expression for the Hooge parameter (α_H) which quantifies the 1/*f* noise can be modified, allowing for bunches of charge qe, to the following expression:

$$\alpha_H = \frac{4\alpha_o}{3\pi} \left(\frac{q}{e}\right)^2 \left(\frac{F_a(0)}{c}\right)^2. \qquad (2)$$

In this expression α_o is the fine-structure constant (1/137), c the speed of light and $F_a(0)$ the low-frequency Fourier transform of the acceleration, a(t), of the carrier. The differences with Handel's original expressions are that now bunches of charge, as they appear in vacuum devices, can be accounted for and second, that the vectorial velocity change that appears in Handel's equation can be derived from semi-classical (no quantum mechanics) arguments as the Fourier transform of the acceleration.

2.2 1/*f* noise characterization of n^+-p and n-i-p $Hg_{1-x}Cd_xTe$ detectors (see p. B6 for full paper)

In this experimental study the noise behavior of $Hg_{0.7}Cd_{0.3}Te$ n^+-p diodes supplied by Rockwell International was investigated in the temperature range from 80-300 K under small reverse bias conditions. The theoretical values for α_H were estimated as follows:
(i) Coherent state 1/f noise $\alpha_H = 4.6\times10^{-3}$,
(ii) Umklapp 1/f noise $\alpha_H = 5\times10^{-5}$ for T = 273 K,
(iii) Normal collision 1/f noise $\alpha_H = 1\times10^{-7}$ for T = 77 K.
In this bias regime the noise spectral density of the current fluctuations is given by:

$$S_I(f) = \alpha_H \frac{eI}{f\tau} F(V). \qquad (3)$$

Here, F(V) is a factor dependent on the bias voltage V that comes about when one integrates the locally generated noise along the device length to find the noise at the terminals. It has been shown earlier that F(V) has the following form for a reverse biased diode:

$$F(V) = \frac{1}{3} - \frac{1}{2a} + \frac{1}{a^2} - \frac{1}{a^3} \ln(1+a) \qquad (4)$$

where $a = \exp(qV/kT) - 1$.
The time constant τ was extracted from measurements of the complex admittance of the diode and fitted to:

$$y(\omega) = g_o(1+j\omega\tau)^{\frac{1}{2}}. \qquad (5)$$

This yielded values for the lifetime that were commensurate with the values of the Honeywell lifetime tables.

The experiments resulted in the following observations:
(i) in the temperature range from 113 - 193 K the values for the Hooge parameter (α_H) were $(3-5)\times10^{-3}$ indicating the presence of the coherent state noise.
(ii) around T = 273 K one device exhibited a value of 5×10^{-5} as one would expect for the Umklapp noise.
(iii) normal collision $1/f$ noise has not been observed. This noise contribution is probably masked by the other two sources.

The second part of this study concerned the noise performance of $Hg_{0.78}Cd_{0.22}Te$ p-i-n diodes supplied by Santa Barbara Research Center. These diodes were tested at 80 K. In an earlier contribution [5] measurements of the admittance of a silicon power diode were used to obtain the lifetime of the carriers. This lifetime is essential when one wants to determine the Hooge parameter from Eq. 3. This expression follows from substituting qN/τ for one of the factors I, into Eq. 1. This analysis resulted in lifetimes of the order of 10^{-7} s, comparable to the Honeywell lifetime tables. The value of α_H was found to be 4×10^{-3}, and this value agrees with the predictions made according to the coherent state $1/f$ noise, $2\alpha/\pi$, which is equal to 4.6×10^{-3}.

2.3 Secondary emission $1/f$ noise revisited (see p. B11 for full paper)

A case is made here that noise measurements, taken in 1960, of the $1/f$ noise in secondary emission pentodes conform to predictions made by Handel's $1/f$ noise theory. The analysis is carried out with one adjustable parameter, the distance between the dynode and the anode, and assuming Handel's predictions are correct. Two sets of measurements taken on each of two devices: one set involved a constant anode current and varying anode-to-dynode voltage, and the other set involved a constant anode-to-dynode voltage and varying anode current. From a fit of the $1/f$ noise measurements the dynode-to-anode distance was found to be 4.8 ± 0.3 mm for one device and 7.0 ± 0.6 mm for the other. The physical distance is estimated at 6 mm. In light of the fact that the dynode and anode are not parallel plates but curved surfaces one can argue that the electron beam might traverse a path length that differs slightly from the

estimated physical distance between the electrodes. It seems reasonable to assume that the values deduced from the noise measurements agree with the physical dimension. This then supports Handel's prediction for the magnitude of the $1/f$ noise in a vacuum device where electrons do not suffer collisions while in transit.

2.4 Generation-recombination-type $1/f$ noise in n-i-p diodes (see p. B14 for full paper)

For devices, such as resistors, that have homogeneous carrier numbers (N) and current densities (I) it is postulated that $1/f$ contribution to the spectral intensity of the current fluctuations (Si) can be described by:

$$S_i = \frac{\alpha_H I^2}{f N}. \qquad (6)$$

In the case that the device is not homogeneous a different approach must be used. The procedure is as follows: the device is divided in slices of thickness Δx and the contribution (ΔS_i) of that slice to the total noise is calculated. In particular, it is assumed here that the noise is associated with the generation- and/or recombination (g-r) processes of carriers interacting with traps. The development of the model then proceeds by replacing I with $(dI/dx)\Delta x$, N with $(dN_T/dx)\Delta x$, and realizing that $dI = q\, dN/\tau$, so that we find:

$$\Delta S_i = \frac{q\, \alpha_H}{f\, \tau} \frac{dI}{dx} \Delta x. \qquad (7)$$

Upon integration of Eq. 7 we find:

$$\Delta S_i = \frac{q\, \alpha_H\, I}{f\, \tau}. \qquad (8)$$

This expression was used to calculate the Hooge parameter from noise measurements taken on $Hg_{0.8}Cd_{0.2}Te$ p-i-n diodes at liquid nitrogen temperatures. This analysis resulted in values varying from 2×10^{-6} to 2×10^{-5}.

The reason this noise was interpreted as g-r-type $1/f$ noise follows from the observation that the frequency dependence of the best fit to the measured spectra behaves as $1/f^{\gamma}$, with γ larger than 1. Therefore the values we give for the Hooge parameter need to be viewed as upper limits; the $1/f$ noise is certainly not larger than the values given. As we reported earlier (Sect. 2.2) it is expected that Umklapp noise gives rise to a value of 10^{-5} for the Hooge parameter. We find smaller values here. Collision $1/f$ noise would result in values of 10^{-8}, two orders of magnitude smaller than the upper limits we found. Possibly, this collision $1/f$ noise

contribution is masked by the g-r noise.

2.5 Burst-type noise mechanisms in bipolar transistors (see p. B17 for full paper)

When one observes the noise signal in the time domain, let us say by using an oscilloscope, it shows an average level on which both upward and downward spikes are superimposed. The occurrence of the spikes as well as their amplitude are "random". In some devices deviations from this time domain signal have been observed. Pulses of varying duration seem to be superimposed on the ordinary noise signal, raising the average locally, and then dropping to the "normal" average. The occurrence of the pulses is "random" in time but their amplitude is fixed. This type of noise is called burst noise. One can hear a distinct popping sound when one feeds this amplified signal to a loud speaker. This explains why this kind of noise is sometimes referred to as popcorn noise.

The occurrence of the pulse in the time domain translates to a Lorentzian, $1/(1+\omega^2\tau^2)$, shaped contribution to the noise spectrum, in addition to the usual $1/f$ noise. Here, measurements of the collector current noise are taken on two different kinds of devices, a discrete bipolar junction transistor (BJT) and a BJT on a chip. Two distinct noise spectra were observed, best described by the theoretical fits to the spectra:

$$\text{discrete BJT} \qquad S_I = \frac{A\tau^2 + B/f}{1 + \omega^2\tau^2}, \tag{9}$$

$$\text{chip BJT} \qquad S_I = \frac{A\tau^2}{1 + \omega^2\tau^2} + B/f. \tag{10}$$

By inspecting Eq. 9 we see that for large frequencies $S_I \propto 1/f^2$ for the discrete device whereas Eq. 10 indicates $S_I \propto 1/f$ at large frequencies for the chip BJT. At the low-frequency side of the spectra both equations predict identical behavior.

The observation of two distinctly different burst noise spectra, mixed with $1/f$ noise, as measured in two different devices is explained by assuming either a modulation of the $1/f$ noise by the burst noise (Eq. 9) indicating a common source for the fluctuations or a superposition of the two noise sources indicating unrelated origins for the fluctuations.

2.6 $1/f$ noise in double-heterojunction AlGaAs/GaAs laser diodes on GaAs and Si substrates (see p. B21 for full paper)

In this study a comparison is made between the noise in the electrical drive current of double-heterojunction AlGaAs/GaAs lasers built on a silicon substrate and ones built on a GaAs

substrate. It might be advantageous, for purposes of easy integration, to fabricate lasers for optical communications on the silicon. Of course the materials issues of growing GaAs on Si need to be addressed, but also the electrical and optical performance of the devices need to be characterized and possibly explained.

Often the laser behavior is modelled in terms of rate equations describing the evolution in time of the number of carriers and the number of photons. These rate equations are coupled and it is expected that fluctuations in the drive current will give rise to fluctuations in the optical output of the laser. Yamamoto [6] speculated that the spectrum of the frequency deviations (phase noise) of the laser output is limited at small frequencies by the fluctuations in the electrical current.

Measurements of the low-frequency noise in the drive current of the laser diodes as a function of the drive are the result of this investigation. Both types of devices showed the magnitude of the noise divided by the current to be independent of the current for currents smaller than 0.1 mA and to decrease for larger currents. The quantity $S_I f/I$ is proportional to α_H/τ, see Eq. 8. If anything, one would expect the lifetime of the carriers to be reduced when more carriers are injected as the current increases, due to an increased recombination. This would increase the ratio α_H/τ. Therefore we must conclude that α_H decreases as the current increases. A similar effect was observed in Si n^+-ν-n^+ and p^+-π-p^+ structures [7].

The two curves, see figure 4 on p. B23, of $S_I f/I$ versus the current for the two types of devices run parallel, with the noise of the devices fabricated on the Si substrate about 50 times as noisy as the ones on the GaAs substrate. Because the current flows through the substrate it is possible that the misfit dislocations due to the lattice mismatch at the Si-GaAs substrate, give rise to excess noise. This would explain the noisier behavior of the lasers on the Si substrate.

2.7 Low-frequency noise in small InGaAs/InP p-i-n diodes under different bias and illumination conditions (see p. B25 for full paper)

With the advances made in the 1.3-1.55 μm wavelength communications it is natural that high-speed photodetectors are considered to allow for high data rates. The InGaAs/InP p-i-n diode is such a fast detector. It is able to detect signals up to a few Gbits/s. It is important to characterize the noise performance of the detectors as signal levels become smaller.

Here the noise is studied in devices that are reverse biased and illuminated and the results are compared with noise data taken on devices that are forward biased and not illuminated. The most remarkable result that the frequency exponent of the spectra of four devices was the same under the two operating conditions we just mentioned, although it differed from device to device. Two devices exhibited a slope of -1 in the noise spectrum whereas the

other two showed a slope of -0.8. The fact that the spectral shape is the same when the devices are forward biased and reverse biased tends to indicate that the mechanisms responsible for the noise are present under both bias conditions. Second, the extrapolated value of $S_I(1\ Hz)/I^2$, averaged over at least five current values, for the devices under reverse bias and illumination was found to be $0.7x10^{-11}$ and $2.6x10^{-11}$ /Hz for two devices (spectral shape $f^{-1.0}$) and about $9.5x10^{-11}$ /Hz for the devices with a spectral shape of $f^{-0.8}$. See table I on p. B26. Although there is some difference between the noise magnitudes of these two sets of devices, they are within one order of magnitude. This again suggests that the same mechanisms govern the noise production. Third, under forward bias, no illumination the value of $S_I(1\ Hz)/I$, again averaged over at least five current values, is virtually the same for all devices: $5x10^{-15}$ A/Hz. This in spite of the differences in the shape of the noise spectra for the different devices. See table II on p. B28.

It is speculated that fluctuations in the quantum efficiency of the detector can result in the I^2 dependence of the noise when the diodes are reverse biased and illuminated. This is the subject of a following paper, Section 2.9.

2.8 Extension of the Hooge equation and the Hooge parameter concept (see p. B30 for full paper)

The Hooge equation should be applied strictly to noise spectra that are proportional to $f^{-1.0}$. However, many spectra exhibit a frequency exponent γ that deviates from -1.0. It is proposed here to modify the Hooge equation to read:

$$S_I(f) = \frac{\alpha_H I^2}{N f^{\gamma}} . \qquad (11)$$

When we allow this α_H is not a dimensionless parameter anymore, but has units $Hz^{\gamma-1}$. This formulation would allow the comparison of the noise parameter of different devices by comparing the value of the spectral intensity at 1 Hz. Since we now allow for the spectral shape to be different that comparison is not easily extended to different frequencies.

2.9 Noise in quantum efficiency of p$^+$-n diodes due to fluctuations in the surface recombination of carriers (see p. B32 for full paper)

In a brief note it is shown that spectral intensity of fluctuations in the quantum efficiency of the p$^+$-n diodes due to fluctuations in the surface recombination of the carriers scales with the quantum efficiency squared. Since the current due to incident light on the detector is proportional to the quantum efficiency the noise in the current will be proportinal to the

current squared.

2.10 Current fluctuations in double-barrier quantum well resonant tunneling diodes (see p. B33 for full paper)

Resonant tunneling diodes are some of the devices with possible operating frequencies close to 1 THz. Applications that make use of these devices are for instance mixers. The noise performance of the diodes in such applications is important because the low-frequency noise will appear as phase noise in the mixed signal. In this study measurements of the noise taken on a device with AlAs barriers are compared with data taken on identical devices that have $Al_{0.3}Ga_{0.7}As$ barriers in stead of the AlAs barriers. The measured spectra are made up of a $1/f$ noise contribution and contributions related to trapping of carriers, g-r noise.

In both devices the magnitude of the $1/f$ noise did not change with temperature in the temperature range from 78-400 K when the diodes were biased close to the peak. Since the tunneling component of the current is independent of the temperature it seems to suggest that the $1/f$ noise is related to the tunneling current. Also, the magnitude of the $1/f$ noise is the same for both types of devices in spite of the different barrier materials. When the diodes are biased at voltages larger than the valley voltage the devices are less noisy at the same operating current.

From the g-r noise measurements the activation energies of the traps were extracted. We observed five traps in the AlAs barrier device and two in the AlGaAs barrier device with activation energies equal to two of the activation energies of the AlAs device. This seems to suggest that increasing the Al mole fraction of the barrier material introduces more traps

3. Results not yet published.

3.1 Noise in BJTs and HBTs (Ph. D. Thesis Alister Young) (for Abstract see p. C2)

It was proposed by van der Ziel that it would be possible to identify the physical location of the sources responsible for the noise in bipolar transistors by measuring the noise in the collector current and the base current when the transistor is biased in the common emitter configuration and when the transistor bias configuration includes a resistor between the emitter and ground. Based on a small signal equivalent circuit model that includes possible independent noise sources the analysis proceeds by fitting the magnitude of the noise sources as well as the base spreading resistance to the four noise measurement data. This procedure, although developed earlier, has never been applied to study the noise behavior of actual devices. In this thesis, the

first experimental test of the procedure is presented. Noise measurements were taken on commercial high-frequency silicon bipolar transistors (Motorola MRF941 and Motorola MRF951) as well as on experimental AlGaAs/GaAs heterojunction bipolar transistors (HBT) fabricated by Rockwell International and by Tektronix.

Silicon Bipolar Transistor (MRF941 and MRF951)

The small signal equivalent circuit model includes three noise sources: (i) a source between base and collector, i_{bc}, due to the generation in the base-collector spce charge region, (ii) a source between the base and the emitter, i_{be}, resulting from recombination in the base, and (iii) a source between the collector and emitter, i_{ce}, associated with the diffusion of carriers from the emitter to the collector. By varying the resistance in the emitter lead we manipulate the relative contributions of these sources to the terminal noise current. The following observations are made:

a. The magnitude of i_{bc} is much smaller than that of i_{be}. This can be expected from improvementsthat have been made in the processing of the materials.

b. The collector current noise is dominated by the contribution of source i_{ce}.

c. Depending on the bias current values between 10 and 100 Ω were found for the base spreading resistance, reasonable for the device structure and doping levels.

d. The values of the Hooge parameter were estimated as follows:

MRF941 base current: 0.1 - 55 μA α_H: 6×10^{-7} - 5×10^{-5}
MRF951 base current: 0.01 - 15 μA α_H: 7×10^{-8} - 1×10^{-4}

MRF941 collector current: 0.1 - 1650 μA α_H: 2×10^{-9} - 2×10^{-3}
MRF951 collector current: 0.1 - 1250 μA α_H: 2×10^{-9} - 2×10^{-4}

In general the value of α_H seems to increase with the current and the MRF951 appears to be quieter than the MRF941. At the moment more careful analysis is under way. We expect to publish the results of this more detailed study shortly.

Heterojunction Bipolar Transistors (AlGaAs/GaAs from Rockwell and Tektronix)

Both types of devices are considered experimantal and no detailed information is available to us concerning the precise device structure. Both are vertical n-p-n transistors and have a cut-off frequency of 200 GHz. The maximum value of h_{FE} is 2.5 for the Rockwell device and 60 for the Tektronix device.

The base current noise spectra as well as the collector current noise spectra show a frequency dependence described by $f^{-\gamma}$, with γ between 0.6 and 1.4. This indicates to us that there is a considerable amount of generation-recombination noise present. It is well known that the exposed base area is likely to have many surface states that can act as trapping centers for the carriers. It is not useful therefore to try to extract values of the Hooge

parameter from these measurements. The magnitude of the base current noise is proportional to the current squared, deviating from a junction noise theory developed by Kleinpenning [8] that did apply to the silicon BJTs. These observations are reminiscent of a surface type 1/f noise [9]. The Rockwell device is noisier than the Tektronix device at the same base current.

The collector current noise spectra show again that the Rockwell device is much noisier, about 100 times, than the Tektronix HBT. Due to the relative small current gain of the HBTs, when compared with the BJT, it is difficult to supply sufficient feedback to reduce the contribution of the noise sources at the input of the transistor. As a result we cannot estimate the magnitude of the source i_{ce}.

The HBTs are inherently noisier than the BJTs we measured on. The $1/f$ noise sources are generally masked by g-r noise processes.

3.2 Noise in JFETs (Master's Thesis Ioannis Stephanakis)

(for Abstact see p. C5)

Measurements of the channel noise in JFETs are analyzed using a model in which the channel is split up in an ohmic part, where the crrier velocity is proportional to the electric field strength, and a saturated part, where the carrier speed is the saturation velocity. In this model the value of α_H is assumed to be constant throughout the channel and the noise measurements are used to extract this parameter. Long-channel JFETs, both p- and n-channel, are studied as well as short n-channel devices.

The 30-μm long n-channel JFETs exhibited values for the Hooge parameter on the order of 10^{-8} for drain currents of about 1 mA. These values are consistent with normal collision noise and Umklapp $1/f$ noise.

The 30-μm long p-channel JFETs showed values of $(5\text{-}10)\times10^{-6}$ for the Hooge parameter for drain currents of 1-2 mA. These values are much larger than expected for incoherent state $1/f$ noise but much smaller than the values expected for coherent state $1/f$ noise. Possibly the extracted values point to an operating regime where a transition is observed from one mechanism to the other.

The 2-μm long n-channel JFETs featured Hooge parameter values in the range from $(3\text{-}11)\times10^{-10}$, about an order of magnitude smaller than the smallest theoretically expected values. During these measurements the devices were operated at large drain currents, 20 mA. There have been other reports in the literature where very small values of the Hooge parameter have been observed.

It is expected that these findings will be published shortly.

4. References

1. A. L. McWorther, 1/f noise and related surface effects in germanium, Lincoln Lab. Rep. **80**, Boston MA, May 1955

2. F. N. Hooge, 1/*f* noise is no surface effect, Phys. Lett. **29A**(3), 139-140 (1969)

3. G. Bosman, R. J. J. Zijlstra, and A. D. van Rheenen, 1/f noise of thermal and hot carriers in silicon, Physica B+C **112**, 188 (1982)

4. P. H. Handel, 1/f Noise - an infrared phenomena, Phys. Rev. Lett. **34**, 1492 (1975)

5. P. Fang, L. He, A. D. van Rheenen, A. van der Ziel, and Q. Peng, Noise and lifetime measurements in Si p^+-i-n power diodes, Solid-State Electron. **32**(5), 345 (1989)

6. Y. Yamamoto, IEEE J. Quantum Electron. **QE-19**, 34 (1983); **QE-19**, 47 (1983)

7. G. Bosman R. J. J. Zijlstra, and A. D. van Rheenen, Physica B+C **112**, 88 (1982)

8. T. G. M. Kleinpenning, 1/*f* noise in p-n diodes, Physica B **98**, 289 (1980)

9. A. van der Ziel, Formulation of surface 1/*f* noise processes in bipolar junction transistors and in p-n diodes in Hooge type form, Solid-State Electron. **32**(1), 91-93 (1989)

5. Scientific Personnel

University of Minnesota

Aldert van der Ziel	Professor Emeritus (deceased)
Arthur D. van Rheenen	Assistant Professor
Ruzong Fang	Research Associate
Lei He	Graduate student
Yayun Lin	Graduate student
Ioannis Stephanakis	Graduate student
Brahim Mezghani	Graduate student
Alister Young	Graduate student

University of Missouri-St. Louis

Peter H. Handel	Professor

6. Degrees granted

Lei He	MSEE
Brahim Mezghani	MSEE (partly supported from other funds)
Ioannis Stephanakis	MSEE
Alister Young	Ph. D.

Degree expected

Lei He	Ph. D.	December 1991
Yayun Lin	MSEE	December 1991

Appendix A

List of papers published during the grant period.

(i) Journals

1. "Extensions of Handel's 1/f noise equations and their semiclassical theory", A. van der Ziel, A. D. van Rheenen, and A. N. Birbas, Phys. Rev. B. **40**(3), pp. 1806-1809, July 15, 1989

2. "1/f noise characterization of n^+-p and n-i-p $Hg_{1-x}Cd_xTe$ detectors", A. van der Ziel, P. Fang, L. He, X. Wu, and A. D. van Rheenen, J. Vac. Sci. Technology **A-7**(2), pp. 550-554, Mar/Apr 1989

3. "Secondary emission 1/f noise revisited", A. van der Ziel, P. Fang, and A. D. van Rheenen, J. Appl. Phys. **66**(6), pp. 2736-2738, 15 September 1989

4. "Generation-recombination-type 1/f noise in n-i-p diodes", A. van der Ziel, L. He, A. D. van Rheenen, and P. Fang, Solid-State Electron. **32**(10), pp. 905-907, 1989

5. "Burst-type noise mechanisms in bipolar transistors" X. L. Wu, A. van der Ziel, A. N. Birbas, and A. D. van Rheenen, Solid-State Electron. **32**(11), pp. 1039-1042, 1989

6. "1/f noise in double-heterojunction AlGaAs/GaAs laser diodes on GaAs and Si substrates", R. Z. Fang, A. D. van Rheenen, A. van der Ziel, A. C. Young, and J. P. van der Ziel, J. Appl. Phys. **68**(8), pp. 4087-4090, 15 October 1990

7. "Low-frequency noise in small InGaAs/InP p-i-n diodes under different bias and illumination conditions" L. He, Y. Lin, A. D. van Rheenen, A. van der Ziel, A. C. Young, and J. P. van der Ziel J. Appl. Phys. **68**(10), pp. 5200-5204, 15 November 1990

8. "Extension of the Hooge equation and the Hooge parameter concept", A. van der Ziel and A. D. van Rheenen, Solid-State Electron. **33**(12), pp. 1647-1648 (1990)

9. "Noise in quantum efficiency of p^+-n diodes due to fluctuations in the surface recombination of carriers", A. van der Ziel, Y. Lin, L. He, and A. D. van Rheenen, Solid-State Electron. **33**(12), p. 1649 (1990)

Accepted for publication.

10. "Current fluctuations in resonant tunneling diodes", Y. Lin, A. D. van Rheenen, and S. Y. Chou, Appl. Phys. Lett. scheduled to appear in the August 26 1991 issue.

(ii) Conference contributions

1. "Experiments on quantum 1/f noise", L. He and A. van der Ziel, IV. Symposium on quantum 1/f noise and other low-frequency fluctuations in electronic devices, Minneapolis, May 10-11 1990.

2. "1/f noise in silicon bipolar junction transistors", A. C. Young and A. van der Ziel, Ibid.

3. "1/f noise in double heterojunction AlGaAs/GaAs laser diodes on GaAs and Si substrates", R. Z. Fang, A. D. van Rheenen, A. van der Ziel, A. C. Young, and J. P. van der Ziel, Ibid.

4. "Low-frequency noise in small InGaAs/InP p-i-n diodes under different bias and illumination conditions", L. He, A. D. van Rheenen, A. van der Ziel, A. C. Young, and J. P. van der Ziel, Ibid.

5. "Report on 1/f noise in p-i-n diodes", Y. Lin, L. He, A. C. Young, F. Feng, A. D. van Rheenen, and A. van der Ziel, Ibid

6. "The present status of the quantum 1/f noise problem", A. van der Ziel, Ibid.

Appendix B

Full text of individual journal publications.

Extensions of Handel's $1/f$-noise equations and their semiclassical theory

A. van der Ziel, A. D. van Rheenen, and A. N. Birbas
Electrical Engineering Department, University of Minnesota, Minneapolis, Minnesota 55455
(Received 16 March 1989)

By replacing the change in velocity Δv by the low-frequency Fourier transform $F_a(0)$ of the electron acceleration $a(t)$, Handel's equations for the Hooge parameter α_H are put in equivalent forms that are not only applicable to collision $1/f$ noise in semiconductors but also to acceleration $1/f$ noise in long semiconductor resistors. To prove these expressions semiclassically, one evaluates first the bremsstrahlung energy dE of a single radiation pulse in a frequency interval df, and then defines $dn = dE/hf$ as the number of photons of a single radiation pulse in a frequency interval df and finally $dr = dn/\tau_a = dE/hf\tau_a$ as the rate of photon emission in a single pulse in a frequency interval df. It is then found that the expression for dr already contains the Hooge parameter α_H. It thus seems that the Hooge parameter depends only on the bremsstrahlung emission process but not on the details of the electron-photon interaction. This may explain why Handel's expressions for α_H so often agree with experiment. One must now bear in mind that the elementary current event is described by a current pulse $i(t)$ of duration τ_a having a Fourier transform $F_i(0)$. If one next defines $S_I''(f) = dr/df$, then the current noise spectrum is obtained by multiplying $S_I''(f)$ first by $2F_i^2(0)$, to obtain the effect of a single elementary event per second, and then multiply by λ, the number of elementary events per second. This leads immediately to the Hooge equation and to the Hooge parameter α_H.

I. INTRODUCTION

According to Handel's quantum $1/f$-noise theory[1,2] the $1/f$ current noise in electronic devices is associated with the low-frequency bremsstrahlung emitted by accelerated or decelerated electrons. This $1/f$ noise is characterized by the Hooge parameter α_H which, in turn, is defined by the Hooge equation[3]

$$S_I(f) = I^2\alpha_H/fN , \tag{1}$$

where $S_I(f)$ is the spectrum, I the current, f the frequency, N the number of carriers in the system, and α_H the Hooge parameter. Handel's quantum $1/f$-noise theory gives expressions for α_H.

van der Ziel *et al.* have experimentally verified Handel's expressions for α_H for a number of cases.[4] To understand what is involved here, we start from Handel's equation for *collision*-free devices (vacuum tubes). In that case,

$$\alpha_H = \frac{4\alpha_0}{3\pi}\frac{\Delta v^2}{c^2} . \tag{2}$$

Here, c is the velocity of light, Δv is the change in velocity along the carrier path, and $\alpha_0 = \frac{1}{137}$ is the fine-structure constant for electrons.[5]

For *collision-dominated devices* involving a *single* collision process, Δv^2 must be replaced by Δv^2, where the averaging is carried out in wave-vector space over all scattering events. For multiple-collision processes the discussion is easily extended.[6] Often alternate equivalent formulations are necessary.

Handel's theory of quantum $1/f$ noise is not generally accepted. However, this should not prevent anybody from experimentally verifying or refuting Eq. (2). Verification means that Eq. (2) has heuristic validity but does not guarantee the validity of its *derivation*.

van der Ziel[7,8] recently gave a semiclassical derivation of Handel's expression for α_H and introduced a new $1/f$-noise source in semiconductors, the so-called *acceleration* $1/f$ noise. This is the semiconductor counterpart of $1/f$ noise in collision-free devices and can easily be incorporated into Handel's schematic.

It is the aim of this note to extend and generalize Handel's equations to new cases and to establish the degree of validity of the various steps in van der Ziel's semiclassical theory.

II. EXTENSION AND GENERALIZATION OF HANDEL'S EXPRESSIONS FOR α_H

We now give various generalized expressions for the Hooge parameters of electron devices. Then we apply Eq. (2) to old and to new situations.

A. Cases where the electrons flow in bunches

In cases where the charges q carrying the current differ from the electron charge e, Eq. (2) has been extended as follows. The charges flow through the device as a unit and hence generate bremsstrahlung as a unit. Consequently, the fine-structure constant α_0 for electrons must be replaced by the fine-structure constant α for charges q; since α is proportional to q^2, one expects $\alpha = \alpha_0(q/e)^2$. Hence Eq. (2) should be written

$$\alpha_H = \frac{4\alpha_0}{3\pi}\left|\frac{q}{e}\right|^2\left|\frac{\Delta v}{c}\right|^2 . \tag{3}$$

where $u_d=\mu_n E$ and τ is the average time between collisions,

$$\tau=m_n^*\mu_n/e \ . \tag{8}$$

Consequently,

$$\alpha_H=\frac{4\alpha_0}{3\pi}\frac{\mathbf{F}(0)^2}{c^2}=\frac{4\alpha_0}{3\pi}\left|\frac{d}{c\tau}\right|^2 . \tag{8a}$$

We therefore see that acceleration $1/f$ noise fits into Handel's extended schematic, and that it does not require the semiclassical theory.

Experimentally, $\tau\simeq 10^{-12}$ sec, in reasonable agreement with Eq. (8). For $d>200$ μm, α_H may saturate to Handel's coherent-state value, $(2-5)\times 10^{-3}$.[11] The experiments were performed on large numbers of MOSFET's operating in the linear mode, but not all MOSFET types show the effect.

III. BREMSSTRAHLUNG NOISE SPECTRA

We now make a Fourier analysis of the bremsstrahlung pulse emitted by an accelerated charge conglomerate of charge q. As shown in textbooks on electromagnetic radiation, the bremsstrahlung pulse $P(t)$ of such a charge conglomerate is[12] (Larmor equation)

$$P(t)=\frac{2q^2}{3c^3}|\mathbf{a}(t)|^2 \tag{9}$$

for $0<t<\tau_a$, where τ_a is the duration of the pulse and $a(t)$ is the acceleration.

The Fourier transform of $a(t)$ is

$$\begin{aligned}\mathbf{F}_a(j\omega)&=\int_0^{\tau_a}\mathbf{a}(t)\exp(-j\omega t)dt\\&=\mathbf{F}_a(0)\frac{\mathbf{F}_a(j\omega)}{\mathbf{F}_a(0)} ,\end{aligned} \tag{10}$$

where

$$\begin{aligned}\mathbf{F}_a(0)&=\int_0^{\tau_a}\mathbf{a}(t)dt\\&=\mathbf{v}(\tau_a)-\mathbf{v}(0)\\&=\Delta v\end{aligned} \tag{10a}$$

is the low-frequency value of $\mathbf{F}_a(j\omega)$ and $\mathbf{F}_a(j\omega)/\mathbf{F}_a(0)$ is the complex "form factor" of the pulse. It is carried along to make $\int_0^\infty|\mathbf{F}_a(j\omega)|^2df$ converge at the upper limit; for most frequencies of practical interest, the form factor is unity and can be omitted.

We now evaluate the total energy E in the radiation pulse by applying Parseval's theorem. According to the definition of E

$$\begin{aligned}E&=\int_0^{\tau_a}P(t)dt\\&=\frac{2q^2}{3c^3}\int_0^{\tau_a}[\mathbf{a}(t)]^2dt\\&=\frac{4q^2}{3c^3}\int_0^\infty|\mathbf{F}_a(j\omega)|^2df ,\end{aligned} \tag{11}$$

since according to Parseval's theorem

$$\int_0^{\tau_a}[\mathbf{a}(t)]^2dt=2\int_0^\infty|\mathbf{F}_a(j\omega)|^2df \ .$$

The energy dE in a frequency interval df in a single pulse is therefore

$$dE=\frac{4q^2}{3c^3}|\mathbf{F}_a(j\omega)|^2df=S_E'(f)df \ , \tag{11a}$$

where $S_E'(f)=dE/df=(4q^2/3c^3)|\mathbf{F}_a(j\omega)|^2$ is the energy spectrum of photons of frequency f in a single pulse of duration τ_a.

Dividing (11a) by hf yields, for the number, dn, of photons in a frequency interval df for a single pulse of duration τ_a,

$$df=\frac{dE}{hf}=\frac{4q^2}{3c^3}\frac{|\mathbf{F}_a(j\omega)|^2}{hf}df=S_n'(f)df \ , \tag{11b}$$

where $S_n'(f)=dn/hf=(4q^2/3c^3)[|\mathbf{F}_a(j\omega)|^2/hf]$ is the number spectrum of photons of frequency f in a single pulse of duration τ_a.

Dividing (11b) by τ_a yields, for the rate, dr, of photon emission in a frequency interval df for a single pulse of duration τ_a,

$$\begin{aligned}dr&=\frac{dn}{\tau_a}=\frac{dE}{hf\tau_a}\\&=\frac{4q^2}{3c^3}\frac{|\mathbf{F}_a(j\omega)|^2}{hf\tau_a}df\\&=S_r'(f)df \ ,\end{aligned} \tag{11c}$$

where $S_r'(f)=dr/df=(4q^2/3c^3)[|\mathbf{F}_a(j\omega)|^2/hf\tau_a]$ is the spectrum of the photon-emission rate for photons of frequency f in a single pulse of duration τ_a.

The spectra $S_E'(f)=dE/df$, $S_n'(f)=dn/df$, and $S_r'(f)=dr/df$ have no further meaning than that given by the definitions. Those who object to the symbol S may replace it by any symbol of their liking. Usually $|\mathbf{F}_a(j\omega)|^2=\mathbf{F}_a^2(0)$ for all frequencies of interest.

So far, we are on firm ground. We now try to connect $S_n'(f)$ and (or) $S_r'(f)$ to the current noise spectrum $S_I(f)$. To that end, we introduce the Hooge parameter α_H,

$$\begin{aligned}\alpha_H&=\frac{4\alpha_0}{3\pi}\left|\frac{q}{e}\right|^2\frac{F_a^2(0)}{c^2}\\&=\frac{8e^2}{3hc}\left|\frac{q}{e}\right|^2\frac{F_a^2(0)}{c^2} ,\end{aligned} \tag{12}$$

where $\alpha_0=2\pi e^2/hc$, so that $4\alpha_0/3\pi=(4/8\pi)(2\pi e^2/hc)=8e^2/3hc$. In this notation,

$$\begin{aligned}S_n'(f)&=\frac{\alpha_H}{2f} ,\\S_r'(f)&=\frac{\alpha_H}{2f\tau_a} ,\\S_I'(f)&=\frac{S_I(f)}{\lambda}=\frac{\alpha_H}{2f\tau_a}2e^2\end{aligned} \tag{12a}$$

B3

The occurrence of the factor $(q/e)^2$ has been verified experimentally, both in vacuum photodiodes[9] and in secondary-emission multipliers,[10] so that it has at least heuristic validity.

B. Replacing Δv

We next turn to the change Δv in velocity along the electron path in a semiconductor, introduced in Eq. (2), to further elucidate its meaning. If $\mathbf{a}(t)$ is the acceleration of the electrons, and if τ_a is the carrier transit time, then

$$\Delta v = \int_0^{\tau_a} \mathbf{a}(t)dt = \mathbf{F}(0) \tag{4}$$

is the low-frequency Fourier transform of $a(t)$. Hence Eq. (2) becomes

$$\alpha_H = \frac{4\alpha_0}{3\pi}\frac{[\mathbf{F}(0)]^2}{c^2} . \tag{5}$$

We shall see that this expression has many applications.

C. Collision 1/f noise

We first apply it to collision $1/f$ noise. Here, τ_a is the time between collisions and $\mathbf{a}(t)=(h/m^*)d\mathbf{k}/dt$, where $\mathbf{k}$ is the wave vector, so that $\mathbf{F}(0)=(h/m^*)\Delta\mathbf{k}$. This must now be applied to the various collision processes.[6]

Process 1: *normal collision process due to electron-phonon interactions in the conduction band.* Here, $\mathbf{F}^2(0)$ must be evaluated by averaging contributions $\Delta\mathbf{k}$ over all collisions.

Process 2: *umklapp 1/f noise by transitions of electrons into the next Brillouin zone.* The lattice thereby exchanges an average momentum h/a with the electron, where a is the lattice spacing. This process can only occur in degenerate semiconductors or in narrow-gap semiconductors. Hence,

$$\alpha_H = \alpha_{H_u} = \frac{4\alpha_0}{3\pi}\left|\frac{h}{m^* ac}\right|^2 . \tag{6}$$

Process 3: *umklapp and intervalley scattering 1/f noise in n-type Si.* In n-type Si the conduction band has *six* equivalent valleys. This leads to the following collision processes: (a) *normal* collisions involving transitions within the *same* valley; (b) there are also transitions possible to an *opposite* valley [they are also called *umklapp transitions* and give rise to an expression similar to Eq. (6)]; and (c) in addition, there are transitions possible to an *adjacent* valley [they are called *intervalley* transitions and give rise to an expression similar to Eq. (6)].

It should be noted that each valley has *one opposite* valley and *four adjacent* valleys and that each adjacent valley contributes to the intervalley $1/f$ noise equally and independently.

Since there can now be multiple-collision processes, the definition of α_H must be extended.[6] To that end one attributes a mobility μ_i and a Hooge parameter α_{H_i} to each process, and writes

$$\frac{1}{\mu}=\sum_i\frac{1}{\mu_i},\quad \frac{\delta\mu}{\mu^2}=\sum_i\frac{\delta\mu_i}{\mu_i^2},\quad \alpha_H=\sum_i\alpha_{H_i}\left|\frac{\mu}{\mu_i}\right|^2 , \tag{7}$$

$$\alpha_{H_i}=\frac{S_I(f)_i}{I^2}fN=\frac{4\alpha_0}{3\pi}\frac{[\mathbf{F}_i(0)]^2}{c^2} . \tag{7a}$$

In process 2 or 3(b) one finds $\mu/\mu_i=\exp(-\Theta_D/4T)$, where Θ_D is the Debye temperature. In n-type Si *both* processes 3(b) and 3(c) contribute; this has not been properly analyzed so far and, therefore, the accurate comparison between theory and experiment still needs to be carried out. The experiments yield $\alpha_{H_n}=2.5\times10^{-8}$ at $T=300$ K and the temperature dependence of α_{H_n} is compatible with the factor $\exp(-\Theta_D/2T)$. In p-type Si there is only one central valley, so that only normal collision $1/f$ noise contributes. Experimentally, $\alpha_{H_i}\simeq10^{-8}$ at $T=300$ K, in reasonable agreement with theoretical estimates.[4]

We thus see that the introduction of the parameters $\mathbf{F}(0)$ gives a generalized description of all collision $1/f$ noises.

D. Acceleration 1/f noise

Next we turn to *acceleration* $1/f$ noise in semiconductor resistors. The duration of a collision is of the order of 10^{-14} sec and the average time between collisions is of the order of 10^{-12} sec in most semiconductors. During the time *between* collisions, the electrons are *accelerated* by the applied electric field E and emit bremsstrahlung. During the much shorter collision times the electrons are accelerated or decelerated by the *collision* field E_C and also emit bremsstrahlung. The electron interacts with its emitted bremsstrahlung, and produces current $1/f$ noise in either case. Note that E has a constant magnitude and direction, whereas E_C has a fluctuating magnitude and direction.

The bremsstrahlung components due to individual collision processes are independent and add *quadratically* so that α_H is independent of the device length d, whereas the bremsstrahlung components generated *between* collisions are fully correlated and add *linearly*, so that α_H varies as d^2 (see below), where d is the length of the device in the direction of the field. For long devices the latter process therefore predominates; the noise is called *acceleration* $1/f$ *noise* and was observed for long Si metal-oxide-semiconductor field-effect transistors (MOSFET's), both p and n type. The collision noise itself predominates for short devices, since it is independent of d.

We now calculate $\mathbf{F}(0)$ for the acceleration $1/f$ noise. If E is the applied field, the acceleration $a(t)=eE/m^*$, where m^* is the effective mass. Since $u_d=\Delta x/\Delta t=\mu_n E$ is the drift velocity of the carriers,[11] we can write

$$\mathbf{F}(0)=\int_0^d\frac{eE}{m^*}\frac{\Delta t}{\Delta x}dx$$

$$=\int_0^d\left|\frac{eE}{m^* u_d}\right|dx$$

$$=\int_0^d\frac{eE}{m^*\mu_n E}dx=d/\tau ,$$

B4

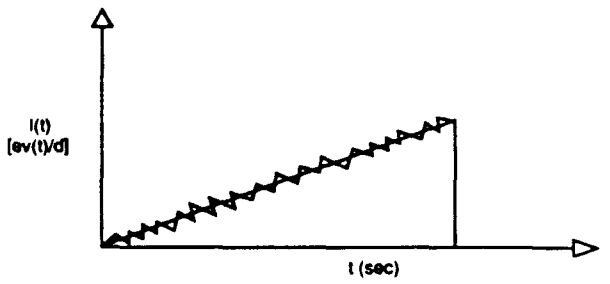

FIG. 1. The current pulse $I(t)=ev(t)/d$ modulated by the $1/f$ noise caused by the random emission of photons by the electron.

and $S_I'(f)$ is the noise for the case of one electron per second where $\lambda=I/e$. Consequently,

$$S_I'(f)=S_r'(f)2e^2 , \tag{13}$$

$$S_I'(f)=S_n'(f)\frac{2e^2}{\tau_a} . \tag{13a}$$

We shall see that (13) has physical meaning, but that (13a) has not.

Due to the random emission of photons by the electron, the pulse $I(t)=ev(t)/d$ has $1/f$ noise superimposed on it (Fig. 1). The ensemble average at the instant t, $\overline{I(t)}=e\overline{v(t)}/d$ gives shot noise $S_I(f)=2e^2\lambda$, whereas the $1/f$ noise, described by $S_r'(f)$, modulates it. Therefore, $S_I'(f)=2e^2S_r'(f)$, and, hence,

$$S_I(f)=2e^2\lambda S_r'(f)=\alpha_H\frac{eI}{f\tau_a} ,$$

as had to be proved.

On the other hand, $2e^2/\tau_a$ represents the shot noise for the case in which there is, on the average, *one electron* in the system; however, the combination (13a) makes no physical sense.

IV. CONCLUSIONS

We conclude the following.

(1) Handel's expressions for the Hooge-parameter (α_H) $1/f$ noise can be generalized to

$$\alpha_H=\frac{4\alpha_0}{3\pi}\left[\frac{q}{e}\right]^2\left[\frac{F_a(0)}{c}\right]^2 ,$$

where the current is carried by charge conglomerates and $F_a(0)$ is the low-frequency Fourier transform of the carrier acceleration $a(t)$. This holds for collision-free and collision-dominated devices including acceleration $1/f$ noise in semiconductor resistors.

(2) This formula can also be derived semiclassically in a more rigorous manner than in van der Ziel's original papers. To that end, one first derives the energy dE of a single radiation pulse in a frequency interval df with the help of Parseval's theorem. Next, one defines $dn=dE/hf$ as the number of photons of a single pulse in a frequency interval df and, finally, defines $dr=dn/\tau_a=dE/hf\tau_a$ as the *rate* of photoemission in a single pulse of duration τ_a in a frequency interval df. It is then found that the expression $S_r''(f)=dr/df$ already contains the Hooge parameter α_H.

(3) If $S_I(f)df$ is the current noise in a frequency interval df and λ the number of pulses per second, then $S_I''(f)df=[S_I(f)/\lambda]df$ is the current noise for a single pulse in a frequency interval df. Since each emitted photon contributes both to $S_r''(f)df$ and to $S_I''(f)df$, the two terms are proportional. Hence, if α_H occurs in $S_r''(f)$ it will also occur in $S_I''(f)$ and, hence, in $S_I(f)$.

(4) We can evaluate $S_I(f)$ directly. An elementary event gives rise to a radiation pulse $P(t)$ that leads to $S_r''(f)$ and to a current pulse $i(t)$ both of duration τ_a. Let $i(t)$ have a low-frequency Fourier transform $F_i(0)$; then, $S_I''(f)=S_r''(f)F_i^2(0)$ and, hence, $S_I(f)=S_I''(f)\lambda=S_r''(f)F_i^2(0)\lambda$. This leads immediately to the Hooge equation.

ACKNOWLEDGMENTS

This work was supported by the U.S. Army Research Office under Contract No. DAAG-29-85-K-0253.

[1]P. H. Handel, Phys. Rev. Lett. **34**, 1492 (1975).
[2]P. H. Handel, Phys. Rev. **22**, 745 (1980).
[3]F. N. Hooge, Phys. Lett. **29A**, 139 (1969); Physica B+C **83B**, 9 (1976).
[4]For a survey, see A. van der Ziel, Proc. IEEE **76**, 233 (1988).
[5]A. van der Ziel, P. H. Handel, X. C. Zhu, and K. H. Duh, IEEE Trans. Electron. Devices **ED-32**, 667 (1985).
[6]G. K. Kousik, C. M. Van Vliet, G. M. Bosman, and P. H. Handel, Adv. Phys. **34**, 663 (1985).
[7]A. van der Ziel, J. Appl. Phys. **63**, 2456 (1988).
[8]A. van der Ziel, J. Appl. Phys. **64**, 904 (1988).
[9]P. Fang, H. Kang, L. He, Q. Peng, and A. van der Ziel, J. Appl. Phys. (to be published).
[10]P. Fang and A. van der Ziel, Physica B+C **174B**, 311 (1987).
[11]Q. Peng, A. Birbas, A. van der Ziel, A. D. van Rheenen, and K. Amberiadis, J. Appl. Phys. **64**, 907 (1988).
[12]J. D. Jackson, *Classical Electrodynamics*, 2nd ed. (Wiley, New York, 1975), pp. 654ff.

B5

1/f noise characterization of n^+–p and n–i–p $Hg_{1-x}Cd_xTe$ detectors

A. van der Ziel, P. Fang,[a] L. He, X. L. Wu,[b] and A. D. van Rheenen
Electrical Engineering Department, University of Minnesota, Minneapolis, Minnesota 55455

P. H. Handel
Physics Department, University of Missouri-St. Louis, St. Louis, Missouri 63121

(Received 11 October 1988; accepted 8 November 1988)

1/f noise in n^+–p and n–i–p $Hg_{1-x}Cd_xTe$ photodiodes is discussed. The n^+–p diodes have coherent-state 1/f noise or umklapp 1/f noise. The n–i–p diodes have much lower values for the Hooge parameter α_H and their noise is probably due to generation–recombination-type (trapping) 1/f noise.

I. INTRODUCTION

In electronic devices the relative 1/f noise spectra $S_I(f)/I^2$ can usually be represented by a Hooge-type equation[1]:

$$\frac{S_I(f)}{I^2}=\frac{\alpha_H}{f^\gamma N}, \tag{1}$$

where the exponent γ is close to unity, N is the number of carriers in the system, and α_H is a constant parameter, the so-called Hooge parameter; it has the dimension $(\mathrm{Hz})^{\gamma-1}$. It can always be defined, and can be used as a measure for the noisiness of the system under investigation, but may not always have physical meaning. This is, e.g., the case for classical 1/f noise caused by surface traps. In other cases α_H can often be identified with distinct physical processes, each resulting in a characteristic value for α_H, dependent on the process involved.

For example, Hooge[1] found $\alpha_H=2\times10^{-3}$ for relatively long semiconductor resistors, independent of the material and the doping, as long as the doping was not too large. This may be identified with Handel's coherent state 1/f noise process with

$$\alpha_H=2\alpha_0/\pi=4.6\times10^{-3}, \tag{1a}$$

where $\alpha_0=1/(137)$ is the fine-structure constant.[2]

In short devices α_H can be much smaller.[3-5] It can be identified with collision processes (normal collision 1/f noise, umklapp 1/f noise, and intervalley scattering 1/f noise) or hole–electron pair generation and recombination 1/f noise processes. For a single-collision process Handel has proposed the quantum 1/f noise equation[6]:

$$\alpha_H=\frac{4\alpha_0}{3\pi}\frac{\overline{\Delta v^2}}{c^2}, \tag{2}$$

where Δv is the vectorial change in velocity during the collision process. If several collision 1/f noise processes are operating simultaneously, Kousik *et al.*[7] proposed

$$\alpha_H=\sum_i \alpha_{H_i}(\mu/\mu_i)^2, \tag{2a}$$

where α_{H_i} is associated with the ith collision process, and μ_i is the mobility associated with that process. In generation–recombination 1/f noise processes $\overline{\Delta v^2}$ can be calculated as $2E/m^*$, where E is the energy associated with the processes[8,9] (see the Appendix).

If normal and umklapp processes are both present, Eq. (2a) yields[3]

$$\alpha_H=\frac{4\alpha_0}{3\pi}\left(\frac{h}{m^*ac}\right)^2\exp\left(-\frac{\theta_D}{2T}\right). \tag{2b}$$

Here m^* is the effective mass, a is the lattice spacing, and θ_D is the Debye temperature of the material, Eq. (2b) takes into account that in an umklapp collision the lattice takes up or gives up a momentum h/a and that the weight factor $(\mu/\mu_i)^2=\exp(-\theta_D/2T)$. The small contribution of normal collision 1/f noise has been neglected.

We now discuss how α_H can be measured experimentally.[9] If the noise can be represented by a "lumped" model, as in vacuum tubes, Eq. (1) can be used directly, and

$$\alpha_H=\frac{f^\gamma S_I(f)N}{I^2}=\frac{S_I(1)N}{I^2}, \tag{3}$$

as long as $S_I(f)=S_I(1)/f^\gamma$ with constant γ. There is one difficulty left, however. Equation (1) implies $N\gg1$, but in a vacuum tube or solid-state diode N can have a value less than unity. In that case we put $I=Ne/\tau$, where τ is a transit time or a lifetime; consequently Eq. (3) becomes

$$\alpha_H=\frac{S_I(1)\tau}{Ie};\quad \text{or } S_I(1)=\alpha_H\frac{eI}{\tau}. \tag{3a}$$

This equation remains valid for $N<1$ and hence Eq. (3a) should replace Eq. (3) in that case.

In many diodes, however, Eq. (1) must be written in the distributed form[9]

$$\frac{S_I(x,f)}{I^2(x)}=\frac{\alpha_H}{f^\gamma N(x)\Delta x}, \tag{4}$$

for a section Δx at x, where $N(x)$ is the number of carriers per unit length at x and $I(x)$ is the minority-carrier current at x.

One now introduces a random noise course $H(x,t)$, evaluates its spectrum $S_H(x,x',f)$ from Eq. (4), and so determines the spectrum $S_I(f)$ in the external circuit by integration. This yields

$$S_I(f)=\alpha_H\frac{eI}{f^\gamma\tau}F(V), \tag{5}$$

where V is the (back) bias of the diode and $F(V)$ is evaluated in the integration process. The time constant τ can be mea-

B6

sured by measuring the device admittance as a function of frequency.[10]

If all parameters are known, α_H can be evaluated.

II. n^+–p $Hg_{1-x}Cd_xTe$ PHOTODIODES

We now turn to various $Hg_{1-x}Cd_xTe$ n^+–p diodes supplied by Rockwell International.[10] They are relatively long diodes, with a cadmium content of 30%; they have n^+ contacts of 150-μm diameter. The length of the p region (w_p) is larger than the diffusion length (L_n). The current flow is by diffusion, as follows from the diode admittance

$$y = g_0(1 + j\omega\tau)^{1/2}. \tag{6}$$

The low-frequency admittance g_0 is equal to dI/dV.

Measuring $y(j\omega)$ near zero bias yielded $\tau \simeq 2\times 10^{-7}$ s at 193 K in good agreement with the Honeywell lifetime tables.[18] Far from zero bias the experimental data could be fitted to the function $g_0(1 + j\omega\tau)^{\gamma_0}$ with $\gamma_0 \simeq 0.7$–0.9. In that case the values of τ deviated from the Honeywell tables and were considered unreliable.

Since the noise seems to be diffusion $1/f$ noise, the following Hooge parameters are expected[11]:

(i) Coherent state $1/f$ noise: $\alpha_H = 4.6\times 10^{-3}$ [Eq. (1a)].

(ii) Umklapp $1/f$ noise to next Brillouin zone: $\alpha_H = 5\times 10^{-5}$ at $T = 273$ K [Eq. (2b)] and $x = 0.30$.

(iii) Normal collision $1/f$ noise: $\alpha_H = 10^{-7}$ at $T = 77$ K and $x = 0.20$ (estimated).

For normal elastic collisions[3]

$$\alpha_H = \frac{4\alpha_0}{3\pi}\frac{6kT}{m^*c^2}, \tag{6a}$$

corresponding to $\alpha_H = 0.34\times 10^{-7}$ at $T = 77$ K; for $x = 0.20$, $m = 0.0073\, m_0$, where $m_0 = 9.11\times 10^{-31}$ kg, the mass of the free electron. If the inelasticity of the collisions was taken into account in the case of electrons in silicon α_H was found to be ~ 3.5 times larger. Assuming the same correction factor for $Hg_{1-x}Cd_xTe$ yields $\alpha_H = 1.2\times 10^{-7}$ in close agreement with our estimate of 10^{-7}.

When we applied Eq. (5) and plotted $S_I(f)/[IF(V)]$ at a fixed frequency f vs V, we found that $S_I(f)/[IF(V)]$ was constant. The theory predicted that

$$F(V) = \frac{1}{3} - \frac{1}{2a} + \frac{1}{a^2} - \frac{1}{a^3}\ln(1+a);$$
$$a = \exp(eV/kT) - 1, \tag{7}$$

so that $F(0) = 0$, as follows from a Taylor expansion of $\ln(1 + a)$ for small a up to the a^3 term. This function was used in Fig. 1. Since $S_I(1)/[IF(V)]$ was independent of bias, α_H/τ was apparently independent of bias (Fig. 1), even when γ_0 had values of 0.7 to 0.9.

The spectra were of the form $1/f^\gamma$ with γ very close to unity (Fig. 2), as expected for quantum $1/f$ noise. Figure 3 shows α_H as a function of back bias, indicating that a high γ_0 and a high α_H go together. Since α_H/τ is constant, the error in α_H is due to a corresponding error in τ.

Measuring $S_I(f)$ at $T = 113$ and at 193 K, we found in all units near zero bias $\alpha_H = (3$–$5)\times 10^{-3}$, indicating that the $1/f$ noise was *coherent state 1/f noise*. Similar values of

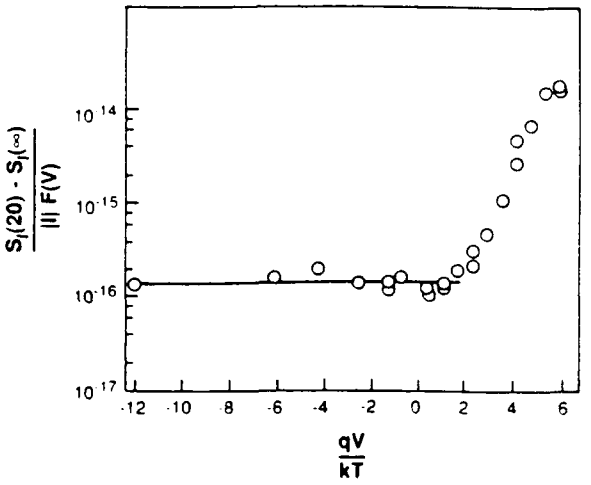

FIG. 1. The relation between $[S_I(f) - S_I(\infty)]/[IF(V)]$ and the bias voltage V for n^+–p diode 3-454 is represented by a horizontal bar.

α_H were obtained for $\gamma = 0.7$–0.9 by using the τ values of the Honeywell lifetime tables.

At 273 K one unit had $\alpha_H = 5\times 10^{-5}$ as expected for *umklapp 1/f noise* to the next Brillouin zone. This unit had $\tau = 1.2\times 10^{-7}$ s according to the lifetime tables.

What happens if $w_p \ll L_n$? In that case the admittance is[12]

$$y = g_0\frac{(2j\omega\tau_d)^{1/2}}{\tanh(2j\omega\tau_d)^{1/2}} \simeq g_0(1 + \tfrac{1}{3}j\omega\tau_d), \tag{8}$$

where $\tau_d = w_p^2/2D_n$, w_p is the length of the p region, and D_n is the diffusion constant of the electrons in the p region. Calculating $S_I(f)$ and applying Eq. (5) yields

$$S_I(f) = \alpha_H\frac{eIF(V)}{f^\gamma\tau_d},$$
$$F(V) = \tfrac{1}{2}\ln\left[\frac{D_n/w_p + s_{cn}}{D_n/w_p + s_{cn}\exp(-eV/kT)}\right], \tag{9}$$

where s_{cn} is the recombination velocity of electrons at the p contact. For most materials s_{cn} is of the order of 10^7 cm/s. Note that $F(V) \simeq \frac{1}{2}eV/kT$ for large negative V. Also,

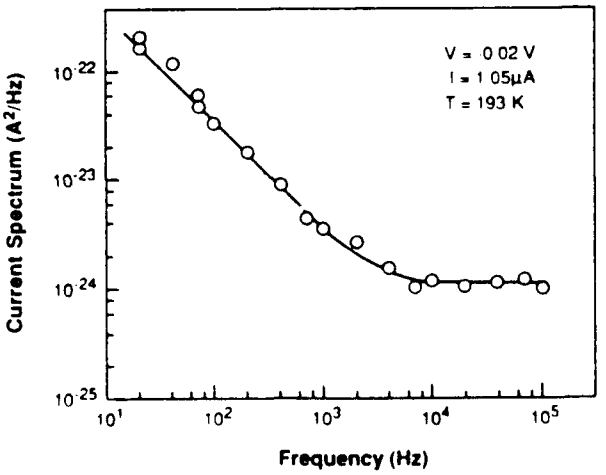

FIG. 2. The spectrum $S_I(f)$ for diode 5-128M at $V = 0.002$ V is of the form $1/f^\gamma$ with γ very close to unity.

B7

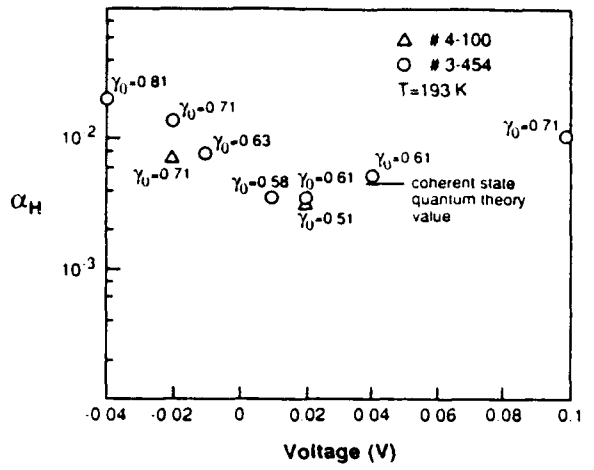

FIG. 3. Hooge parameters α_H vs applied voltage V. Note the effect of the parameter γ_0.

$s_{in} \gg D_n/w_p$ in most cases. (For $D_n = 250\,\mathrm{cm^2/s}$ and $w_p = 5$ μm, $D_n/w_p = 0.5\times 10^6$ cm/s, which is an order of magnitude smaller than s_{in}.)

How can the operation of the detector be improved? To that end one must make P_{eq} or $[S_I(f)]^{1/2}$ as small as possible. This means that one must make (α_H/τ) and $IF(V)$ as small as possible.[13]

The highest value of α_H (5×10^{-3}) occurs for coherent-state 1/*f* noise; this fundamental noise source should therefore be avoided.

The next lower value of α_H (5×10^{-5}) occurs for umklapp 1/*f* noise. It might be achieved by making the device dimensions somewhat smaller, and would give a value of α_H that is ~ 100 times smaller. Hence, if τ does not change very much, as our data seem to indicate, P_{eq} could be lowered by a factor of 10. This needs further investigation, especially as far as the value of τ is concerned. At 273 K the p region was nearly intrinsic, and this might make the theory of Sec. III applicable when $\tau_d = w_p^2/2D_n \ll \tau$.

Can the normal collision 1/*f* noise be reached? We estimated $\alpha_H \simeq 10^{-7}$, but it can probably only be reached for very small w_p, e.g., $w_p < 5\,\mu$m. But in that case τ_d is very small and hence α_H/τ_d may not be much improved. For example, our unit at $T = 273$ K has $\alpha_H = 5\times 10^{-5}$ and $\tau = 1.2\times 10^{-7}$ s, so that $\alpha_H/\tau = 400\,\mathrm{s^{-1}}$. Suppose now that we could achieve $\alpha_H = 10^{-7}$ at $w_p = 5\,\mu$m. Then $\tau_d = w_p^2/2D_n = 5\times 10^{-10}$ s (if we take $D_n = 250\,\mathrm{cm^2/s}$), so that $\alpha_H/\tau_d = 200\,\mathrm{s^{-1}}$. This is an insignificant improvement. So we should search for the normal collision 1/*f* noise in order to complete our catalog of noise sources, and to see whether our pessimistic views about P_{eq} are correct, but we should not keep our hopes up too high. Fortunately, better ways have been found[20] of achieving lower values of P_{eq} (see Sec. III).

The diffusion 1/*f* noises in n^+-p $Hg_{1-x}Cd_xTe$ diodes are so high because the effective mass of the electrons is so small ($= 0.01\,m_0$); as a consequence $(\alpha_H)_{diff} > 5\times 10^{-5}$. Trapping 1/*f* noises, however, when described by a Hooge parameter, usually have $\alpha_H = 10^{-6}$–10^{-5} so that those noise processes will be completely masked by diffusion 1/*f* noise. For that reason we can understand why only one Rockwell unit showed burst noise and none showed trapping 1/*f* noise.[10]

III. $Hg_{1-x}Cd_xTe$ *p–i–n* DIODES

In order to study the *p–i–n* structures we first investigated long *p–i–n* silicon power diodes as far as admittance and noise were concerned.[14] If the i region extends from $-d < x < d$ then a *p–i–n* diode is called "long" if $d > L$, where L is the diffusion length and "short" if $d < L$. The admittance had a complicated structure and showed two resonances. The impedance of the device could be written as $1/Y_j + Z_m$, where $Y_j(\omega) = g_j + j\omega C_j$ is the admittance of the *p–i* junction and z_m is the modulation impedance due to the modulation of the carrier density in the i region by the ac current. Here

$$\frac{1}{Z_m} = \frac{1}{R_m} + \frac{1}{j\omega L_0} + j\omega C, \tag{10}$$

where L_0C_j gives the first resonance and L_0C the second; g_j, C_j, and L_0 may be functions of frequency.

Next we solved the Fletcher equations for ac and found this yielded a term for the high-frequency admittance of the junction[15]:

$$Y_j = g_0 \frac{L}{L'} \frac{\tanh(d/L')}{\tanh(d/L)}, \tag{11}$$

where $g_0 = dI/dV$, $L'/L = (1+j\omega\tau)^{-1/2}$, and τ is the carrier lifetime.

For long diodes ($d/L > 1$), $\tanh(d/L) \simeq 1$, and $\tanh(d/L') \simeq 1$, so that at lower frequencies

$$Y_j = g_0 \frac{L}{L'} = g_0(1+j\omega\tau)^{1/2} = g_j + j\omega C_j, \tag{11a}$$

corresponding to Eq. (6); here g_j and C_j are frequency dependent; this corresponds to Eq. (6). For shorter diodes ($d/L < 1$),

$$Y_j = g_0(L/L')^2 = g_0(1+j\omega\tau) = g_0 + j\omega C_{j0}, \tag{11b}$$

where g_0 and C_{j0} are independent of frequency.

In addition one can evaluate Z_m as a function of frequency for higher frequencies. This leads to a complicated resonance for $d/L > 1$, as described by Eqs. (6) and (10) and to a simple resonance described by Eq. (11b) and Z_m for $d/L < 1$, where

$$Z_m = \frac{1}{2}\frac{R_m \cdot j\omega L_0}{R_m + j\omega L_0}. \tag{12}$$

The simple resonance is now determined by the frequency $\omega_0 = (L_0C_{j0})^{-1/2}$ (Fig. 4).

Calculating all circuit elements numerically we can evaluate τ either from Y_j, when Y_j predominates, or from Z_m when Z_m predominates. Applying this to the long Si p^+-i-n power diode yielded $\tau \simeq 1.4\times 10^{-5}$ s at $T = 400$ K, as expected for such diodes, whereas for the $Hg_{1-x}Cd_xTe$ diodes with $x = 0.22$ and $T = 80$ K all Santa Barbara units gave $\tau = 10^{-7}$ s, comparable to the Honeywell lifetime tables.[18]

We conclude from the latter result that the Santa Barbara diodes are relatively short ($d/L < 1$) *p–i–n* diodes and not n^+-p junction diodes.

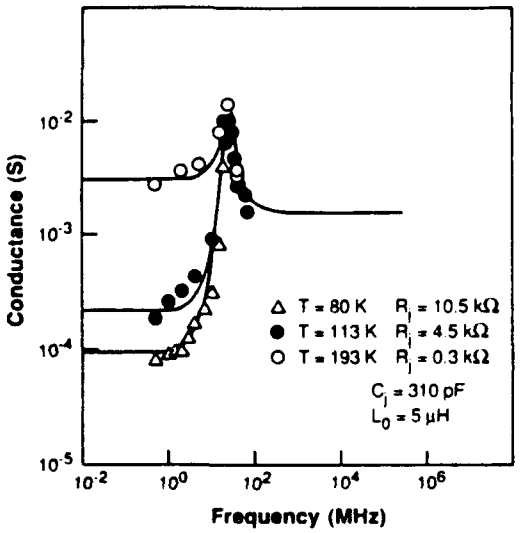

FIG. 4. The conductance $G(f)$ vs frequency for Santa Barbara Research Center devices at 80, 113, and 193 K. Crosses: experiment; full-drawn line: theory ($\tau = 10^{-7}$ s).This representative figure seems to indicate that the devices are *n–i–p* diodes.

We now turn to the $1/f$ noise. The *p–i–n* diode $1/f$ noise has not been evaluated theoretically but by analogy with the previous discussion one would expect a formula of the type

$$S_I(f) = \alpha_H \frac{e|I|F(V)}{f^{\gamma}\tau}, \tag{13}$$

where $F(V)$ is usually a function of V but $F(V)$ may not be equal to zero for $V = 0$. Measuring $S_I(f)$ and τ vs V, we can thus evaluate $f(V)$ from the data.

For long Si *p–i–n* power diodes ($d/L > 1$) Fang[16] found at $T = 400$ K that $S_I(f)/|I|$ was independent of the back bias voltage V; this means that $f(V)$ was independent of V.

Assuming $f(V) = 1$ yielded $\alpha_H = 4.1 \times 10^{-3}$ in good agreement with what the coherent-state $1/f$ noise theory predicts (4.6×10^{-3}). A more accurate theory of $S_I(f)$ is, of course, needed for this case, but the simple results obtained so far look plausible.

For shorter $Hg_{1-x}Cd_xTe$ diodes with $x = 0.22$ at 80 K,

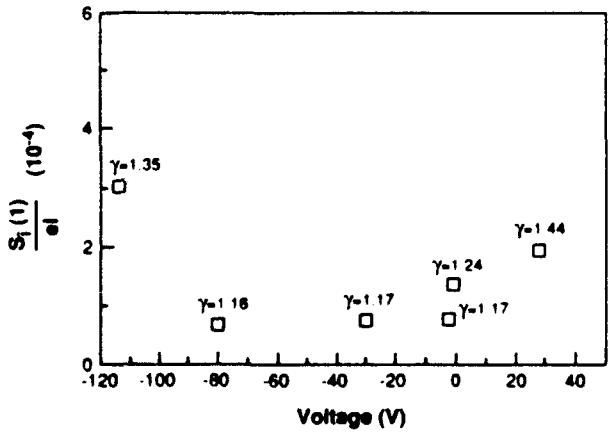

FIG. 5. $S_I(f)/e|I| = \alpha_H F(V)$ vs back bias for diode G14, indicating that $F(V)$ is independent of bias (bias in mV, not V).

TABLE I. α_H values for different diodes at $T = 80$ K.

No.	V_d(mV)	I_d(μA)	$S_I(f)$ (A²/Hz)	$\alpha_H(\tau = 10^{-7}$ s)
M	−0.8	−3.5	2.25×10^{-23}	2.0×10^{-3}
G	−3.0	−3.5	0.95×10^{-23}	1.5×10^{-3}
F	−20	−6.0	4.3×10^{-24}	2.25×10^{-3}
J	−25	−7.0	0.9×10^{-23}	8.0×10^{-4}
K	−30	−10.0	1.0×10^{-23}	3.0×10^{-4}
H	−40	−12.0	0.8×10^{-23}	2.0×10^{-4}

Fang[15] found much lower values for α_H than either the coherent-state theory (4.6×10^{-3}) or the umklapp theory (1.7×10^{-4}) would predict for the case.[11] Measurements by Fang and He[17] indicated that $|F(V)|$ was independent of the back bias $|V|$ (Fig. 5). We therefore assumed $F(V) = 1$ and obtained the results shown in Table I.

The spectra were of the form $1/f^{\gamma}$, where γ deviates significantly from unity (Fig. 6). The latter is incompatible with quantum $1/f$ noise, but can be explained by superimposed trapping processes or classical modulation effects.

How have such low values of α_H been achieved? Only because diffusion $1/f$ noise processes are inactive in this case (see the Appendix). What is then left are various trapping processes, probably at the surface of the *p* region (or the surface of the junction space-charge region), or at other crystal defects. The noise is not fully describable in terms of quantum $1/f$ noise processes, though they may play a part; classical modulation effects might enhance it, just as is the case in Si bipolar junction transistors (see the Appendix).

The α_H values of Table I vary by a factor of 10. This is explainable in terms of trapping effects, for $S_I(f)$ should be proportional to the trap density and can therefore vary from unit to unit even in a single array.

But there could be a lower limit set by *direct* hole–electron pair generation or recombination. We can make the following estimate. If a hole–electron pair is generated, the average energy of the free electron is $3kT/2$ and the average energy of

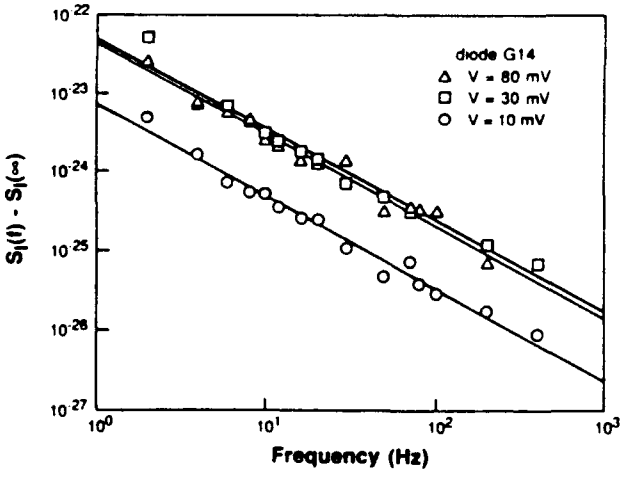

FIG. 6. $[S_I(f) - S_I(\infty)]$ vs frequency for diodes G14 indicating that the spectrum is proportional to $1/f^{\gamma}$ with $\gamma \neq 1$. *R* is the parameter characterizing the computer fit.

B9

the free hole $3kT/2$, so that the total energy involved is $E = 3kT$ and hence $\overline{\Delta v^2} = 3E/m^*$, or[8,9]

$$\alpha_H = \frac{4\alpha_0}{3\pi}\left(\frac{2E}{m^*c^2}\right) = \frac{4\alpha_0}{3\pi}\frac{6kT}{m^*c^2}, \tag{14}$$

corresponding to the elastic theory of normal collision $1/f$ noise. Van der Ziel[9] has explored the possibility of adding a term E_g to E, where E_g is the gap width. It is unlikely that this conjecture can be justified theoretically.

It should be understood from Table I that the lower limit for α_H has not yet been reached. Hence Eq. (14) has not been verified and can only be used as a guide for interpreting data.

Jones and Radford[20] found $\alpha_H = 5\times 10^{-5}$ for similar units. They also found that the temperature dependence of the $1/f$ noise was proportional to $\exp(E_g/2kT)$, as expected for g–r-type $1/f$ noise processes. On the other hand, the $1/f$ noise in n^+–p $Hg_{1-x}Cd_xTe$ photodiodes has an $\exp(E_g/kT)$ temperature dependence, as expected for diffusion-type $1/f$ noise processes.

ACKNOWLEDGMENTS

This work was supported by ARO Contract No. DAAG 29-85-K 0235. The n^+–p devices were supplied by G. R. Williams, Rockwell International, Thousand Oaks, CA, and the n–i–p diodes came from W. A. Radford, Santa Barbara Research Center, Goleta, CA. We thank E. G. Kelso, CNVEO, Fort Belvoir, VA, for reviewing the manuscript.

APPENDIX

1. *n–i–p* diode

We can elucidate the admittance and the noise properties of the p–i–n diode by considering the dc solution of the Fletcher equations. Here $p(x) \simeq n(x)$ in the i region. Let the i region extend from $-d$ to $+d$ and let L be the diffusion length of the carriers. Then, according to Fletcher,[15]

$$p(x) = p(I)\frac{\cosh(x/L)}{\cosh(d/L)}, \quad (-d < x < d), \tag{A1}$$

with $p(x) = p(I)$ at $x = \pm d$.

For long diodes ($d \gg L$) $p(x)$ depends strongly on x; there is a carrier density gradient at the end points $\pm d$ and hence there is diffusion at the boundaries. It is therefore not surprising that Eq. (11a) agrees with Eq. (6). For short diodes ($d/L \ll 1$) $p(x)$ is independent of x [$p(x) \simeq p(I)$ for $-d < x < d$]; there is no carrier density gradient and hence no diffusion. For Eq. (11b) one would expect $g_0 = dI/dV$. Furthermore, for lack of diffusion one would not expect diffusion $1/f$ noise.

According to Handel, the quantum $1/f$ noise due to bulk or surface traps can usually be written in the form[8]

$$\alpha_H = \frac{4\alpha_0}{3\pi}\frac{2E}{m^*c^2}, \tag{A2}$$

where E always contains a term $(3kT/2)$ or $3kT$. In addition, there can be another energy term E' due to potential barriers, built-in voltages, etc. But it is doubtful whether values of $\alpha_H > 10^{-6}$ can be achieved in this manner.

Since our measurements of α_H are in the range 2×10^{-6}–2×10^{-5}, it seems that they cannot be interpreted by quantum effects. We believe that classical modulation of (surface) recombination centers by the fluctuating occupancy of traps in the surface oxide might explain the discrepancy.[19] In addition the frequency dependence of most spectra also rules out a quantum $1/f$ noise interpretation.

[a] Present address: EE Department, University of Southern Florida, Tampa, FL.
[b] Present address: Unisys, San Diego, CA.

[1] F. N. Hooge, Phys. Lett. A **29**, 139 (1969); Physica B **83**, 9 (1976). We added the exponent γ.
[2] P. H. Handel, in *Noise in Physical Systems and 1/f Noise*, edited by M. Savelli, C. Lecoy, and J. P. Nougier (Elsevier, New York, 1983), p. 97; P. H. Handel, *Noise in Physical Systems and 1/f Noise*, edited by A. d'Amico and P. Mazetti (Elsevier, New York, 1986), p. 456.
[3] A. van der Ziel, P. H. Handel, X. C. Zhu, and K. H. Duh, IEEE Trans. Electron Devices **32**, 667 (1985).
[4] K. H. Duh and A. van der Ziel, IEEE Trans. Electron Devices **32**, 662 (1985).
[5] X. C. Zhu and A. van der Ziel, IEEE Trans. Electron Devices **32**, 658 (1985).
[6] P. H. Handel, Phys. Rev. Lett. **34**, 1492 (1975); Phys. Rev. **22**, 745 (1980).
[7] G. Kousik, C. M. van Vliet, G. Bosman, and P. H. Handel, Adv. Phys. **34**, 663 (1985).
[8] A. van der Ziel, P. H. Handel, X. L. Wu, and J. B. Anderson, J. Vac. Sci. Technol. A **4**, 2205 (1986).
[9] A. van der Ziel, Proc. IEEE **76**, 233 (1988) (review paper).
[10] X. L. Wu, J. B. Anderson, and A. van der Ziel, IEEE Trans. Electron Devices **34**, 602 (1987).
[11] X. C. Zhu, X. L. Wu, A. van der Ziel, and E. G. Kelso, IEEE Trans. Electron Devices **32**, 1353 (1987).
[12] A. van der Ziel, *Solid State Physical Electronics*, 3rd Ed. (Prentice–Hall, Englewood Cliffs, NJ, 1976).
[13] The standard definition of the equivalent noise power of a detector is

$$P_{eq} = \frac{V_{ph}}{(1-R)\eta}[S_i(f)]^{1/2},$$

where V_{ph} is the energy of the incoming photons in eV, η is the quantum efficiency, and R the reflection coefficient of the surface.
[14] P. Fang and A. van der Ziel, in *Noise in Physical Systems*, edited by C. M. Van Vliet (World Scientific, Singapore, 1987), p. 410.
[15] N. Fletcher, Proc. IRE **45**, 862 (1957).
[16] P. Fang, Ph.D. thesis, University of Minnesota, 1988.
[17] P. Fang, L. He, A. van der Ziel, and A. D. van Rheenen (see Fig. 5).
[18] G. Hanson and T. Casselman, "Fundamental parameters in mercury cadmium telluride, Vol. 3, Table of lifetimes in $Hg_{1-x}Cd_xTe$," Honeywell Corporate Research Center, Minneapolis, MN, Technical Report, 1982.
[19] A. van der Ziel, Solid-State Electron. (in press).
[20] C. E. Jones and W. A. Radford, in *Ninth International Conference on Noise in Physical Systems*, edited by C. M. Van Vliet (World Scientific, Singapore, 1987), p. 393.

B10

Secondary emission 1/*f* noise revisited

A. van der Ziel, P. Fang,[a] and A. D. van Rheenen
Electrical Engineering Department, University of Minnesota, Minneapolis, Minnesota 55455

(Received 6 January 1989; accepted for publication 16 May 1989)

Fang and van der Ziel's analysis of secondary emission 1/*f* noise in secondary emission pentodes is extended to 16 individual data points. It is found that by proper choice of the secondary electron path length d_{da}, good agreement between the experimental values of the Hooge parameter α_H and the theoretical values predicted by Handel's quantum 1/*f* noise theory is obtained for 14 data points. Handel's equations for the Hooge parameter of the tubes thus seem to have heuristic validity. The values of the secondary electron path length d_{da} differ somewhat from tube to tube and may also depend slightly on bias; these effects are attributed to the electron-optical system formed by screen grid, dynode, and anode.

In 1960 Schwantes and van der Zeil[1] observed secondary emission 1/*f* noise in Philips EFP60 secondary emission pentodes but they had no satisfactory explanation of the effect. In 1987 van der Ziel[2] applied the predictions made by Handel's quantum 1/*f* noise theory[3] to the problem and obtained good agreement with experiment after a slight modification of Handel's expression for the Hooge parameter of the system.

[a] Now at the EE Department, University of South Florida, Tampa, FL.

The 1/*f* noise is generated in the region between the secondary emission dynode (d) and the anode (a) collecting the secondary electrons. According to Hooge's equation[4]

$$S_{I_a}(f) = \alpha_H (I_a^2/fN) = \alpha_H (eI_a/f\tau_{da}) = 4kTR_{ns}g_{ma}^2, \quad (1)$$

where α_H is the Hooge parameter, and $N = I_a\tau_{da}/e$ the number of electrons in the system. Furthermore, τ_{da} is the electron transit time from dynode to anode, I_a is the anode current, $g_{ma} = \partial I_a/\partial V_g$ the transconductance of the tube, and R_{ns} the secondary emission noise resistance measured

 0021-8979/89/182736-03$02.40

B11

by Schwantes and van der Ziel.[1] (The paper of Fang and van der Ziel[3] has the obvious misprint $g_{ma} = \partial I_a/\partial V_a$.) Handel's modified expression for the Hooge parameter α_H is[3]

$$\alpha_H = (4\alpha_0/3\pi)\delta^2(\Delta v^2/c^2), \tag{1a}$$

where $\alpha_0 = 1/(137)$ is the fine structure constant for electrons in the system, δ is the secondary emission factor, Δv is the velocity change of the secondary electrons along the electron path from dynode to anode, and c is the velocity of light. The modification consists in adding a factor δ^2 to (1a); it comes about because the secondary electrons are emitted in bunches of charge δe, so that the fine structure constant of the bunches should be $\alpha_0\delta^2$. The factor δ^2 in (1a) was first introduced empirically and subsequently justified by the argument given above.

If the secondary electrons are emitted with near-zero velocity, $(V_a - V_d)$ is the potential difference between dynode and anode and d_{da} is the length of the electron path in the dynode-anode system, we obtain

$$\Delta v^2 = (2e/m)(V_a - V_d),$$

$$\tau_{da} = 2d_{da}/\Delta v = 2d_{da}/[2e(V_a - V_d)/m]^{1/2}. \tag{1b}$$

van der Ziel[3] found good agreement between theory and experiment by choosing $d_{da} = 0.50$ cm, which was compatible with the device dimensions.

By substituting (1b) and (1a) into (1), obtain

$$S_{I_a}(f) = \alpha_H \frac{eI_a}{2fd_{da}}\Delta v$$

$$= \frac{4\alpha_0}{3\pi}\frac{(2e/m)^{3/2}}{c^2}\frac{e}{2fd_{da}}\delta^2 I_a(V_a - V_d)^{3/2}. \tag{2}$$

Fang and van der Ziel measured the spectral intensity of the fluctuations in the anode current in two EFP60 tubes. They determined $S_{I_a}(f)/(V_a - V_d)^{3/2}$ at constant δ and constant I_a as a function of $(V_a - V_d)$, and also $S_{I_a}(f)/(\delta^2 I_a)$ at constant $(V_a - V_d)$ as a function of the screen grid voltage V_2; they found horizontal lines in both cases. They also deduced[3]

$$S_{I_a}(f)/[(V_a - V_d)^{3/2}\delta^2 I_a]$$

from their data, plotted it versus $(V_a - V_d)^{3/2}\delta^2 I_a$ and found again horizontal lines. The average values were

$$S_{I_a}(10)/[(V_a - V_d)^{3/2}\delta^2 I_a]$$

$$= 1.27\times 10^{-20}\ \text{A Hz}^{-1}\,\text{V}^{-3/2}$$

for tube No. 1 and 0.79×10^{-20} A Hz^{-1} V$^{-3/2}$ for tube No. 2 both at 10 Hz. The average over both tubes is therefore 1.03×10^{-20} A Hz$^{-3/2}$ at 10 Hz. Assuming Eq. (2) to be valid they found $d_{da} = (d_{da})_{av} = 0.56$ cm from this average; individual tubes give $d_{da1} = 0.45$ cm and $d_{da2} = 0.73$ cm, respectively.

Actually, Fang and van der Ziel did eight independent measurements on each tube and each measurement can yield additional information. To retrieve this we introduce the theoretical α_H, denoted by $(\alpha_H)_{theo}$ and the experimental α_H, denoted by $(\alpha_H)_{exp}$. According to Eqs. (1b) and (2)

$$(\alpha_H)_{theo} = \frac{4\alpha_0}{3\pi}\delta^2\frac{\Delta v^2}{c^2};\quad (\alpha_H)_{exp} = \frac{S_{I_a}(f)}{(eI_a\Delta v)}2d_{da}f. \tag{3}$$

TABLE I. Device No. 1, $f = 10$ Hz.

(a) $I_a = 10$ mA, $\delta = 3.6$, $V_2 = 250$ V

$V_a - V_d$ (V)	S_{I_a}(10 Hz) (10^{-18} A^2/Hz)	d_{da}* (mm)
125	2.32	4.48
100	1.56	4.77
75	1.06	4.56
50	0.48	5.48

(b) $V_a - V_d = 125$ V

V_2 (V)	I_a (mA)	δ	S_{I_a}(10 Hz) (10^{-18} A^2/Hz)	d_{da}* (mm)
250	10.00	3.60	2.30	4.52
225	5.88	3.04	0.94	4.64
200	2.94	2.93	0.27	5.16
175	1.44	1.97	0.15	2.99

*$d_{da} = 4.8 \pm 0.3$ mm when the last measurement is left out of the averaging procedure.

We see that $(\alpha_H)_{theo}$ is independent of d_{da}, whereas $(\alpha_H)_{exp}$ varies linearly with d_{da}. By proper choice of d_{da} one can thus bring the two α_H values to coincidence; equating $(\alpha_H)_{exp} = (\alpha_H)_{theo}$ yields d_{da} for each measurement. Actually, due to errors in the measurement, the individual values of d_{da} will scatter.

The aim of this communication is to point out that the averaging process eliminates a large amount of valuable information. Also, it neglects the possibility that the secondary electron path length between the anode and dynode can be different for the two tubes. Therefore, we calculate the value of d_{da} from the measurements for each tube separately using Eq. (3). For each tube two runs of four measurements are available: one run for which the anode-to-dynode voltage $(V_a - V_d)$ is varied between 50 and 125 V while keeping the grid voltage constant and one run where the grid voltage (V_g) is varied between 175 and 250 V when the anode-to-dynode voltage is kept constant. The results are presented in Table I. Similar experiments were done on a second tube and these results are supplied in Table II. The values of d_{da} tend

TABLE II. Device No. 2, $f = 10$ Hz.

(a) $I_a = 8.0$ mA, $\delta = 3.1$, $V_2 = 250$ V

$V_a - V_d$ (V)	S_{I_a}(10 Hz) (10^{-19} A^2/Hz)	d_{da}* (mm)
125	8.7	7.09
100	6.1	7.24
75	4.3	6.67
50	2.6	6.00

(b) $V_a - V_d = 125$ V

V_2 (V)	I_a (mA)	δ	S_{I_a}(10 Hz) (10^{-19} A^2/Hz)	d_{da}* (mm)
250	8.00	3.1	8.7	7.09
225	5.0	2.6	3.4	7.98
200	2.5	2.1	1.3	6.81
175	1.2	1.7	0.3	9.28

*$d_{da} = 7.0 \pm 0.6$ mm when the last measurement is left out of the averaging procedure.

B12

to deviate from the average value for small bias voltages V_2 and $(V_a - V_d)$ or small currents in both devices. Omitting these values from the averaging procedure yields $d_{da} = 4.8 \pm 0.3$ mm for tube No. 1 and $d_{da} = 7.0 \pm 0.6$ mm for tube No. 2 in agreement with Fang and van der Ziel's data.[3] Apart from the fact that these are reasonable values for the anode-dynode distance, the root-mean-square deviation from the average is less than 8% for seven measurements on each device. The eighth measurement in each set deviates strongly from the other seven. These are the measurements at the smallest bias voltages and currents; they do not deviate systematically either to the high or the low side. Hence we consider them poor measurements.

We conclude that Eq. (3) accurately describes the measured noise in secondary emission tubes. Not only is the magnitude correctly predicted but the dependence on the applied voltages and the current as well.

The screen-grid–dynode-anode system guides the primary electron beam towards the dynode and the secondary electrons to the anode. The point where the primary beam hits the dynode will vary from tube to tube due to slight variations in the screen geometry, screen grid distance, grid dynode distance, and may also depend somewhat on bias. Accordingly, the path the electrons travel from dynode to anode will vary from tube to tube, as already demonstrated.

[1] R. C. Schwantes and A. van der Ziel, Physica **26**, 1162 (1982)
[2] A. van der Ziel, Physics **144** B, 205 (1987)
[3] P. Fang and A. van der Ziel, Physica **147** B, 311 (1987)
[4] F. N. Hooge, Phys. Lett. **A-29**, 139 (1969)

Solid-State Electronics Vol. 32, No. 10, pp 905-907, 1989
Printed in Great Britain.
0038-1101/89 $3.00 + 0.00

GENERATION–RECOMBINATION-TYPE $1/f$ NOISE IN n–i–p DIODES

A. VAN DER ZIEL, L. HE, A. D VAN RHEENEN and P. FANG*
Electrical Engineering Department, University of Minnesota, Minneapolis, MN 55455, U.S.A.

(*Received* 13 *March* 1989; *in revised form* 6 *April* 1989)

Abstract—It is shown for p–i–n diodes, in which the current flow is by hole-electron pair generation and (or) recombination, that the $1/f^{\gamma}$ noise is due to generation–recombination processes involving traps and (or) recombination centers and that the spectrum may be written as $S_I(f) = \alpha_H e|I|/[f^{\gamma}\tau]$, where α_H is the Hooge parameter, e the electron charge, $|I|$ the absolute current, τ the time constant associated with the pair generation and pair recombination process, f the frequency and γ is the exponent of the spectrum. This is studied experimentally and the Hooge parameters of various devices are determined.

1. THEORY

According to Hooge[1] the relative $1/f$ noise spectrum of a long uniform resistor is given by the Hooge equation

$$S_I(f)/I^2 = \alpha_H/(fN) \tag{1}$$

where α_H is the Hooge parameter, f the frequency, and N the number of carriers in the system. It was found that α_H had a value of 2×10^{-3} for long resistors, decreased with decreasing device length[2] and was many orders of magnitude smaller for small junction diodes, bipolar junction transistors, and field effect transistors[3].

It should be understood, of course, that in the small devices eqn (1) must be properly modified. For example, since the devices are non-uniform, eqn (1) must be written in differential form. Moreover, since the spectrum is often not exactly $1/f$, f must be replaced by f^{γ}. The contribution of the noise produced in a slice of thickness Δx located at x to the total spectrum is

$$S_I(x,f) = \frac{I(x)^2\alpha_H}{f^{\gamma}N(x)\,\Delta x} \tag{2}$$

where α_H is now not a dimensionless constant but has the dimension $(\mathrm{Hz})^{\gamma-1}$. $N(x)$ is the number of carriers per unit length and $I(x)$ is the minority carrier current at x. This generalized formula is usually valid. For long n^+–p diodes $S_I(x,f)$ and $I(x)$ decrease with increasing x.

The calculation of the spectrum of the current fluctuations in the external circuit is done by properly integrating eqn (2). For an n^+–p $Hg_{1-x}Cd_xTe$ diode in which the current flow is by *diffusion*, this procedure yields[4]

$$S_I(f) = \frac{\alpha_H e|I|}{f^{\gamma}\tau}F(V) \tag{3}$$

where the function $F(V)$ follows from the integration process. For long diodes τ is the life time of the carriers, which can be evaluated from the h.f. device admittance, and for shorter diodes $\tau = \tau_d = w_p^2/2D_n$ is the electron diffusion time, which can be evaluated if the electron diffusion constant D_n and the length w_p of the p-region are known. The Hooge parameter α_H can then be determined; for long diodes[4] $\alpha_H = (3\text{–}5) \times 10^{-3}$, comparable to Hooge's value 2×10^{-3}.

For n–i–p diodes we postulated[5] by analogy

$$S_I(f) = \frac{\alpha_H e|I_d|f(V)}{f^{\gamma}\tau}, \tag{4}$$

where τ is again the carrier lifetime and the function $f(V)$ may differ from the corresponding function in eqn (3). Experimentally $\alpha_H f(V)$ was found to be independent of back bias. Since α_H is supposed to be a constant, $f(V)$ is apparently also a constant. Assuming $f(V) = 1$ we obtained very reasonable values for α_H[5].

It is the aim of this note to prove the validity of eqn (4) and to show that $f(V) = 1$. We do so as follows. Van der Ziel has observed that in the case of $1/f$ noise due to recombination centers the number N of electrons in eqn (1) must be replaced by the number N_T of recombination centers[6]. Moreover, for the distributed form corresponding to eqn (2) $I(x)$ must be replaced by the net current $\Delta I(x)\,\Delta x$ generated in the section Δx at x. We then obtain for the noise generated in the section Δx

$$\Delta S_I(x,f)\,\Delta x = \frac{[\Delta I(x)\,\Delta x]^2\alpha_H}{f^{\gamma}N_T(x)\,\Delta x}, \tag{5}$$

where $N_T(x)\,\Delta x$ is the effective number of recombination centers in the section Δx at x. But, if τ is the time constant associated with the generation–recombination process

$$|\Delta I(x)|\,\Delta x = eN_T(x)\,\Delta x/\tau \tag{6}$$

is entirely due to g–r processes where τ can be

*Now at Electrical Engineering Department, University of South Florida, Tampa, FL 33620, U.S.A.

B14

determined from the h.f. device admittance[5,7]. Substituting eqn (6) into eqn (5) yields

$$\Delta S_I(x,f)\,\Delta x = \frac{e\alpha_H}{f^\gamma\tau}\,|\Delta I(x)|\,\Delta x \qquad (7)$$

and hence by integration

$$S_I(f) = \frac{e\alpha_H}{f^\gamma\tau}\int_0^d |\Delta I(x)|\,\mathrm{d}x = \frac{e\alpha_H\,|I|}{f^\gamma\tau}. \qquad (8)$$

Comparing eqn (8) with eqn (4) shows that eqn (4) is correct and that $f(V) = 1$.

Since the above approach is derived by slicing the device up into sections Δx, it is generally valid, holding both for volume and surface g–r processes.

2. EXPERIMENTS ON $Hg_{1-x}Cd_xTe$ p–i–n DIODES WITH $x = 0.20$ AT 77 K

Noise measurements were performed on relatively short $Hg_{1-x}Cd_xTe$ p–i–n diodes with cadmium molar fraction $x = 0.20$ at 77 K. It was found that $[S_I(f) - S_I(\infty)]/|I|$ was nearly independent of bias for $-100\,\mathrm{mV} < V < 0$; here $S_I(\infty)$ is the shot noise of the devices. This is equivalent to what was found in long n^+p $Hg_{1-x}Cd_xTe$ diodes, where $[S_I(f) - S_I(\infty)]/[If(V)]$ was independent of bias. Applying eqn (8) we thus see that α_H/τ is independent of bias. For $V < -100$ mV the noise increased due to pre-breakdown processes; for $V > 0$ the noise also increased due to carrier injection into the i-region.

The time constant τ, determined with the help of the diode admittance method, was found to be 10^{-7} s and was nearly independent of bias. The resulting values of α_H are shown in Fig. 1 and Table 1; they are also nearly independent of bias.

We now turn to the diode admittance. It was shown[5,7] that for relatively short p–i–n diodes the diode itself can be represented by a (g_i, C_i) parallel circuit, where $g_i = \mathrm{d}I/\mathrm{d}V$ and C_i is the diode capacitance. In addition the i-region has a series resistance $R_s(I)$; it decreases with increasing current because of carrier injection (holes and electrons) into the i-region. If an a.c. voltage is applied to the p–i–n diode, the current I, and hence $R_s(I)$, are a.c. modulated. The net effect is that $R_s(I)$ must be replaced by an (R, L) circuit (modulation impedance), where

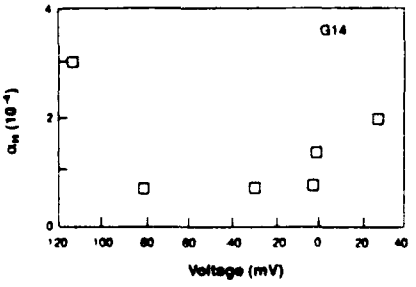

Fig. 1. The Hooge parameter α_H as a function of the diode voltage (diode G-14).

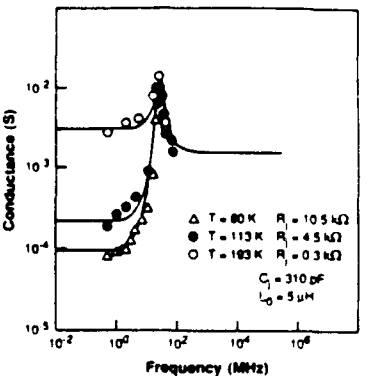

Fig. 2. Conductance of the diode as a function of frequency at different temperatures.

$R = -I\,\mathrm{d}R_s/\mathrm{d}I$ and L is proportional to the carrier lifetime τ. As a consequence the device shows a sharp series resonance (Fig. 2) at the frequency $\omega_0 = (LC_i)^{-1/2}$; from this resonance the life time τ can be determined.

Figures 3 and 4 show $[S_I(f) - S_I(\infty)]$ for diode G-14 as a function of frequency for different bias voltages. The spectra are of the form $1/f^\gamma$ with γ differing significantly from unity. Since quantum $1/f$ noise has a γ-value that is very close to unity[3], it follows that the noise is not of quantum origin. Figure 5 shows γ vs bias for diode G-14.

Since in a p–i–n diode the current flow is by generation–recombination processes, the $1/f$ noise should be associated with these processes. Except perhaps in the cleanest samples, the noise involves traps or recombination centers and $S_I(f)$ should be proportional to the density of these centers. Since the

Table 1

#	V_d (mV)	I_d (μA)	$S_I(f)$ (A^2/Hz)	α ($\tau = 10^{-7}$ s)
M	−0.8	−3.5	2.25×10^{-23}	2.0×10^{-5}
G	−3.0	−3.5	0.95×10^{-23}	1.5×10^{-5}
F	−20	−6.0	4.3×10^{-23}	2.25×10^{-5}
J	−25	−7.0	0.9×10^{-23}	8.0×10^{-6}
K	−30	−10.0	1.0×10^{-23}	3.0×10^{-6}
H	−40	−12.0	0.8×10^{-23}	2.0×10^{-6}

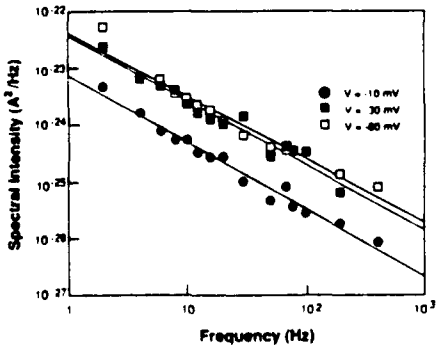

Fig. 3. Noise spectrum under different reverse bias; 10, 30 and 80 mV.

B15

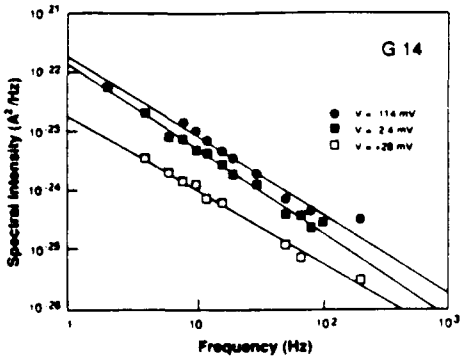

Fig. 4. Noise spectrum under different bias, 2.4, 114 mV (both are reverse biased), and 28 mV (forward bias).

density of the centers will differ from unit to unit, $S_I(f)$ and hence α_H will differ from unit to unit, as experiment indicates (Table 1). Since the spectrum has $\gamma \neq 1$, the noise is not of the quantum $1/f$ noise-type and is non-essential noise. For the $1/f$ noise is proportional to the density of the centers and can be reduced by reducing that density.

The limiting $1/f$ noise is obtained when all recombination centers have been removed; in that case the noise is due to *direct* band to band transitions and has a fundamental nature. It is a form of quantum $1/f$ noise that can be described as follows.

In the generation process an electron and a hole are created simultaneously, each with an average energy $3kT/2$. Therefore the electron mean square velocity is $\overline{v_n^2} = 3kT/m_n^*$ and the hole mean square velocity is $\overline{v_p^2} = 3kT/m_p^*$, where m_n^* and m_p^* are the effective masses. Since $m_n^* \ll m_p^*$, we have $\overline{v_n^2} \gg \overline{v_p^2}$ so that only the electrons give a significant contribution. Hence[5]

$$\alpha_H = \frac{4\alpha_0}{3\pi}\frac{\overline{\Delta v_n^2}}{c^2} = \frac{4\alpha_0}{3\pi}\frac{3kT}{m_n^* c^2} \tag{9}$$

At $T = 77$ K and $x = 0.20$ we have $m_n^* = 0.0073 m_0$, where $m_0 = 9.11 \times 10^{-31}$ kg is the mass of a free electron. Hence $\alpha_H = 1.7 \times 10^{-6}$, which is a factor 100 lower than the lowest α_H value measured so far. It is therefore doubtful whether the quantum limit for p–i–n $Hg_{1-x}Cd_xTe$ diodes will soon be reached.

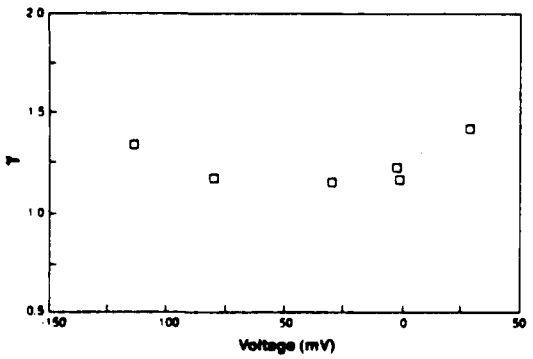

Fig. 5. The exponent γ as a function of the bias voltage for diode G-14.

3. CONCLUSIONS

1. The $1/f$ noise in p–i–n diodes is of the generation–recombination type, involving recombination centers. The noise is proportional to the density of these centers.
2. The best unit measured so far has $\alpha_H \simeq 2 \times 10^{-6}$; the quantum limit lies about a factor 100 lower.
3. A formula for $S_I(f)$ is derived that allows the evaluation of the Hooge parameter α_H from the measured noise.

Acknowledgements—The work was performed under ARO contract DAAG 29-85-K-0235. The p–i–n diodes were supplied by W. A. Radford, Santa Barbara Research Center, Goleta, CA.

REFERENCES

1. F. N. Hooge, *Phys. Lett.* **A-29**, 139 (1969); *Physica* **83B**, 9 (1976).
2. G. Bosman, R. J. J. Zijlstra and A. D. van Rheenen, *Phys. Lett.* **78A**, 385 (1980); **80A**, 57 (1980).
3. K. H. Duh and A. van der Ziel, *IEEE Trans. Electron Devices* **ED-32**, 662 (1985); X. C. Zhu and A. van der Ziel, *IEEE Trans. Electron Devices* **ED-32**, 658 (1985); A van der Ziel, P. H. Handel, X. C. Zhu and K. H. Duh, *IEEE Trans. Electron Devices* **ED-32**, 667 (1985).
4. X. L. Wu, J. B. Anderson and A. van der Ziel, *IEEE Trans. Electron Devices* **ED-34**, 602 (1987).
5. A. van der Ziel, P. Fang, L. He, X. L. Wu, A. D. van Rheenen and P. H. Handel, *J. Vac. Sci. Tech.* **A-7**, In press.
6. A. van der Ziel, *Solid St. Electron.* **32**, 91 (1989).
7. P. Fang and A. van der Ziel, to be published.
8. P. H. Handel, *Phys. Rev. Lett.* **34**, 1492 (1975); *Phys. Rev.* **22**, 745 (1980).

B16

Solid-State Electronics Vol. 32, No. 11, pp. 1039–1042, 1989
Printed in Great Britain.

0038-1101/89 $3.00 + 0.00

BURST-TYPE NOISE MECHANISMS IN BIPOLAR TRANSISTORS

X. L. WU,† A. VAN DER ZIEL, A. N. BIRBAS and A. D. VAN RHEENEN
Department of Electrical Engineering, University of Minnesota, Minneapolis, MN 55455, U.S.A.

(*Received* 27 *March* 1989)

Abstract—Two types of burst noise have been observed in silicon bipolar transistors. They can be characterized by the typical frequency dependence of their current fluctuation spectra. Interestingly, observation of the noise signal in the time domain gives two distinctively different pictures of the bistable waveform. Also, amplification of the noise signal yields different sounds when fed to a speaker. One of the noise spectra is the superposition of $1/f$ noise and a Lorentzian component (burst noise) and the other can be described mathematically as $1/f$ noise modulated by the burst noise. The classification of those two types of burst noise and the mathematical explanation will lead to a better understanding of the bipolar transistor burst noise itself.

1. INTRODUCTION

Bistable current waveforms resembling a random telegraph signal known as burst noise have been reported for the last 30 years. This phenomenon has been observed in forward and reverse biased diodes, bipolar junction transistors, optical isolators and detectors, junction field effect transistors and metal–oxide–semiconductor field effect transistors.

The origin of the burst noise has been attributed to physical mechanisms such as microplasmas related to the dislocations in the crystal, emitter edge dislocations of bipolar transistors, crystallographic defects, generation–recombination (g–r) centers associated with metallic precipitates or extensive defects near the surface of the junction, etc. It has also been established that the burst noise in JFETs is related to point defects in silicon and the burst noise in MOSFETs has been attributed to charge state transitions at traps in the oxide very close to the Si/SiO_2 interface.

The mechanism that causes the burst noise in bipolar transistors is not well understood even though much work has been done in the area. This is due to the poor understanding of the mechanisms for current generation and the spatial nonuniformities in the current flow. However, it is well established that dislocations at the emitter as well as trapping are sources of burst noise and $1/f$ noise. It is the aim of this paper to shine some light on the burst noise originated at the emitter junction of a bipolar transistor as well as its correlation with the locally produced $1/f$ noise.

2. MECHANISMS OF BURST NOISE

Much work has been done in the area of low-frequency noise of silicon planar devices. Various authors have attributed the low-frequency noise to dislocations at the emitter–base junction. Morrison[1] predicted that it could be caused by the dislocations in the bulk whereas Bess[2] attributed the noise to dislocations that communicated with the silicon surface and thus allowed impurity atoms to diffuse to the silicon surface. Green[3] and Jordan have established that the low-frequency noise is affected by the dislocations only when they emerge at a silicon surface near the junction.

Emitter-phosphorus diffusion normally used for fabrication of silicon planar n–p–n transistors may create two kinds of dislocations: (i) diffusion-induced dislocations, which appear inside diffused emitter areas, and (ii) emitter-edge dislocations, which appear around the planar edges of the diffused emitter areas, usually after the emitter oxidation step. While researchers in the past have attributed the low-frequency noise of silicon planar n–p–n transistors to both diffusion-induced dislocations and emitter-edge dislocations[4], studies of modern planar devices show that the low frequency noise in n–p–n transistors is affected only by emitter-edge dislocations[5]. The effect is enhanced rapidly in n^+ emitters for emitter doping densities larger than $4.3 \times 10^{20}\,cm^{-3}$[6].

We can now discriminate between various mechanisms responsible for the low-frequency noise. If the emitter doping exceeds the $4.3 \times 10^{20}\,cm^{-3}$ value, then there are a number of edge dislocations. It is also well known that considering the regularity of the pulse amplitude (about 10^{-8} A) associated with the burst noise, it is inconceivable that we are dealing with the statistics of a large number of carriers. It seems more feasible that a single carrier controls the flow of 10^8 carriers in a reasonably periodic fashion producing a pulse duration about 1 ms. Indeed, a defect associated with the edge of the emitter–metallurgical junction can produce burst noise

†Present address: Unisys Corp., San Diego, CA 92127, U.S.A.

B17

due to the modulation of the current. The modulation is caused by the change in occupancy of a generation–recombination center located in the space-charge region adjacent to the defect[7]. Furthermore, when a lot of dislocations are present trapping of carriers can occur at that point. If there is a uniform distribution of the time constants associated with the trapping and detrapping then the resulting noise spectrum is proportional to $1/f$. In conclusion we see that in the case of a heavily doped emitter the dislocations produce low-frequency noise. The trapping effect of one of those dislocations (the closest to the metallurgical junction with the appropriate time constant) may give burst noise and the superposition of the others may be giving $1/f$ noise if there is a uniform distribution of their time constants. Both the burst and the $1/f$ type of noise are due to the dislocations, they originate from the same region of the device and since they are due to the same physical mechanism they are related and the one type modulates the other.

If dislocations are not present at the emitter edge then the burst noise can be produced at the space-charge region of the device if a trap is present[7]. Then the burst modulation current will be given by $\Delta I_B = q^2 I/2\pi\epsilon kT(\sqrt{\pi A})$[7] where all the quantities have the normal meaning, and A is the effective cross sectional area at a forward bias junction with a boundary at the surface (planar BJT). In addition to the burst noise in that case we can have $1/f$ noise associated with the emitter–base junction recombination current which is not transmitted to the collector. In modern transistors we rather have diffusion $1/f$ noise and in good low noise devices mobility fluctuation $1/f$ noise[8]. In this case the burst noise and the $1/f$ noise come from the same region but they are due to different mechanisms; so they are unrelated, act in parallel and their spectra are superimposed.

3. SWITCHING MODEL OF THE BURST NOISE

We now turn to the formulation of the two cases of the joint appearance of $1/f$ and burst noise mechanisms described in Section 2. Burst noise is a form of g–r noise. It consists typically of random current pulses of variable duration and equal height, but sometimes the random pulses seem to be superimposed upon each other. The random switch model[8] considers that the burst noise is caused by an assembly of random switches, each carrying a fixed current when closed and no current when open. During the time interval dt let an open switch have the probability dt/τ_1 of closing, and a closed switch a probability dt/τ_2 of opening. Let furthermore $H(t)$ be a random source function describing spontaneous fluctuations in the rate at which switches open or close.

At a given time t N_1 switches are open and N_2 switches are closed. Develop around the equilibrium values we find: $N_1 = \bar{N}_1 + \Delta N_1$ and $N_2 = \bar{N}_2 + \Delta N_2$. The rate at which open switches will close is given by:

$$\frac{d(\bar{N}_1 + \Delta N_1)}{dt} = -(\bar{N}_1 + \Delta N_1)\frac{1}{\tau_1} + [\bar{N}_2 - \Delta N_1]\frac{1}{\tau_2} + H(t) \quad (1)$$

where $H(t)$ is a random source function describing spontaneous fluctuations in the rate at which switches open or close.

Because of the constraint on $\bar{N}_1$ and $\bar{N}_2(\bar{N}_1 + \bar{N}_2 = N =$ total number of switches) we see that $\Delta N_1 = -\Delta N_2$. Additionally $d\bar{N}_1/dt = 0$ by definition. Therefore eqn (1) reduces to:

$$\frac{d\,\Delta N_1}{dt} = -\frac{\Delta N_1}{\tau_0} + H(t); \quad \tau_0^{-1} = \tau_1^{-1} + \tau_2^{-1} \quad (2)$$

and

$$\frac{\bar{N}_1}{\tau_1} = \frac{\bar{N}_2}{\tau_2}$$

from which we find

$$\bar{N}_1 = N\frac{\tau_1}{\tau_1 + \tau_2}, \quad \bar{N}_2 = N\frac{\tau_2}{\tau_1 + \tau_2}$$

and

$$\Delta\bar{N}_1^2 = N\frac{\tau_1\tau_2}{(\tau_1 + \tau_2)^2}$$

since we have a binomial distribution.

Once we find the rate equation (eqn 2), the spectral intensity of the fluctuations in the number of open switches is computed by Fourier transforming eqn (2) and averaging. The spectrum will be

$$S_{\Delta N1} = \frac{S_H\tau_0^2}{1 + \omega^2\tau_0^2}. \quad (3)$$

In this equation S_H is the spectrum of the driving force $H(t)$.

4. BURST NOISE AND $1/f$ NOISE

(a) In Section 3 eqn (1) describes the burst noise produced by the rate fluctuations

Let's now turn to the application of this equation to an electronic device where carrier number fluctuations ($1/f$ noise) appear along with the burst noise. We consider that an $1/f$ modulation occurs of the number of carriers (N_1 open switches) along with the burst noise modulation $H_b(t)$ and let this be described by a source function $H_f(t)$. Then eqn (1) is modified to:

$$\frac{d(\Delta N_1 + \bar{N}_1)}{dt} = -[\bar{N}_1 + \Delta N_1 + H_f(t)]\frac{1}{\tau_1} + [\bar{N}_2 - \Delta N_1 - H_f(t)]\frac{1}{\tau_2} + H_b(t) \quad (4)$$

The d.c. part of this equation is the same as that described in eqn (2). Then the time dependent part of

B18

eqn (4) may be written

$$\frac{d\Delta N_1}{dt} = -\frac{\Delta N_1}{\tau_0} - \frac{H_f(t)}{\tau_0} + H_b(t);$$

$$\tau_0^{-1} = \tau_1^{-1} + \tau_2^{-1} \quad (5)$$

Keeping in mind that $H_f(t)$ and $H_b(t)$ are independent and after Fourier transforming we get:

$$S_{\Delta N_1}(f) = \frac{S_H(0)\tau_0^2 + S_f(f)}{1+\omega^2\tau_0^2} = \frac{A\tau_0^2 + B/f}{1+\omega^2\tau_0^2} \quad (6)$$

since $S_H(0) = A$ and $S_f(f) = B/f$.

The resulted spectrum is a modulation of the Lorentzian (burst noise) by the $1/f$ noise.

(b) $1/f$ noise and burst (Lorentzian) noise occur in parallel and have independent spectra because they come from fluctuations in independent parameters

The time dependent Langevin Equation for the burst noise is then:

$$\frac{d\,\Delta N_1}{dt} + \frac{\Delta N_1}{\tau_0} = H_b \quad (7)$$

where: H_b is the burst noise source; after Fourier transforming and averaging we get the first term of the right hand side of eqn (3) where we replace S_H by S_{Hb}. Furthermore, if we consider that a $1/f$ noise source which corresponds to an independent process occurring either in the same or in a different region of the device then a $1/f$ source H_f has to be superimposed on the burst noise. This $1/f$ response $\{S_M(f) = B/f\}$ is independent of the burst noise and will give the second term of the right hand side of eqn (8).

The total spectrum will be:

$$S(f) = \frac{A^2\tau^2}{1+\omega^2\tau^2} + \frac{B}{f}, \quad (8)$$

In this case the resulting spectrum is a superposition of the burst noise and the $1/f$ noise.

5. EXPERIMENT AND DISCUSSION

Measurements of the electric noise in two different devices illustrate nicely the different spectra. The spectrum of the collector-current of a discrete silicon BJT is shown in Fig. 1. The solid line in this figure is the best fit using eqn (6). At the high frequency end the spectrum reaches the thermal noise limit of 3.8×10^{-19} A²/Hz. The most interesting feature of this spectrum is that it decreases as f^{-2} at larger frequencies until it reaches the thermal noise floor. The effect is more dramatic when one subtracts the thermal noise floor from the data. This is done for the last 6 data points and indicated by the open squares in Fig. 1. The f^{-2} dependence is even more pronounced. This observation is in accordance with the expression in eqn (6). At higher frequencies the right hand side of eqn (6) is dominated by the first term and falls off as f^{-2}.

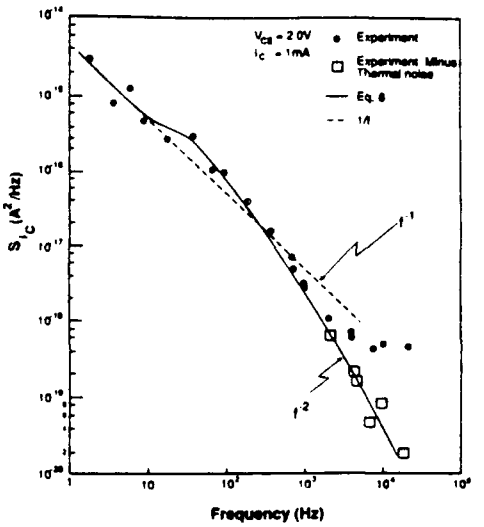

Fig. 1. The experimental spectrum (●) of the discrete silicon BJT and the theoretical spectrum following eqn (6) (—). The open squares (□) are experimental data points with the thermal noise floor subtracted. At the high frequency end the spectrum falls off faster than f^{-1}.

As an example of the second type of burst noise (Section 4b) we present the fluctuation spectrum of the base current of a BJT on a chip, in Fig. 2. The spectrum behaves as predicted by eqn (8). By inspecting eqn (8) we find that at the higher frequencies it should fall off as f^{-1}. We observe this phenomenon in Fig. 2.

When comparing the two equations (6 and 8) there is no difference between the spectra at the low-frequency end (provided that we choose the same values for the constants A, B and τ_0). However, the difference between the two models can be observed at the high-frequency end of the spectra. Spectra following

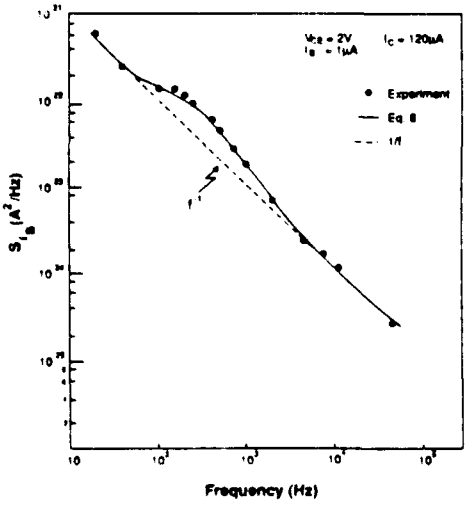

Fig. 2. The experimental spectrum (●) of the BJT on the chip and the theoretical curve following eqn (8). At the high frequency end the spectrum falls off as f^{-1}

B19

Fig. 3. The oscilloscope picture of the burst noise of type a. The duration of the total time signal is 40 ms.

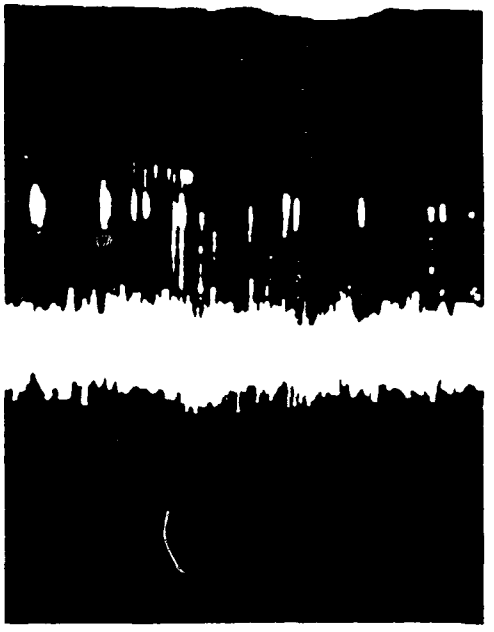

Fig. 4. The oscilloscope picture of the burst noise type b. The duration of the total time signal is 40 ms.

eqn (6) will fall off as f^{-2} and spectra following eqn (8) will fall off as f^{-1}.

In the time domain the two burst noise types have two distinct patterns as is shown in Figs 3 and 4. The noise signal in the time domain (Fig. 3) shows two levels with noise in each level. The duration of the total time trace is 40 ms. The duration of the up pulse is of the same order as the one of the down pulse. This is in contrast with the time signal of the chip transistor which we depict in Fig. 4. On this photograph we see a broad noise base line and short pulses on top of it. When this signal was amplified and fed to a speaker a distinctive popping sound could be heard. This phenomenon showed itself only with the chip transistor and not with the discrete one.

The discrete device has a heavily doped emitter and we expect a lot of dislocations in the emitter–base space-charge region. Therefore, we were not surprised to see the noise spectrum to follow eqn (6) (see Section 2), apparently the chip transistor did not appear to have too many dislocations and therefore shows a different noise spectrum, more in line with the predictions of eqn (8).

6. CONCLUSION

The observation of two distinctly different burst noise spectra, mixed with $1/f$ noise, as measured in two different devices is explained by assuming either a modulation of the $1/f$ noise by the burst noise indicating a common source for the fluctuations or a superposition of the two noise types indicating unrelated sources for the fluctuations.

Acknowledgement—The authors would like to thank M. Mihaila for providing one of the devices.

REFERENCES

1. S. R. Morrison, *Phys. Rev.* **104**, 619 (1956).
2. L. Bess, *Phys. Rev.* **105**, 72 (1956).
3. D. Green and A. G. Jordan, *Int. J. Electron.* **27**, 159 (1969)
4. Nishida, *IEEE Trans.* **ED-20**, 221 (1973).
5. N. D. Stojadinovic, *Electron. Lett.* **15**, 340 (1979).
6. M. Mihaila and K. Amberiadis, *Solid-St. Electron.* **26**, 109 (1983).
7. S. T. Hsu, R. J. Whittier and C. A. Mead, *Solid-St. Electron.* **13**, 1055 (1970).
8. A. van der Ziel, *Noise in Solid State Devices and Circuits*. Wiley Interscience, New York (1986).
9. X. L. Wu, Ph.D. thesis, University of Minnesota (1987).

B20

1/f noise in double-heterojunction AlGaAs/GaAs laser diodes on GaAs and on Si substrates

R. Z. Fang,[a] A. D. van Rheenen, A. van der Ziel, and A. C. Young
Electrical Engineering Department, University of Minnesota, Minneapolis, Minnesota 55455

J. P. van der Ziel
AT&T Bell Laboratories, Murray Hill, New Jersey 07974-2070

(Received 15 September 1989; accepted for publication 6 June 1990)

Low-frequency electrical current noise measurements are reported on double-heterojunction AlGaAs/GaAs laser diodes fabricated on GaAs and on Si substrates. The noise spectra show a frequency dependence proportional with $f^{-\gamma}$ with γ close to unity. The spectral intensity is proportional to the current for smaller currents (< 0.1 mA) and levels off at larger currents (> 1 mA). The diodes built on the GaAs substrate are 50 times less noisy than the ones built on the Si substrate. This effect is attributed to the fact that the density of dislocations at the Si interface is much larger than at the GaAs substrate/device interface.

I. INTRODUCTION

The data rates needed in communications systems have increased to the point where the only viable links are optical. The interest in these systems has grown enormously in the last several years. These links consist of semiconductor laser with associated driver and perhaps multiplexing and demultiplexing circuitry, optical fibers, and semiconductor detectors with their associated amplifier and possibly multiplexing or demultiplexing circuitry. The level of noise generated in the components is crucially important to know particularly in long-distance systems where signal levels can be low and distance between repeaters is determined by the noise.

With the emergence of lasers, and semiconductor laser diodes in particular, as useful light sources there has been an enormous interest in the description of the operation of the lasers. The noise, specifically in the light output, has been the subject of a large body of publications that appeared starting in the 1960's. Different formalisms to describe this quantum noise were developed. The two basic methods are the Langevin method and the density matrix method. Exponents of the former are quantum-mechanical rate equations with fluctuating terms,[1,2] the Fokker–Planck equation for the photon amplitude probability density,[3] and the van der Pol equation with a noise source as the driving force.[4,5] The density matrix method has been studied by Scully and Lamb[6] and Lax[7] who established that both formulations yield the same result when the photon number (i.e., pump rate) is large enough. Corrections for small photon numbers were discussed by Smith.[8]

Because the Q factor is relatively low in a semiconductor laser as compared to gas lasers and solid-state lasers the quantum noise will be of enormous importance in such applications where semiconductor lasers are an integral part of optical fiber communication systems. Components of these systems include transmitters, modulators, optical amplifiers, local oscillators, and detectors. Yariv[9] identifies three noise quantities, the field spectrum, the intensity spectrum, and the frequency deviation spectrum (phase noise), that describe the fluctuations in the laser oscillation field.

Almost all of these studies deal with the laser field and hardly any work is done to relate the fluctuations in the electrical current to fluctuations in the laser output. Yamamoto[10] made the observation that the spectrum of the frequency deviations seems to be limited by the electrical current noise spectrum at small frequencies.

For purposes of easy integration of silicon electronics with optical devices people are investigating the possibilities to fabricate GaAs base structures on Si substrates. With this in mind we set out to study the electrical noise properties of identical laser diode configurations composed on Si and GaAs substrates.

II. EXPERIMENTS AND RESULTS

The device structure we investigated is presented in Fig. 1 where we indicate the layer configuration and layer thicknesses. These double-heterojunction injection AlGaAs/GaAs devices are designed to have a low threshold voltage, a high quantum efficiency, and to operate at room temperature. Diodes No. 1 and No. 3 were grown on silicon substrates by metalorganic chemical vapor deposition whereas diodes No. 5, No. 6, and No. 7 were fabricated on gallium-arsenide substrates using the same growth technique.

The current-voltage characteristics of all the diodes are shown in Fig. 2. All of these curves can be represented by

$$I = I_s \exp[(V - IR_s)/nV_T]. \quad (1)$$

In Eq. (1) I is the current, I_s the reverse saturation current, V the voltage, R_s the diode series resistor, n the ideality factor, and V_T the thermal voltage ($k_B T/q$). Table I gives a listing of the values of the ideality factor and the series resistance of each diode.

During the electrical noise measurements the diodes were connected in series with a 10-kΩ resistor which allowed us to measure the current noise produced by the lasers. The signal is fed into a low-noise amplifier and passed on to a dynamic signal analyzer. The measurement technique is designed to allow for the noise produced by the amplifier and

 0021-8979/90/204087-04$03.00

B21

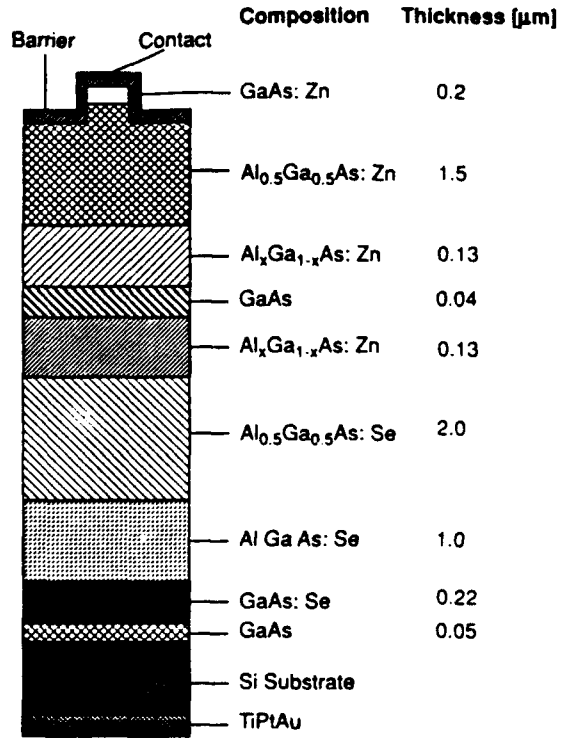

FIG. 1. Structure of the laser diodes.

possible nonflatness of the gain of the amplifier over the frequency band. The current noise spectra are measured in the range from 10 Hz to 100 kHz.

Typical examples of the spectral intensity of the current fluctuations of both types of diodes, diode No. 1 on a Si substrate and diode No. 5 on a GaAs substrate, are presented in Fig. 3. The noise spectra are measured when the currents are as indicated in the figure. Even when we measured at frequencies up to 100 kHz did we not see any significant

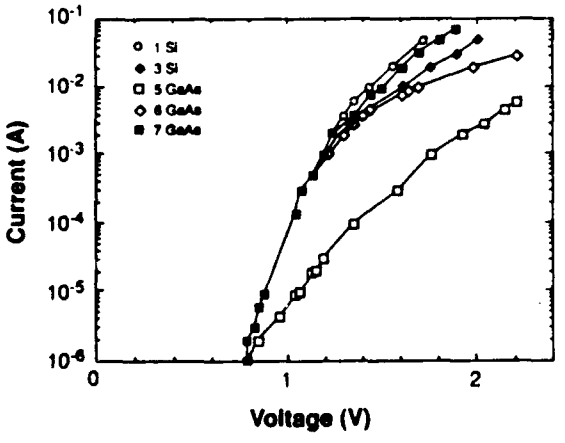

FIG. 2. Current-voltage characteristics of the diodes.

TABLE I. Collected values of the series resistance (R_s) and ideality factor (n) of the diodes.

Diode	R_s (Ω)	n
1	11	2.0
3	21	2.0
5	111	3.5
6	31	2.0
7	14	2.0

leveling off of the spectra. This indicates that the shot noise associated with the carriers crossing the p-n junction and the thermal noise associated with the series resistance R_s of the diodes are well below the measured excess noise in this frequency range. One would expect the shot noise and thermal noise contributions to add according to

$$S_i = \frac{R_d^2}{(R_d + R_s)^2} 2qI + \frac{R_s^2}{(R_d + R_s)^2} \frac{4k_B T}{R_s}. \tag{2}$$

In this equation R_d is the small signal resistance of the diode:

$$R_d = \frac{dV}{dI} = \frac{nV_T}{I}. \tag{3}$$

For small currents (R_d is large) $S_i = 2qI$ whereas for large currents (R_d is small) $S_i = 4k_B T/R_s$. The measured excess noise was much larger than this white noise.

The low-frequency parts of the spectra exhibited a frequency dependence of $f^{-\gamma}$ with γ close to 1, within 10%. In Fig. 4 we present the value of the spectral intensity extrapolated to $f = 1$ Hz divided by the current for both laser diodes No. 1 and No. 5. Two interesting observations can be made: (i) the value of $S_i(1\text{ Hz})/I$ for the laser built on the GaAs substrate (diode No. 5) is much smaller (factor of 50) than the value of $S_i(1\text{ Hz})/I$ for the diode built on the Si substrate over the whole range of currents (1 μA–10 mA); and (ii) the relative noise is constant up to ~1 mA and then starts to decrease for both diodes.

III. DISCUSSION

In order to be able to compare the magnitude of the $1/f$ noise produced by different types of devices the following expression[11] is often used:

$$S_i(f) = \alpha_H I^2/fN. \tag{5}$$

In this equation N is the number of carriers in the device and α_H is a dimensionless parameter that measures the noisiness of the device. This parameter is defined by Eq. (5). In Ref. 12 it is shown that this expression can be rewritten as

$$S_i(f) = \alpha_H qI/f\tau, \tag{6}$$

where it is assumed that the noise is produced in the vicinity of the lasing medium. In this expression the $1/f$ noise is assumed to be due to a distribution of recombination centers and τ is the lifetime of the minority carriers. Equation (6) predicts the current dependence that we found for the low-frequency noise in our diodes (see Fig. 4), at least for the

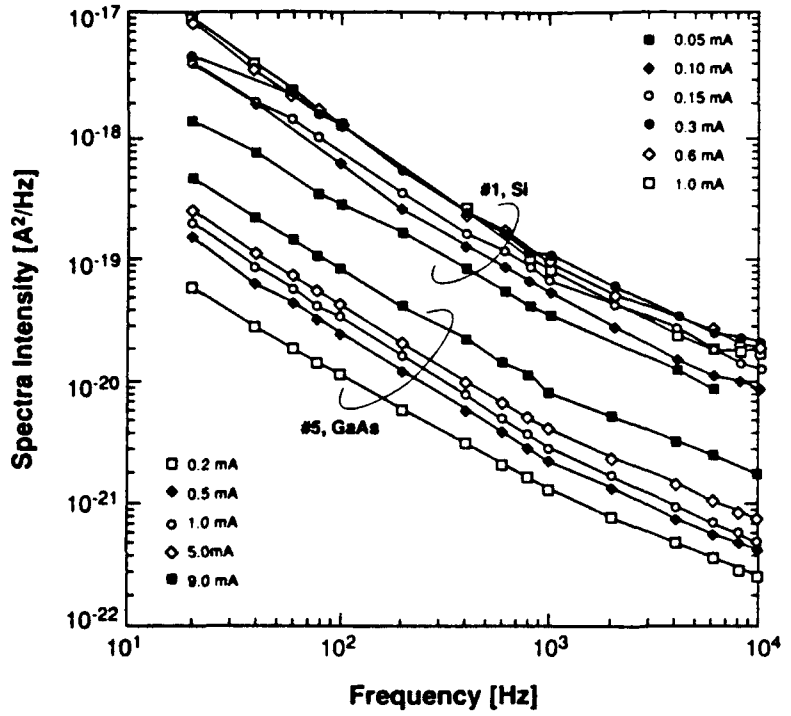

FIG 3 Spectral intensity of the current fluctuations of a typical diode on a Si substrate and of a typical diode on a GaAs substrate for different current.

smaller currents (<0.1 mA). Another way of looking at it is to say that α_{H}/τ [see Eq. (6)] is independent of the current for small currents and decreases for larger currents (>1 mA). If anything, one would expect the lifetime of the carriers to be reduced when more carriers are injected as the current is increased. This would increase the ratio α_{H}/τ. Therefore, we must conclude that α_{H} is decreasing as the current increases. A similar effect was observed in Si n^{+}-γ-n^{+} and p^{+}-π-p^{+} structures.[13]

More significant is that our data indicate that diodes built on GaAs substrates are 50 times quieter than identical structures built on Si substrates. It is known that the dislocation density at the Si/GaAs interface is much larger than at the GaAs/GaAs interface. Since the current is flowing vertically through the device (Fig. 1) it is not surprising that generation-recombination processes show up in the noise. However, this observation cannot be quantified in terms of Eq. (6) since the expression used for the current $I = qN/\tau$ is applicable to the diode region, not to the device-substrate interface region.

IV. SUMMARY

We have reported here electrical current noise measurements that were taken on identical double-heterojunction, low-threshold voltage, high-quantum-efficiency AlGaAs/GaAs laser diodes fabricated on Si and GaAs substrates.

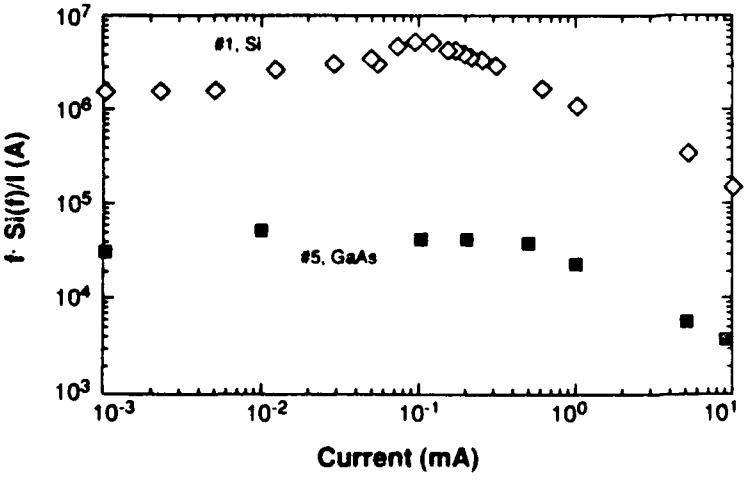

FIG 4 Extrapolated value of the noise spectra at 1 Hz divided by the current as a function of the current both for a diode on a Si substrate and for a diode on a GaAs substrate

The main observations are as follows: (i) The spectral intensity of the current fluctuations scale with the current for smaller (<0.1 mA) values of the current whereas it levels off for larger currents. This is true for devices built on both substrates. (ii) The diodes built on the Si substrate are 50 times noisier than the ones built on GaAs substrates in the range of measured currents ($1\ \mu$A–10 mA).

ACKNOWLEDGMENT

This work was partly supported by ARO Contract No. DAAL03-89-K-0009.

[1] D. E. McCumber, Phys. Rev. **141**, 306 (1966).
[2] H. Haug, Phys. Rev. **184**, 338 (1969).
[3] H. Risken, Z. Phys. **196**, 85 (1965).
[4] H. Haug and H. Haken, Z. Phys. **204**, 262 (1967).
[5] A. Yariv and W. M. Caton, IEEE J. Quantum Electron. **QE-10**, 509 (1974).
[6] M. O. Scully and W. C. Lamb, Jr., Phys. Rev. **179**, 368 (1968).
[7] M. Lax, J. Quantum Electron. **7**, 37 (1967); Phys. Rev. **157**, 213 (1967).
[8] W. A. Smith, Opt. Commun. **12**, 236 (1974).
[9] A. Yariv, *Quantum Electronics*, 3rd ed. (Wiley, New York, 1989).
[10] Y. Yamamoto, IEEE J. Quantum Electron. **QE-19**, 34 (1983); **QE-19**, 47 (1983).
[11] F. N. Hooge, Phys. Lett. A **29**, 139 (1969); Physica **83B**, 9 (1976).
[12] A. van der Ziel, Proc. IEEE **76**, 233 (1988).
[13] G. Bosman, R. J. J. Zijlstra, and A. D. van Rheenen, Physica B + C **112**, 88 (1982).
[14] D. J. Jackson, J. Y. Josefowicz, D. B. Reusch, and D. L. Persedrini, Proc. SPIE **839**, 161 (1987).
[15] S. J. Wojtczuk, J. M. Ballantyne, S. Wanuga, and Y. K. Chen, IEEE J. Lightwave Technol. **5**, 1365 (1987).
[16] D. L. Rogers, J. M. Woodall, G. D. Pettit, and D. McInturff, IEEE Electron Dev. Lett. **9**, 515 (1988).
[17] M. Makiuchi, H. Hamagueli, T. Kumai, M. Ito, O. Wada, and T. Sakurai, IEEE Electron Dev. Lett. **EDL-6**, 634 (1985).
[18] W. T. Tsang, J. C. Campbell, and G. J. Qua, IEEE Electron Dev. Lett. **EDL-8**, 294 (1987).
[19] A. van der Ziel, *Noise in Measurements* (Wiley, New York, 1976).
[20] L. Zenterro, IEEE J. Lightwave Technol. **7**, 39 (1989).
[21] H. E. Lassen, P. B. Hansen, and K. E. Stubkjaer, IEEE J. Lightwave Technol. **6**, 1559 (1988).

Low-frequency noise in small InGaAs/InP *p-i-n* diodes under different bias and illumination conditions

L. He, Y. Lin, A. D. van Rheenen, A. van der Ziel, and A. Young
Electrical Engineering Department, University of Minnesota, Minneapolis, Minnesota 55455

J. P. van der Ziel
AT&T Bell Laboratories, Murray Hill, New Jersey 07974-2070

(Received 4 June 1990; accepted for publication 31 July 1990)

Low-frequency noise measurements are reported on small InGaAs/InP *p-i-n* photodiodes under different bias and illumination conditions. In the first experiment measurements were taken when the diodes were reverse biased and illuminated with incandescent light. At high frequencies the noise is shot noise and at low-frequencies the noise has a spectrum proportional to f^{γ} with $\gamma = -1.0$ for one set of two devices and $\gamma = -0.8$ for another set of two devices. At low-frequencies the spectral noise intensity is proportional to the current squared. In a second experiment the diodes were forward biased (no illumination) and the spectral intensity of the low-frequency noise was proportional to the current. Under these bias conditions it was possible to extract the parameter α_H. The obtained values for this parameter are not compatible with quantum $1/f$ noise but do seem to coincide with values related to $1/f$ noise due to recombination centers.

I. INTRODUCTION

In this paper we report electrical noise measurements on small (75-μm-diam) *p-i-n* InGaAs/InP photodiodes designed to be used in optical communication systems. In certain applications the sensitivity of the photodetectors might be limited by the noise and it is therefore of interest to quantify the noisiness of the detectors to be able to compare the noise performance of different device structures. The magnitude of the noise might for instance determine the number of repeater stations necessary to send a signal a certain distance. In addition, measurements of the noise of devices with different structures or as a function of the bias will reveal the preferred device configuration or the optimum operating conditions. With this in mind we have set out to investigate the bias dependence of the current noise of two batches of two different devices.

II. EXPERIMENTS AND RESULTS

A. Illuminated, reverse biased

In this first set of experiments the diodes were subjected to reverse-bias voltages of -0.5 and -3 V. The diodes were illuminated through the InP substrate with incandescent light. The magnitude of the current (1–14 μA) was controlled by the amount of light we shined on the diode. To be able to measure the voltage noise due to the current fluctuations in the diode a resistor R_B (10 kΩ) was connected in series with the diode. This voltage signal is fed into a low-noise amplifier and passed on to a spectrum analyzer. When calculating the spectra allowance was made for the noise produced by the amplifier.

In Fig. 1 we present the current noise spectra of the illuminated diode D_1 biased at $V = -3$ V. The spectra were measured for different currents: 1, 3, 5, 7, and 10 μA. At low frequencies the spectra are proportional to f^{γ} with γ very close (within 6%) to -1. The magnitude of this component of the noise is proportional to the current squared. These results are summarized in Table I.

At higher frequencies the spectra are independent of the frequency and are very well described by

$$S_I(\infty) = 2qI + 4k_BT/R_B. \tag{1}$$

In this equation $S_I(\infty)$ is the spectral intensity at high frequencies, q the electronic charge, I the current, k_B is Boltzmann's constant, and T is the ambient temperature.

In Fig. 2 the current spectra of diode L_1 are plotted. The diode was also biased at -3 V and the light intensity was controlled so that the currents were 0.5, 1.0, 5.0, and 10.0 μA. The spectra seem to have the same shape as the spectra of diode D_1 with the main difference being that the slopes of the low-frequency components are equal to -0.83 ± 0.01. The high-frequency parts of the spectra are again well described by Eq. (1). In Fig. 2 the thermal noise of resistor R_B has already been subtracted from the spectra for $I = 0.5$ and 1.0 μA but not for the other two current values. This allows us to better estimate the magnitude of the low-frequency part of the spectra. Again, the magnitude of the low-frequency part of the spectra scales with the current squared.

From Fig. 3 it is clear that the influence of the bias voltage in the range from -0.5 to -3 V on the spectra is very small. This result presented here for diode L_1 is representative of all four diodes.

In Table I we summarized the significant results we obtained from measuring the noise spectra of all four diodes under reverse bias: D_1, D_2, L_1, and L_2. For each diode we measured the spectra for at least five different currents in the range from 0.5 to 14 μA. For each current we calculated the normalized magnitude, $S_I(1\text{ Hz})/I^2$, and the slope γ and then averaged these values over the currents. The most significant observation to be made is the difference in the slopes of the low-frequency parts of the spectra.

 0021-8979/90/225200-05$03.00

B25

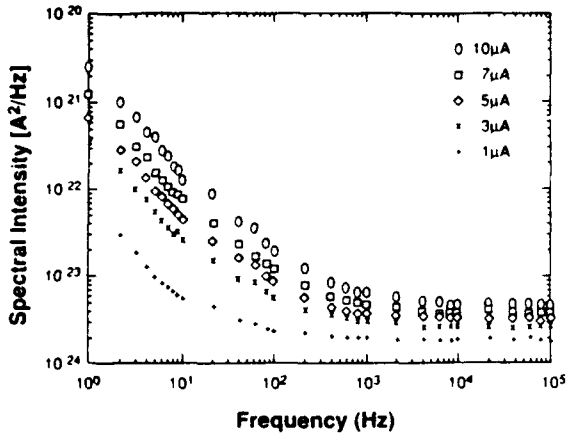

FIG. 1. Current noise spectra of the reverse-biased and illuminated diode D_1 for different currents.

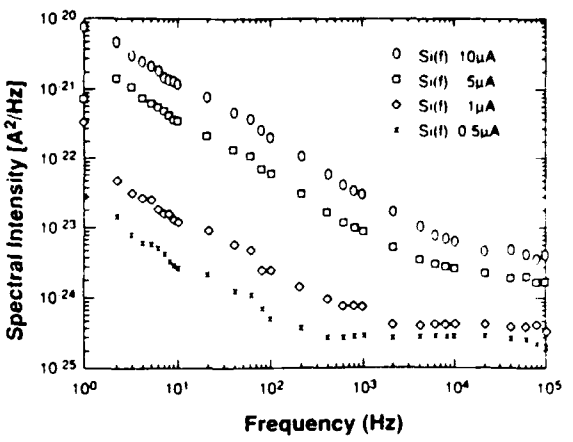

FIG. 2. Current noise spectra of the reverse-biased and illuminated diode L_1 for different currents. In order to be able to better estimate the magnitude of the low-frequency part of the spectra it was necessary to subtract the contribution of the thermal noise of the bias resistor only from the two small-current spectra.

The exponent of the spectra of both diodes D_1 and D_2 are very close to -1 whereas the exponents for diodes L_1 and L_3 are both close to -0.8. Additionally, the normalized magnitude of the spectra is smaller for diodes D_1 and D_2 by about a factor of 4 than it is for diodes L_1 and L_3. This is also obvious from Fig. 4 where we present the spectral intensity at $f = 1$ Hz versus the current for the four devices. The solid line indicates a proportionality with the current squared. The spectral intensities of diodes L_1 and L_3 are almost identical and larger than the noise of diodes D_1 and D_2. The noise of diode D_2 is about an order of magnitude smaller than that of diodes L_1 and L_3.

B. Not illuminated, forward biased

In this second set of experiments the diodes were kept in the dark and a forward voltage was supplied so that the currents would be equal to the ones during the first experiments. In Figs. 5 and 6 the current spectra of diodes D_1 and L_1 are presented, respectively, for different currents. The general shape of the spectra is very similar to what we found when the diodes were reverse biased. The high-frequency parts of the spectra follow Eq. (1) and at smaller frequencies we observe a frequency dependence proportional to f^{γ} where $\gamma = -1.0$ for the spectra of diode D_1 and $\gamma = -0.8$ for the spectra of diode L_1. The magnitude of the low-frequency noise is linearly proportional with the current. This is in contrast to what we observed for the reverse-biased diode spectra. Figure 7 shows this current dependence of the noise spectra for three of the diodes. By the time we took the forward-biased data diode D_2 had expired. The spread in the magnitude of the noise is smaller when compared with the previous experiment. Some of these observations are summarized in Table II where we give the average values of the current spectra at 1 Hz divided by the current as well as the average of the slope of the low-frequency parts of the spectra.

TABLE I. The measured average noise intensity at 1 Hz [$S_I(1\text{Hz})$] of the diodes under *reverse* bias and illumination, normalized by the square of the current. The slope of the measured low-frequency spectra is γ. The entries in the table are averaged over at least five different currents ranging from 1 to 14 μA.

Diode No.	$S_I(1\text{Hz})/I^2(10^{-11}\text{ Hz}^{-1})$	γ
D_2	0.7 ± 0.1	-0.99 ± 0.03
D_1	2.6 ± 0.4	-0.99 ± 0.06
L_1	8.9 ± 0.8	-0.83 ± 0.01
L_3	9.8 ± 0.8	-0.80 ± 0.03

III. DISCUSSION

The most remarkable result is that the exponents (γ) of the low-frequency parts of the spectra are -1.0 for diodes D_1 and D_2 both under forward and reverse bias and this exponent is -0.8 for diodes L_1 and L_3, again both under forward and reverse bias. Intriguing as well is the fact that the magnitudes of the noise spectra when the

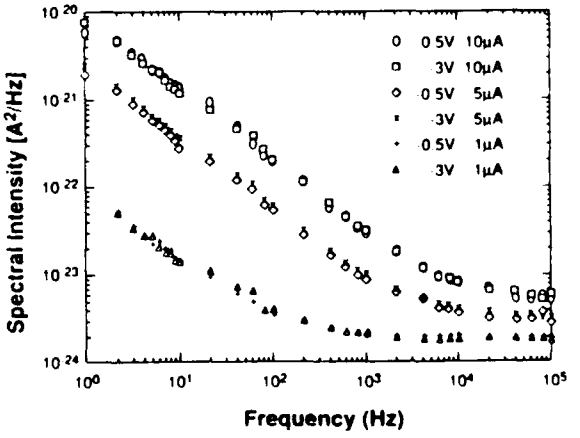

FIG. 3. Current noise spectra of the reverse-biased and illuminated diode L_1 for different currents and different voltages.

B26

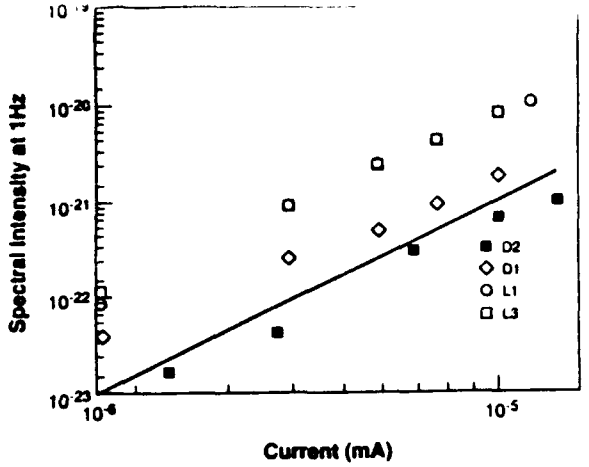

FIG. 4. Current dependence of the noise intensity at 1 Hz for the four diodes under reverse bias and illumination. The slope of the line is + 2.

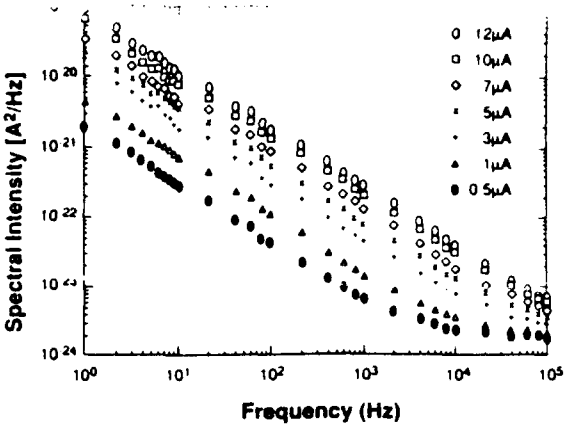

FIG. 6. Current noise spectra of the forward-biased (no illumination) diode L_1 for different currents.

diodes are forward biased are almost equal for diodes D_1, L_1 and L_3 (see Table II). Although there is some difference between the two sets of devices when the diodes are reverse biased the spectral densities are within one order of magnitude (see Table I). Both these observations seem to indicate that the mechanisms that are responsible for the noise are present whether the diodes are forward or reverse biased. This is surprising when one considers that the dc current flow is governed by different mechanisms under the two bias conditions. This statement is supported by the fact that the current dependence of the magnitude of the noise is different for the two bias conditions (see Figs. 4 and 7).

Another method that has been used to separate out the different noise producing mechanisms is to evaluate the parameter α_H as it is defined by Eq. (2):

$$S_I(f)/I^2=\alpha_H/fN. \tag{2}$$

In this equation[1] $S_I(f)$ is the spectral intensity of the current fluctuations, I the dc current, f the frequency, and N the number of carriers in the system. If nothing else, α_H is a dimensionless measure for the noisiness of the device and permits as such a comparison between devices. By comparing the derived values of α_H with theoretical predictions made by Handel,[2] which are only applicable to true $1/f$ spectra and many of which have been verified,[3] the noise processes can be identified. However, this method is hard to apply in the case of reverse biased diodes since we do not have an independent way to establish the number of free carriers in these diodes.

When the diodes are forward biased the current flow is governed by a transit time or lifetime (τ) of the carriers. In that case $N=I\tau/q$ and upon substitution into Eq. (2) one finds

$$S_I(f)/I=\alpha_H q/\tau f. \tag{3}$$

Measurements of the ac impedance of the diode have been used before[4] to obtain this time constant from resonances in the real part of the impedance. Even when the spectra have an exponent unequal to -1.0 can we define

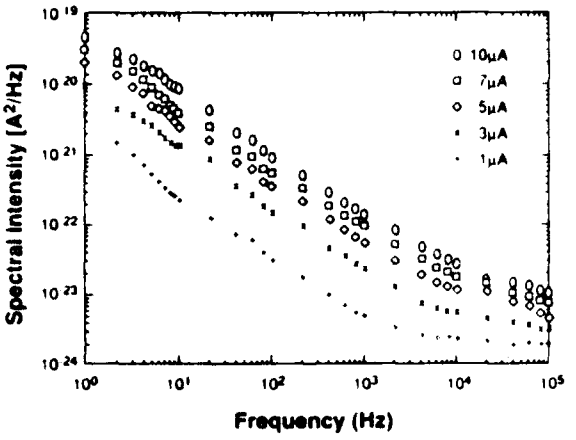

FIG. 5. Current noise spectra of the forward-biased (no illumination) diode D_1 for different currents.

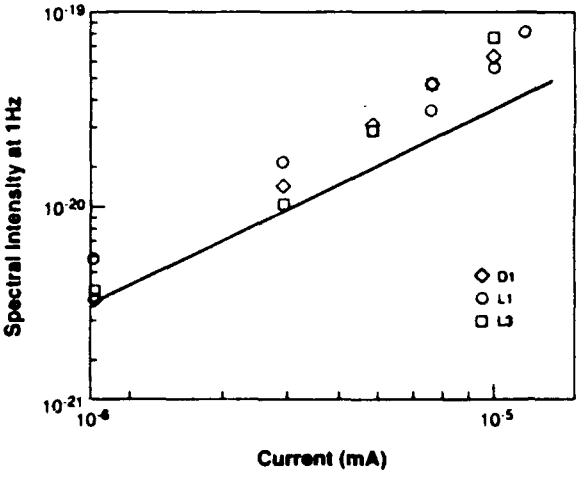

FIG. 7. Current dependence of the noise intensity at 1 Hz for the three diodes under forward bias (no illumination). The slope of the line is + 1.

B27

TABLE II. The measured average noise intensity at 1 Hz [$S_i(1\ \text{Hz})$] of the diodes under *forward* bias and no illumination, normalized by the current. The slope of the measured low-frequency spectra is γ. The entries in the table are averaged over at least five different currents ranging from 1 to 14 μA.

Diode No.	$S_i(1\text{Hz})/I(10^{-15}\ \text{A/Hz})$	γ
D_1	5.1 ± 1.1	-0.99 ± 0.66
L_1	5.4 ± 0.7	-0.82 ± 0.03
L_3	5.1 ± 1.5	-0.82 ± 0.02

$$\alpha_H = \frac{[S_i(f)f]_{f=1\ \text{Hz}}\tau}{qI} = \frac{S_i(1\ \text{Hz})\tau}{qI}, \tag{4}$$

where α_H is not dimensionless anymore, it just defines the noisiness at $f = 1$ Hz. The diodes have been shown to be very-high-speed devices; they have been operated at a few GHz. Therefore, the lifetime in these devices has to be at least 10^{-9} s, resulting in values for α_H that are larger than 3×10^{-5}. Note that the values of α_H/τ are very close for the three diodes (see Table III). The value for α_H (α_H) found here does not coincide with the values predicted by Handel's quantum $1/f$ noise theory, apart from the fact that the frequency exponent of the low-frequency parts of the spectra are not equal to -1.0. Accordingly, we cannot attribute the noise we observe to these mechanisms. On the other hand, the fact that the values for $\alpha_H(\alpha_H)$ are almost identical for the three diodes might suggest that apart from a surprising uniformity that we have not observed as yet, the noise is of a fundamental nature. It requires further study of what other fundamental noise sources can exist besides quantum $1/f$ noise.

In this light it should be considered that earlier experiments on $Hg_{1-x}Cd_xTe$ *p-i-n* diodes revealed values for α_H in the range of 2×10^{-6}–2×10^{-5}; the frequency exponents were smaller than -1.0 in these devices as well.[5] The noise was attributed to a distribution of generation-recombination centers having different activation energies. This would result in noise spectra that are summations of Lorentzians $[1/(1+\omega^2\tau^2)]$. This so-called generation-recombination $1/f$ noise might also be the source of the noise in our InGaAs diodes.

IV. QUANTUM EFFICIENCY

In the search for a fundamental source of noise one might want to consider fluctuations in the quantum efficiency. One should realize that this would only be a source of noise when light is shone on the devices as we did when we reverse biased the devices. This would not explain the noise in the devices under forward bias. Let n photons arrive at the surface per second and let the reflection coefficient of the surface be r; then $m = n(1-r)$ of these photons will enter the semiconductor. They will have probability η to generate an electron-hole pair resulting in the production of $N = \eta n(1-r)$ electron-hole pairs per second. It is shown that the variance of N equals

$$\text{var}(N) = [\text{var}(n) - \langle n \rangle](1-r)^2\eta^2 + \langle N \rangle. \tag{5}$$

The angular brackets ($\langle\ \rangle$) indicate taking the ensemble average. If the incandescent light has a Poissonian distribution [$\text{var}(n) = \langle n \rangle$] then the distribution of the electron-hole pairs will be Poissonian as well and the high-frequency shot noise will be $2qI$. If the distribution of the photons is super-Poissonian [$\text{var}(n) > \langle n \rangle$] then $\text{var}(N) > \langle N \rangle$ and the shot noise will be enhanced. We have not observed the enhancement of the shot noise in either diode and therefore conclude that the light source gives a Poissonian distribution of photons.

A possible source for low-frequency fluctuations might be the quantum efficiency, resulting in a $1/f$-like spectrum. Since the photocurrent is proportional to the quantum efficiency one can show that the relative spectrum of the fluctuations in the current is equal to the relative spectrum of the fluctuations in the quantum efficiency:

$$S_I/I^2 = S_\eta/\eta^2. \tag{6}$$

Since η is practically independent of the current, the same is true for S_η/η^2 so that S_I varies as I^2.

This model would explain qualitatively the current dependence of the current spectra when the diodes are reverse biased and illuminated. It would not explain the magnitude of the noise we observed.

V. SUMMARY

The following observations were made from the measured current noise spectra of two types of InGaAs/InP photodiodes under reverse bias and illumination and under forward bias without illumination:

(1) For each set of devices the slopes of the low-frequency spectra where the same under both bias conditions.

(2) Under forward bias both sets of devices showed a current dependence of the noise that is linear.

(3) Under reverse bias both sets of devices showed a current dependence of the noise that is quadratic.

(4) The values of α_H obtained from the noise spectra under forward bias are not compatible with Handel's quantum $1/f$ noise; they seem to be indicative of $1/f$ noise due to a distribution of recombination centers.

From the first observation one might infer that the mechanism responsible for the noise is the dominant one under both bias conditions. This is not obvious since the mechanism controlling the current flow under the two conditions is different. The second and third observation support the fact that the current flow in the diodes is controlled by different mechanisms under the two conditions.

TABLE III. The values of α_H from the current noise spectra of the forward biased diodes. Equation (4) is used to calculate α_H and it is assumed that $\tau = 1 \times 10^{-9}$ s.

Diode No.	α_H (in units of 10^{-5})	γ
D_1	6.4	1.0
L_1	6.8	0.8
L_3	6.6	0.8

We have shown that fluctuations in the quantum efficiency could give rise to the quadratic current dependence of the noise intensity. Of course, this mechanism cannot explain the noise when the diodes are forward biased and not illuminated.

A distribution of traps with different activation energies seems to be a likely candidate to explain our observations. It would explain the identical slope of the spectra under the two bias conditions. The different current dependence of the noise under these two conditions would be explained by the different mechanisms controlling the current flow. The latter ones determine how a local noise source contributes to the noise as it appears at the terminals. We would like to emphasize that for the three diodes under forward bias the value of $S_I(1\text{Hz})/I$ is remarkably close (Table II). This might be indicative of a more fundamental noise source.

ACKNOWLEDGMENT

This work was partly supported by U. S. Army Research Office contract No. DAAG-29-85-K-0253.

[1] F. N. Hooge, Phys. Lett. A **29**, 139 (1969); Physica B **83**, 9 (1976).
[2] P. H. Handel, Phys. Rev. Lett. **34**, 1492 (1975), Phys. Rev. B **22**, 745 (1980), in *Noise in Physical Systems and 1/f Noise*, edited by M. Savelli, G. Lecoy, and J. P. Nougier (Elsevier, New York, 1983), p. 97; *ibid.* edited by A. d'Amico and P. Mazzetti (Elsevier, New York, 1986), p. 465.
[3] See the review paper by A. van der Ziel, Proc. IEEE **U76**, 233 (1988).
[4] P. Fang, L. He, A. D. van Rheenen, A. van der Ziel, and Q. Peng, Solid-State Electron. **32**, 345 (1989).
[5] A. van der Ziel, P. Fang, L. He, X. L. Wu, and A. D. van Rheenen, J. Vac. Sci. Technol. A **7**, 550 (1989).

B29

Solid-State Electronics Vol. 33, No. 12, pp. 1647–1648, 1990
Printed in Great Britain

0038-1101/90 $3.00 + 0.00
Pergamon Press plc

NOTES

EXTENSION OF THE HOOGE EQUATION AND OF THE HOOGE PARAMETER CONCEPT

(Received 30 June 1988; in revised form 9 June 1990)

INTRODUCTION

The Hooge equation is extended to the case where the noise spectrum is of the form $1/f^{\gamma}$ with γ slightly different from unity. This leads to a generalization of the Hooge parameter that corrects an earlier ambiguity.

DISCUSSION

In 1969 Hooge published his well-known equation[1]

$$\frac{S_I(f)}{I^2} = \frac{\alpha_H}{fN} \tag{1}$$

giving an empirical description of the releative $1/f$ noise of a uniform semiconductor sample carrying a current I. Here $S_I(f)$ is the spectral intensity of the current fluctuations, N the number of carriers in the sample and α_H is an empirical constant, known as the Hooge parameter, that characterizes the noise.

Later, eqn (1) was extended to include mobility and diffusion $1/f$ noise and applied to devices. Equation (1) may then be written[2,3] as

$$\frac{S_\mu(f)}{\mu^2} = \frac{\alpha_H}{fN}; \quad \frac{S_D(f)}{D^2} = \frac{\alpha_H}{fN}. \tag{1a}$$

The two equations are connected by means of the Einstein relation $qD = kT_\mu$.

In the case of spatially distributed $1/f$ noise sources eqn (1) can be written as

$$\frac{S_I(x,f)}{I^2} = \frac{\alpha_H}{fN(x)\,\Delta x}. \tag{1b}$$

Here $S_I(x,f)$ is the current spectrum in a section Δx at x; $N(x)$ is the number of carriers per unit length at x.

Equation (1) can be used for evaluating α_H from the measured spectrum $S_I(f)$. If the spectrum is *exactly* $1/f$, we may write $S_I(f) = S_I(1)/f$; solving for α_H yields

$$\alpha_H = \frac{NfS_I(f)}{I^2} = \frac{NS_I(1)}{I^2}. \tag{2}$$

The value of α_H, thus obtained, is independent of the frequency f at which $S_I(f)$ is measured.

At first the first half of eqn (2) was also used without having ascertained that the spectrum *was exactly* $1/f$. That is α_H was expressed as

$$\alpha_H = \frac{NfS_I(f)}{I^2} \tag{3}$$

irrespective of the frequency dependence of $S_I(f)$. But this led to ambiguous results, in that α_H now depended on the frequency f. For if $S_I(f)$ had a $1/f^{\gamma}$ dependence: $S_I(f) = S_I(1)/f^{\gamma}$, one finds by substitution

$$\alpha_H = \frac{NS_I(1)}{I^2} f^{1-\gamma} \tag{3a}$$

which depends on the frequency f and is only equal to eqn (2) at 1 Hz. Usually the error is relatively small, however. Note that $S_I(1)$ has the dimension $-\mathrm{A}^2(\mathrm{Hz})\gamma^{-1}$.

To remedy the situation we generalize eqn (1). If the spectrum $S_I(f) = S_I(1)/f^{\gamma}$ with $\gamma \neq 1$, the simplest generalized form is

$$\frac{S_I(f)}{I^2} = \frac{\alpha_H}{Nf^{\gamma}}. \tag{4}$$

Substituting for $S_I(f)$ yields

$$\alpha_H = \frac{Nf^{\gamma}S_I(f)}{I^2} = \frac{NS_I(1)}{I^2} \tag{4a}$$

which is identical with eqn (2). The expression for α_H is now independent of the measuring frequency and does not contain the exponent γ explicitly. Note that α_H has the dimension $(\mathrm{Hz})\gamma^{-1}$.

If we compare eqns (3a) and (4a) we see that the correction factor is $f^{1-\gamma}$, where f is the measurement frequency. For $f = 1$ Hz the correction factor is unity for all values of γ; for $f = 10$ Hz and $\gamma = 0.90$ the correction factor is 1.26, whereas for $f = 100$ Hz and $\gamma = 0.90$ it is 1.58. For reasonable accuracy one should measure close to 1 Hz[4]. Finally eqn (4) may be written

$$f^{\gamma}S_I(f) = \frac{\alpha_H}{N} I^2 = S_I(1) \tag{5}$$

This is easily adapted to devices with distributed noise sources such as MOSFETs and short p–n junction diodes.

As a first example consider a MOSFET operating in the linear mode ($V_d \ll V_{dn}$)[5]. If the device has a length L, a drain voltage V and a current I, and μ is the carrier mobility, then

$$S_I(f) = \frac{\alpha_H e\mu I_d V_d}{f^{\gamma}L^2}, \quad \text{or} \quad f^{\gamma}S_I(f) = S_I(1) = \frac{\alpha_H e\mu I_d V_d}{L^2}. \tag{6}$$

As a second example consider a short n^+–p diode. The spectrum is now[3,5]

$$S_I(f) = \frac{\alpha_H eI}{2f^{\gamma}\tau_{dn}} \ln\left[\frac{N(0)}{N(W_p)}\right]; \quad \frac{N(0)}{N(W_p)} = 1 + \frac{S_{cn}W_p}{D_n}. \tag{7}$$

Here W_p is the length of the p-region, S_{cn} the electron recombination velocity at the p-contact (6×10^6 cm in n-type Si), D_n the diffusion constants for electrons and $\tau_{dn} = W_p^2/2D_n$ the diffusion time of the electrons through the p-region. Hence

$$f^{\gamma}S_I(f) = S_I(1) = \frac{\alpha_H eI}{2\tau_{dn}} \ln\left(1 + \frac{S_{cn}W_p}{D_n}\right). \tag{7a}$$

The extension does not apply too well to GaAs MESFETs since the spectrum has g–r "bumps" superimposed upon a $1/f$ background[6]. If one does not require great accuracy, however, eqn (3a) or eqn (4a) can be used as approximations to find "order of magnitude" values of α_H.

If one wants to compare the quantum-theoretical[7,8] and the experimental values of the Hooge parameter α_H, ones uses the experimental values given by eqns (4a), (6) or (7a), whereas the theoretical values are taken from Handel's equation[7,8].

$$\alpha_H = \frac{4\alpha_0}{3\pi}\frac{\overline{\Delta v^2}}{c^2} \tag{8}$$

where $\alpha_0 = 1/(137)$ is the fine structure constant, c the velocity of light and Δv the vectorial change in carrier velocity in the collision process.

It should furthermore be borne in mind that the quantum theory of $1/f$ noise results in a $1/f^{\gamma}$ spectrum with γ very close to unity. If deviations occur, either in γ or in α_H, one should investigate whether a superposition of spectra might be present. In some FETs a generation–recombination type $1/f^2$ spectrum sometimes masks the wanted $1/f$ spectrum; this unwanted noise source must then be corrected for[9]. In vacuum photodiodes a quantum $1/f$ spectrum and a classical surface $1/f^{1/2}$ spectrum are present simultaneously and must be separated before an analysis can be attempted[10]. Care must be taken that conclusions are not made prematurely.

Electrical Engineering Department A. VAN DER ZIEL
University of Minnesota A. D. VAN RHEENEN
Minneapolis, MN 55455, U.S.A

REFERENCES

1. F. N. Hooge, *Phys. Lett.* **A-29,** 139 (1969).
2. F. N. Hooge, *Physica* **114B,** 39 (1982).
3. T. G. M. Kleinpenning, *Physica* **98B,** 289 (1980).
4. Compare e.g. A. Pawlikiewicz and A. van der Ziel, *IEEE Electron Device Lett.* **EDL-6,** 497 (1986). Here the uncertainty in α_H is relatively small.
5. A. van der Ziel, *Proc. IEEE* **76,** 233 (1988).
6. B. Hughes, N. G. Fernandez and J. M. Glastone, *IEEE Electron Devices Lett.* **ED33,** 1852 (1986).
7. P. H. Handel, *Phys. Rev. Lett.* **34,** 1992 (1975).
8. P. H. Handel, *Phys. Rev. Lett.* **22,** 745 (1980).
9. Q. Peng, A. N. Birbas, A. van der Ziel and A. D. van Rheenen, to be published.
10. P. Fang, L. He, H. Kang, Q. Peng and A. van der Ziel, *J. appl. Phys.*, in press.

B31

Solid-State Electronics Vol. 33, No. 12, p. 1649, 1990
Printed in Great Britain.

0038-1101/90 $3.00 + 0.00

NOISE IN THE QUANTUM EFFICIENCY η OF p^+–n DIODES DUE TO FLUCTUATION IN THE SURFACE GENERATION–RECOMBINATION OF CARRIERS

(Received 7 April 1990; in revised form 31 May 1990)

According to Melngailis and Harman[1] the quantum efficiency η in a p^+–n photodiode with surface generation and recombination of carriers is given by

$$\eta = \frac{1-r}{\cosh(d/L_p) + (s\tau_p/L_-)\sinh(d/L_n)} \tag{1}$$

Here r is the photon reflection coefficient at the surface, τ_p the carrier lifetime, d the depth of the junction, L_p is the hole diffusion length, and s the surface recombination velocity.

We now calculate the noise specturm of η. Since s fluctuates in a $1/f$ fashion, η will fluctuate in the same fashion. Hence

$$\delta\eta = -\frac{(1-r)[(\tau_p/L_p)\sinh(d/L_p)]}{[\cosh(d/L_p) + (s\tau_p/L_p)\sinh(d/L_p)]^2}\,\delta s \tag{2}$$

Putting $Q(s, \tau_p, d) = (s\tau_p/L_p)\tanh(d/L_n)$ yields

$$\frac{\delta\eta}{\eta} = -\frac{Q(s,\tau_p,d)}{1+Q(s,\tau_p,d)}\,\frac{\delta s}{s} \tag{3}$$

Making a Fourier analysis and calculating the power spectrum yields

$$S_\eta(f)/\eta^2 = \left[\frac{Q(s,\tau_p,d)}{1+Q/(s,\tau_p,d)}\right]^2 \frac{S_s(f)}{s^2} \tag{4}$$

For long diodes $d/L_p \gg 1$ and hence $\tanh(d/L_p) = 1$, so that

$$\frac{S_\eta(f)}{\eta^2} = S_s(f)\left(\frac{\tau_p/L_p}{1+s\tau_p/L_n}\right)^2 \tag{4a}$$

If $d/L_p \ll 1$, we have $\tanh(d/L_n) \simeq d/L_p$ and $Q^2 \ll 1$, so that

$$\frac{S_\eta(f)}{\eta^2} = Q^2\,\frac{S_s(f)}{s^2} = S_s(f)(\tau_p d/L_p^2)^2 \tag{4b}$$

In either case $S_s(f) = \text{const}\, s/f$ so that $S_\eta(f)$ has a spectrum that is nearly independent of current[2].

In modern p^+–i–n diodes recombination–generation usually occurs in the bulk[3]. In that case the above theory does not apply.

Electrical Engineering Department A. VAN DER ZIEL
University of Minnesota Y. LIN
Minneapolis L. HE
MN 55455, U.S.A. A. D. VAN RHEENEN

REFERENCES

1. I. Melngailis and T. C. Harman, *Semiconductors and Semimetals*, Vol. 5, Chap. 4, p. 111, Appendix A1. Academic Press, New York (1970) (Review paper)
2. We follow here Fonger's definition of $S_s(f)$: W. Fonger, in *Transistors I*, p. 259. RCA Lab, Princeton, NJ (1956).
3. L. He, Y. Lin, A. van der Ziel, A. D. van Rheenen, A. Young and J. P. van der Ziel, *J. appl. Phys.*, in press.

B32

Current Fluctuations In Double Barrier Quantum Well Resonant Tunneling Diodes

Yayun Lin, Arthur D. van Rheenen, and Stephen Y. Chou

Electrical Engineering Department
University of Minnesota
200 Union Street SE, Minneapolis, MN 55455

Abstract:

Reported here are measurements of the spectral intensity of the current fluctuations in double-barrier quantum well resonant tunneling diodes as a function of temperature and bias current. Two types of devices were studied: one with AlAs barriers and GaAs well and contact regions, and the other has $Al_{0.3}Ga_{0.7}As$ barriers. The frequency range covered is 1 Hz to 100 kHz and the temperature range is 78 K to 400 K. The noise spectra are decomposed in a 1/f part, resulting in the magnitude of the 1/f noise, and contributions due to carrier trapping, resulting in the activation energies of the traps. It is found that a reduction of the Al contents of the barrier material reduces the number of traps and further the magnitude of the 1/f noise is practically independent of the temperature and of the Al content of the barrier.

Double-barrier resonant tunnelling structures (DBRTS) have attracted much attention recently because of their functionality in a wide variety of applications that include frequency multipliers, parity generators, multi-state memory, analog-digital converters[1], opto-electronic devices[2], etc. While there would be variations of present or potential applications of resonant tunnelling devices, DBRTS offer not only the key attributes for the applications mentioned above, but also tender opportunities for experimental studies on quantum effects in carrier transport[3,4]. In the last ten years the impressive advances in the molecular beam epitaxy have contributed greatly to the amelioration of the DBRTS making possible more refined studies of the characteristics of the devices such as the noise performance as it correlates with the presence of defects, impurities, and tunnelling processes. We report here on an extensive study of just this low-frequency noise behavior of two types of DBRTS: one with Al barriers and GaAs electrodes and well, and another type with AlGaAs barriers and GaAs electrodes and well. The measured current noise spectra are interpreted in terms of 1/f noise and generation-recombination (g-r) noise. The noise spectroscopy has been applied before, to bulk semiconductors[5,6] as well as to DRTBS[7], and has proven to be very successful in identifying carrier traps.

The noise behavior of two types of devices was investigated. The symmetric tunnel structures were grown by MBE on an n^+ substrate and are identical except for the barriers which are 3nm thick AlAs for one device type and 5 nm thick $Al_{0.3}Ga_{0.7}As$ for the other type. The details of the layer structure are presented in Fig. 1. In all the doped layers Si was used as a dopant. Current-voltage characteristics of the two devices both at 77 K and 300 K are shown in figures 2a and 2b. The peak-to-valley ratio of the current of the AlAs barrier device is about 13 at 77 K and decreases to about 3 at room temperature. For the AlGaAs barrier device the current peak-to-valley ratio is about 5 at 77 K, dropping to 2.2 at room temperature, and further decreasing to 1.3 at 400 K.

In order to measure the noise as a function of temperature the devices were mounted in a flow cryostat. The noise signal was fed into a low-noise amplifier and detected by a Fast Fourier Transform dynamic signal analyzer. In calculating the spectra allowance was made for the amplifier noise as well as the non-flatness of the amplifier gain. The resultant noise spectra usually consisted of a 1/f component, Lorentzian shaped bumps due to trapping and de-

trapping of carriers, and a white part due to the thermal noise.

The experimental investigation is divided into three parts: (i) Spectral intensity of the current fluctuations as a function of temperature at a fixed current, (ii) Current dependence of the noise for voltages smaller than the peak-voltage (V_p), and (iii) Current dependence of the noise for voltages larger than the valley-voltage (V_v).

To study the temperature dependence of the noise the diodes were biased at a constant current of 0.7 mA, relatively close to the peak, and the temperature was varied between 78 K and 400 K. The spectra consist of a 1/f part and Lorentzian-shaped bumps due to generation and recombination (g-r noise) of the carriers. Upon multiplication of the spectra by the frequency the 1/f contribution will appear independent of frequency and the bumps associated with the g-r noise will appear as peaks. From these graphs one can readily extract the magnitude of the 1/f noise and the frequencies (f_p) for which the g-r peaks occur. A subsequent plot of the square of the temperature T divided by f_p as a function of the reciprocal temperature permits the calculation of the activation energies of the traps from the slopes of the curves.

In Fig. 3 we show these Arrhenius plots for the device with the AlAs barriers and for the device with the $Al_{0.3}Ga_{0.7}As$ barriers. For the mentioned range of temperatures five trapping levels could be detected in the AlAs barrier device with activation energies of 0.017, 0.15, 0.21, 0.38, and 0.55 eV. Under the same bias current and in the same temperature range the device with the $Al_{0.3}Ga_{0.7}As$ barriers showed only two traps with activation energies of 0.16 and 0.55 eV: these energies are close to two of the energies we found in the first device. Since the aluminum content of the barrier material is the main difference in the device structures we attribute the presence of the three other traps to the larger Al mole fraction. Apparently, there is some trap assistance in the tunneling process and sweeping the temperature allows us to probe these traps by making noise measurements.

In Fig. 4 we present the magnitude of the 1/f component we observed in the noise spectra as a function of the temperature. The bias current (I_d) was held constant at 0.7 mA for both devices. We want to mention here that the frequency exponent of the spectra is equal to -1.00 ± 0.05. Due to the magnitude of the g-r noise in the AlGaAs barrier device (solid triangles) at temperatures below 190 K it was not possible reliably to extract the magnitude of the 1/f noise.

Our measurements indicate that the magnitude of the 1/f noise component is relatively constant over the entire temperature range for both devices when the diodes are biased close to the peak (0.7 mA). This strongly suggests that the 1/f component is associated with the tunneling current since this current is independent of the temperature in first order. Because the device is biased relatively close to the peak we expect the main current component to be due to tunneling. We also observe that the magnitude of the 1/f noise is practically the same in the two different devices. This seems to imply that the physics (tunnelling through the barrier at this operating point) that governs the transport, and therefore the noise, is the same for these devices, although the materials properties of the barriers differ.

The last part of our study of the noise behavior of resonant tunnel diodes involved the current dependence of the 1/f noise component both at different temperatures as well as for bias points with $0 < V < V_p$ and for bias points with $V > V_v$ for the two devices. The peak current occurs for $V=V_p$, the valley current occurs for V_v. In Fig. 5 we show the spectral intensity of the current fluctuations at 1 Hz versus the bias current measured at room temperature for the AlAs barrier device. The solid circles indicate biaspoints with $V < V_p$ and the solid triangles represents the noise for the biaspoints for which $V > V_v$. In the domain where the current is due mostly to tunneling through the barriers the noise increases with the current and can be described by $I^{1.6}$. When the voltage is larger than V_v the current dependence of the noise is even stronger, close to I^2. The latter current dependence is expected for a resistor-like device. In this bias regime the current is due mostly to carriers that are excited over the barriers. It is important to observe that

for the same current the device is noisier when biased at voltages smaller than the peak value.

When the temperature is lowered to 78 K the current dependence of the noise is less strong, the device noise tends to behave more like that of a regular diode, although the magnitude of the noise does not change very much (Fig. 5, open circles).

For the AlGaAs barrier device these measurements were repeated at temperatures of 400, 300, and 200 K (see Fig. 6). At the highest temperature we observe roughly the same behavior as we observed for the AlAs barrier device; the current dependence of the noise for the smaller voltages (circles) is less strong than it is for the voltages larger than V_v (triangles). However, the data for which $V < V_p$ show a knee close to the maximum current point. This is more dramatic for the 300 K data. The 200 K data do not show this behavior very strongly. A point to note is that as the temperature is lowered from 400 K to 300 K to 200 K the noise in the after-valley regime increases with respect to the noise when the device is biased in the before-peak regime. This is consistent with the remarks we made earlier that the 1/f noise in the before-peak-regime is associated with the tunneling process whereas the 1/f noise in the after-valley-regime is due to other processes and has a stronger temperature dependence.

In summary measurements are presented here of the low-frequency noise of two types of resonant tunnelling diodes, one with AlAs barriers and one type with $Al_{0.3}$ $Ga_{0.7}$ As barriers. The temperature dependence of the 1/f noise is investigated when the devices are biased just below the peak in the current-voltage characteristic and found to be very small. Additionally, the magnitude of the 1/f noise is very similar in both device types. Both these observations are believed to be consistent with the main current component in this bias regime: the tunneling through the barriers.

Second, from generation-recombination noise measurements trap activation energies were extracted. We noticed five traps in the AlAs barrier device and two in the AlGaAs barrier device with activation energies equal to two of the trap energies we found in the AlAs barrier device. This seems to support the idea that the larger Al concentration in the barrier material introduces carrier traps in the device.

Third, we compared the current dependence of the 1/f noise in the devices in the two biasing regimes: before the peak and after the valley. We observed a stronger current dependence of the magnitude of the 1/f noise when the device was biased in the tunnelling regime than when it was biased in the field-assisted thermionic emission mode. The magnitude of the noise in the latter mode of operation is smaller consistent with expectations.

Acknowledgment.
Part of this work was supported by the Army Research Office under contract number DAAL03-89-K-0009.

References.

1. F. Capasso, S. Sen, F. Beltram, L. M. Lunardi, A. S. Vengurlekar, P. R. Smith, N. J. Shan, R. J. Malik, and A. Y. Cho, "Quantum functional devices: Resonant-tunnelling devices, circuits with reduced complexity, and multiple-valued logic" in IEEE Trans. Electron Devices, Vol. 36, No 10, pp. 2065-2082 (1989).

2. H. Sakaki, T. Matsusue, and M. Tsuchiya, "Resonant tunnelling in quantum heterostructures: Electron transport, dynamics, and device applications" IEEE J. Quantum Electronics, Vol. 25, No.12, pp. 2498-2504 (1989).

3. J. S. Wu, C. P. Lee, C. Y. Chang, D. G. Liu, and D. C. Liou, "Quantum effect of the source electrode on electrical and optical characteristics of double-barrier resonant tunnelling structures", Technical Digest IEDM, San Fransisco Dec. 1990, pp. 343-346.

4. J. F. Chen, L. Yang, A. Y. Cho, "Investigation of the influence of the well and the barrier thicknesses in GaSb/AlSb/GaSb/AlSb/InAs double-barrier interband tunneling structures", IEEE Electron Dev. Lett. Vol. 11, No. 11, pp. 532-534 (1990).

5. A. D. van Rheenen, G. Bosman, and R. J. J. Zijlstra in "Low-frequency noise measurements as a tool to analyze deep-level impurities in semiconductor devices", Solid-State Electron., Vol. 30, p. 259 (1987).

6. A. D. van Rheenen, G. Bosman, and C. M. Van Vliet, "Decomposition of generation-recombination noise spectra in separate Lorentzians", Solid-State Electron. Vol. 28, p. 457 (1985).

7. M. H. Weichold, S. S. Villareal, and R. A. Lux, "Analysis of defect-assisted tunnelling based on low-frequency noise measurements of resonant tunnel diodes", Appl. Phys. Lett. Vol. 55, No. 7, pp. 657-659 (1989).

Figure Captions

1. Device layer configuration.

2. Current-voltage characteristics of (a) the AlAs barrier and (b) the AlGaAs barrier device at different temperatures.

3. Activation energies as deduced from the generation-recombination spectra for the AlAs barrier (circles) and the AlGaAs barrier (triangles) device. The quiescent current during the noise measurements was 0.7 mA.

4. Spectral intensity of the current fluctuations (1/f component) at f = 1 Hz and an operating current of 0.7 mA as a function of the temperature for the AlAs barrier (circles) and the AlGaAs barrier (triangles) device.

5. Spectral intensity of the 1/f current fluctuations at f = 1 Hz versus the operating current for the AlAs barrier device. The solid circles represent the data taken at room temperature and for voltages smaller than the I-V peak voltage. The solid triangles are room temperature data measured as the voltage was larger than the valley voltage. The open circles specify the data for T = 78 K and voltages smaller than the peak voltage. The letter B labels before the peak, A labels after the valley.

6. Spectral intensity of the current fluctuations at f = 1 Hz of the AlGaAs barrier device versus the operating current at T = 400 K, T = 300 K, and T = 200 K. The circles represent data taken with voltages smaller than the peak voltage and the triangle show the data for applied voltages larger than the valley voltage.

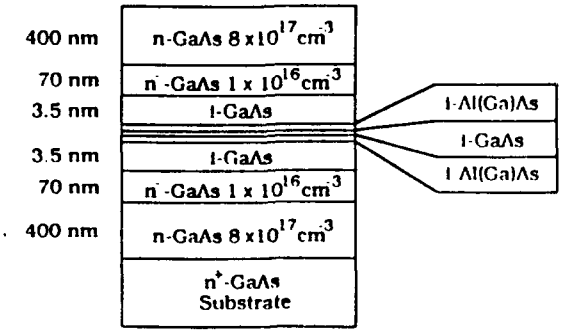

Fig. 1

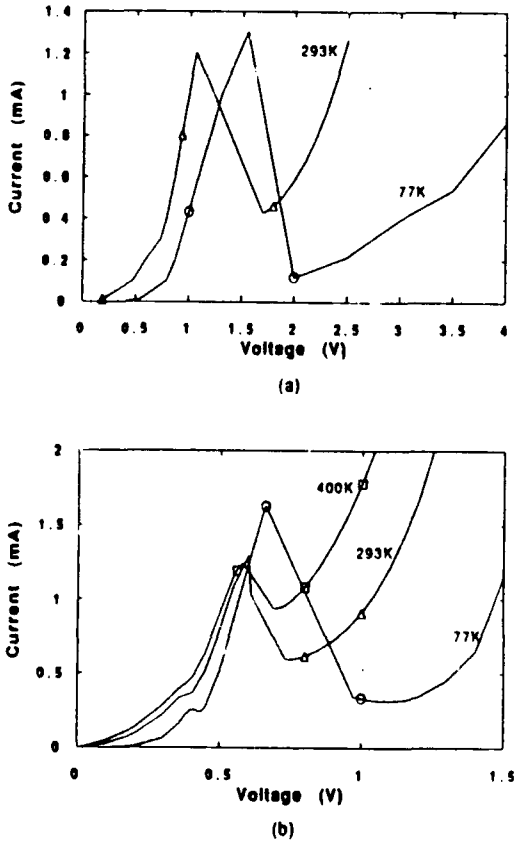

Fig. 2

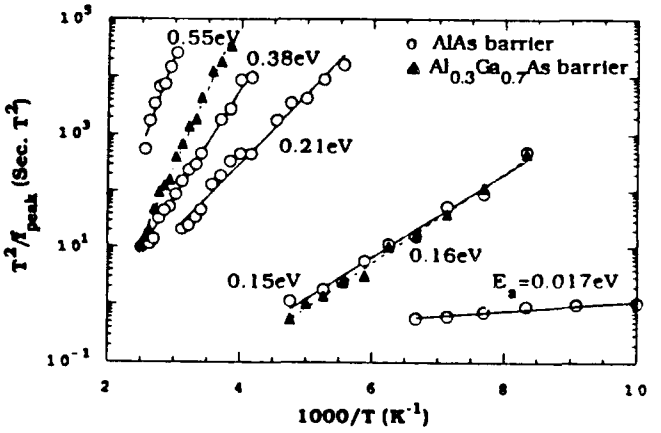

Fig. 3

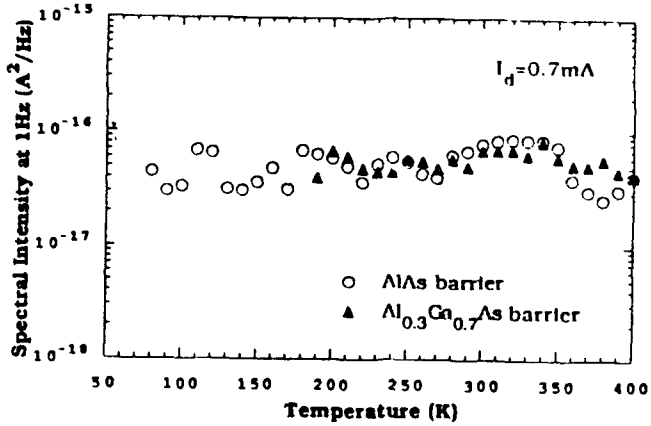

Fig. 4

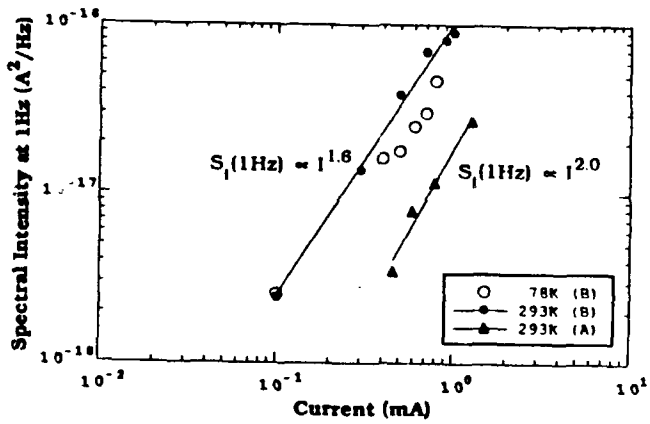

Fig. 5

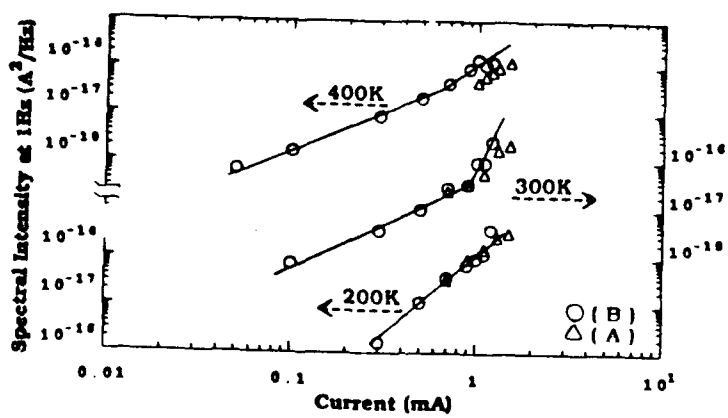

Fig. 6

Appendix C

Abstracts of theses

Arthur van Kheenen
June 90

QUANTUM 1/*f* NOISE IN BIPOLAR JUNCTION TRANSISTORS

A THESIS
SUBMITTED TO THE FACULTY OF THE GRADUATE SCHOOL
OF THE UNIVERSITY OF MINNESOTA

BY
ALISTER CHUN-FUNG YOUNG

IN PARTIAL FULFILLMENT OF THE REQUIREMENTS
FOR THE DEGREE OF
DOCTOR OF PHILOSOPHY

JUNE 1990

C 2

ABSTRACT

It is shown that the present model used to describe the silicon bipolar junction transistors is far from being precise. In general it demonstrates the approximate locations of the constituents of both the base and the collector noise current sources and the relative magnitudes, but shows minimally about the shape and type of the noise sources. For the transistors under investigation, we found that the collector noise spectra are generally $1/f^{\gamma}$ type with $\gamma \approx 2.0$. This could mean that the dominant noise source in the collector current is G-R type noise. Given this fact, the Hooge parameters obtained from these collector noise spectra have either no meaning or can only be interpreted as an upper limit to the α_H. The base noise, on the other hand conforms to the Kleinpenning-van der Ziel $1/f$ diffusion theory. One can therefore determine whether the noise source is of a fundamental nature by comparing and contrasting the experimentally obtained Hooge parameters α_H's with theoretically calculated values.

In Gallium-Arsenide (GaAs) heterojunction transistors, same result was obtained for the collector in some preliminary experiments. We have again G-R type noise appearing in the collector current spectra. As for the base current spectra, it is different than that of the Si transistors, that is, the near $1/f$ base current spectra have a base current dependence as I_B^2; contrary to its counterpart in Si transistors which obey the $1/f$ diffusion theory.

Since α_H alone is not always sufficient to determine the noise source. New quantities $f_C(I_C)$ and $f_B(I_B)$ as $1/f$ cut-off frequencies for both the collector and the base are introduced. These generalized quantities can be used to determine whether the devices have $1/f$ diffusion noise or not. Usually if the cut-off frequency varies slowly with the respective bias current it is $1/f$ diffusion noise, otherwise it is not likely to be.

Finally, α_H's found in the experiments are compared to the theoretical values calculated by Handel, Van Vliet and others to show that we have devices exhibiting collision $1/f$ noise, Umklapp noise and perhaps intervalley scattering noise. In most cases, we have combinational effects therefore the values of α_H's tend to be larger than the individual quantum limits.

1/f NOISE IN P- AND N- CHANNEL JFETS

A THESIS

SUBMITTED TO THE FACULTY OF THE GRADUATE SCHOOL

OF THE UNIVERSITY OF MINNESOTA

BY

Ioannis M. Stephanakis

IN PARTIAL FULFILLMENT OF THE REQUIREMENTS

FOR THE DEGREE OF

MASTER OF SCIENCE EE

APRIL 1991

C5

ABSTRACT

The main body of the thesis is virtually divided into two parts, Chapters I,II,III and Chapters IV,V. In the first three chapters an introduction to noise phenomena is attempted and the basic concepts related to noise are presented. The flicker (1/f) noise is first discuss in Chapter II along with the Hooge parameter α_H which is introduced as an empirical parameter which measures the noisiness of several solid-state devices exhibiting 1/f noise. The incoherent state 1/f noise theory and the coherent state 1/f noise theory are mentioned in Chapter III. The equations yielding the Hooge parameter, α_H, are given in each case along with the theoretical predictions regarding the values of α_H in a number of different devices.

Whereas the first part of the thesis is devoted to the theory of 1/f noise, the second part (Chapters IV and V) is devoted to experimental results taken from p-channel JFETs and both short and long n-channel JFETs. The measurement procedure and the model we assume in order to describe the noise behavior of JFETs are presented in Chapter IV. For a saturated channel JFET, we split the channel into two parts, the ohmic part in which the mobility is regarded to be constant and the saturated part in which the velocity equals the saturation velocity. The noise is accounted for by assuming two current noise sources, one for each part of the channel, characterized by the same α_H. The equation which relates the value of α_H to experimentaly accessible variables is given in this chapter.

Experimental data taken from JFET devices of three different types are presented in Chapter V. The noise behavior of 2N4867 n-channel JFETs with channel length of 30μm is investigated first. Noise measurments at room temperature indicate that the noise originates from Umklapp scattering processes. JFETs with a p-channel of the [illegible] length (U168) are also measured at different temperatures and below saturation. The product of $\alpha_H x \mu$ (mobility) seems to be insensitive to temperature changes for a range of, about, 220 to 350 K for these devices. Finally, noise measurements are carried out on short channel (2.6μm) n-JFETs (2SK152). The dependence of α_H on temperature and drain-to-source voltage, V_{ds} is investigated. The obtain values ($\sim 5 \times 10^{-10}$) are one order of magnitude lower than the theoretical predictions and indicate a possible dependence of α_H on the electic field within the channel.

The references used in the course of this research work are given together at the end of the thesis.

II. THEORETICAL RESULTS

1. Introduction

Progress has been achieved during 1989 and 1990 in the study of nonlinear systems which generate chaotic 1/f fluctuations, in the application of the Quantum 1/f Theory[5-7,9-11] to various materials used in small and ultrasmall electronic devices, and in the application of the Quantum 1/f Theory to electronic devices.

The close similarity of the classical and quantum 1/f theories, and the initial development of the quantum 1/f theory by the author out of his efforts to quantize his classical turbulence theory, have led to sustained efforts of the author aimed to integrate all his theories as various forms or realizations of a fundamental notion of chaos in nonlinear systems. During this grant period, these efforts finally beared fruits. A general sufficient criterion was formulated, allowing to identify the nonlinear systems which exhibit 1/f spectra. This criterion is presented in Sec. 3 below. It is followed in Sec. 4 and in the Appendix by examples, in which the criterion is applied to the classical and quantum mechanical forms of the author's 1/f noise theory. These examples clarify the physical meaning of the new criterion.

For the practical application of the Quantum 1/f Theory it is necessary to derive the quantum 1/f fluctuations of various kinetic (transport) coefficients which characterize the materials used in electronic and microelectronic applications, from the author's fundamental quantum 1/f formula. The latter is applicable only to cross sections and rates of elementary processes. Most important is the calculation of mobility fluctuations in Si, GaAs and $Hg_{1-x}Cd_xTe$. An earlier calculation (Kousik, Van Vliet, Handel, 1985) of mobility fluctuations in Si and GaAs is replaced in Sec. 5 by a more rigorous calculation, based on the new quantum 1/f cross-correlations, presented at the 1989 Conference on Noise in Physical Systems. The new calculation yields increased 1/f noise, and is in vey good agreement with the experiment. Although not presented here yet, we also performed a Monte Carlo simulation for HgCdTe during this period. The simulation has yet to be improved and compared with the experiment.

Primarily, we have tried to improve the application of quantum 1/f theory to the collector noise of bipolar transistors. This short calculation is presented in Sec. 2.

In the same time, many new contributions to the quantum 1/f theory and experiment were published by other workers in the field, considerably advancing the field of infra-quantum physics and quantum 1/f noise in high-technology applications. These new contributions, as well as new PhD thesis work in this field

and contributions presented at the IV Conference on Quantum 1/f Noise and other Low-Frequency Fluctuations and included in the Conference Proceedings[14], are included in the updated General Quantum 1/f Bibliography appended to this Report.

2. Collector quantum 1/f noise in BJTs

1/f noise in bipolar junction transistors (BJT's) was elegantly treated by van der Ziel[1-3] who applied a Hooge-type approach similar to Kleinpenning's treatment[4] of pn junctions, and used experimental data to determine the Hooge constant which was in turn compared with the quantum 1/f theory. However, since the BJT is a minority carrier device, it requires the application of the quantum 1/f equation[5-7] from the beginning, for the correct interpretation of the number of carriers in the denominator of the Langevin noise source.

In the most elementary model[8] of a BJT, the collector current I_C arises from minority carriers injected from the emitter into the base, which diffuse across the width X_B base and are then all swept across the reverse-biased collector junction by the built-in field of the junction. If we neglect the usually small leakage current of the collector junction and the small fraction of the carriers recombining in the base, we get for a n^+pn BJT

$$I_C = AqD_n[n_{oB}\exp(qV_{BE}/kT)/X_B], \qquad (1)$$

where A is the cross sectional area of the base, q=-e is the charge of the minority carriers in the base, D_n their diffusion coefficient in the base, $n_B(0)=n_{oB}\exp(qV_{BE}/kT)$ is the electron concentration at the limit of the emitter space charge region, V_{BE} is the applied base - emitter voltage, and X_B is the width of the base. The expression in rectangular brackets is the electron concentration gradient calculated with the boundary condition of a vanishing electron concentration at the limit of the collector space charge region. We assume the base to be much narrower than the electron diffusion length $L_n=(D_n\tau)$, $X_B<<L_n$, but sufficiently wide to avoid ballistic electron transport across the base. Usually X_B is a fraction of a micron.

Quantum 1/f fluctuations of the collisional cross sections of the electrons in the base will yield fluctuations of the diffusion constant, and of the mobility ($\delta D_n/D_n=\delta\mu/\mu$)

$$\delta I_C = Aq(\delta D_n)[n_{oB}\exp(qV_{BE}/kT)/X_B]. \qquad (2)$$

The corresponding spectral density of fractional fluctuations $I^{-2}S_{Ic}$ is

$$I_C^{-2}\langle(\delta I_C)^2\rangle_f = D_n^{-2}\langle(\delta D_n)^2\rangle = \mu^{-2}\langle(\delta\mu)^2\rangle = \alpha_n/fN. \qquad (3)$$

In the last step our quantum 1/f equation[5-7] was used, where N is the number of carriers which define the scattered, or diffused, current leaving the base and emerging in the collector, while $\alpha_n = \alpha A_n$ is the effective quantum 1/f noise coefficient, or Hooge constant. The number of electrons N is thus determined by the effective lifetime τ of the electrons, which will be slightly lower than the lifetime in the unbounded collector material, due to the collector lead contact processes, and due to lateral surface recombination. Indeed, we can write $N = \tau I_C/q$. Thus we finally obtain the spectral density of the collector current fluctuations

$$S_{Ic} = \alpha_n Iq/f\tau, \qquad (4)$$

in which τ is the effective lifetime of the majority carriers in the collector. This expression is simpler, but similar to the expression derived earlier, with the important difference that now we have a lifetime of the carriers in the denominator, while before it was the usually much smaller diffusion time $\tau_D = X_B^2/D_n$ of the electrons in the base. Eq. (4) also implies that in narrow-base BJTs of various base-widths α_n will be constant, as in other devices, rather than α_n/τ_D.

3. A sufficient criterion for 1/f noise in chaotic nonlinear systems

In spite of the practical success of our quantum 1/f theory in explaining electronic 1/f noise in most high-tech devices, and in spite of the conceptual success of our earlier classical turbulence approach to 1/f noise, the question about the ultimate origin of nature's omnipresent 1/f spectra remained unanswered. During the last three decades, we have claimed repeatedly that nonlinearity is a general cause of 1/f noise. Our new result proves that nonlinearity always leads to a 1/f spectrum if homogeneity is also present in the equation(s) of motion. Specifically, let the system be described in terms of the dimensionless vector function $\mathbf{Y}(\mathbf{x},t)$ by the m^{th} order nonlinear system of differential equation

$$\Phi[t, \mathbf{x}, \mathbf{Y}, \partial\mathbf{Y}/\partial t, \partial\mathbf{Y}/\partial x_1 \ldots \partial\mathbf{Y}/\partial x_n,$$

$$\partial^2\mathbf{Y}/\partial t^2, \partial^2\mathbf{Y}/\partial x_1{}^2 \ldots\ldots \partial^m\mathbf{Y}/\partial x_n{}^m] = 0 \qquad (5)$$

where the vector function Φ may be nonlinear in any of its arguments. If a number θ exists such that Eq. (1) implies

$$\Phi[\lambda^\theta t, \lambda\mathbf{x}, \mathbf{Y}, \partial\mathbf{Y}/\lambda^\theta\partial t, \partial\mathbf{Y}/\lambda\partial x_1 \ldots \partial\mathbf{Y}/\lambda\partial x_n, \partial^2\mathbf{Y}/\lambda 2^\theta\partial t^2, \partial^2\mathbf{Y}/\lambda^2\partial x_1{}^2 \ldots\ldots \partial^m\mathbf{Y}/\lambda^m\partial x_n{}^m) = 0 \qquad (6)$$

for any real number λ, the power spectral density of any chaotic solution for the vector function $\mathbf{Y}$ defined by Eq. (5) is proportional to 1/f. We shall present here a simplified proof, assuming Eq. (5) to contain only the first time derivative.

Consider a n-dimensional nonlinear system described in terms of the dimensionless vector function $\mathbf{Y}(\mathbf{x},t)$ by the m^{th} order nonlinear dynamical equation

$$\partial\mathbf{Y}/\partial t + \mathbf{F}(\mathbf{x}, \mathbf{Y}, \partial\mathbf{Y}/\partial x_1 \ldots \partial\mathbf{Y}/\partial x_n, \partial^2\mathbf{Y}/\partial x_1{}^2 \ldots \partial^m\mathbf{Y}/\partial x_n{}^m) = 0 \quad (7)$$

Here $\mathbf{F}$ is a nonlinear vector function of its arguments which include the vector $\mathbf{x}(x_1, \ldots x_n)$. If

$$\mathbf{F}[\lambda\mathbf{x}, \mathbf{Y}, \partial\mathbf{Y}/(\lambda\partial x_1) \ldots \partial\mathbf{Y}/(\lambda\partial x_n), \partial^2\mathbf{Y}/(\lambda\partial x_1)^2 \ldots\ldots \partial^m\mathbf{Y}/(\lambda\partial x_n)^m] = \lambda^{-p}\mathbf{F}(\mathbf{x}, \mathbf{Y}, \partial\mathbf{Y}/\partial x_1 \ldots \partial\mathbf{Y}/\partial x_n, \partial^2\mathbf{Y}/\partial x_1{}^2 \ldots\ldots \partial^m\mathbf{Y}/\partial x_n{}^m) \quad (8)$$

for any real number λ, Eq. (7) is said to be homogeneous of order -p. Performing a Fourier transformation with respect to the vector $\mathbf{x}$, we get in terms of the Fourier-transformed wavevector $\mathbf{k}$ the nonlinear integro-differential equation

$$\partial\mathbf{y}(\mathbf{k},t)/\partial t + \mathbf{G}[\mathbf{k}, \mathbf{y}(\mathbf{k},t), k_1\mathbf{y}(\mathbf{k},t) \ldots k_n\mathbf{y}(\mathbf{k},t), k_1{}^2\mathbf{y}(\mathbf{k},t) \ldots k_n{}^m\mathbf{y}(\mathbf{k},t)] = 0, \quad (9)$$

where $\mathbf{y}(\mathbf{k},t)$ is the Fourier transform of $\mathbf{Y}(\mathbf{x},t)$. Due to Eq. (8), the nonlinear integro-differential operator $\mathbf{G}$ satisfies the relation

$$\mathbf{G}[\lambda\mathbf{k}, \mathbf{y}, \lambda k_1\mathbf{y} \ldots \lambda k_n\mathbf{y}, (\lambda k_1)^2\mathbf{y} \ldots\ldots (\lambda k_n)^m\mathbf{y}] = \lambda^p\mathbf{G}[\mathbf{k}, \mathbf{y}, k_1\mathbf{y} \ldots k_n\mathbf{y}, k_1{}^2\mathbf{y} \ldots\ldots k_n{}^m\mathbf{y}]. \quad (10)$$

Eq. (9) can thus be rewritten in the form

$$dy/d(t/\lambda^p) + G[\lambda k, y, \lambda k_1 y ... \lambda k_n y, (\lambda k_1)^2 y ..... (\lambda k_n)^m y] = 0, \qquad (11)$$

Taking $\lambda=1/k$, where $k=|\mathbf{k}|=(k_1^2+....+k_n^2)^{1/2}$, and setting $k^p t=z$, we notice that k has been eliminated from the dynamical equation, and only $\mathbf{k}/k$ is left. This means that there is no privileged scale left for the system in $\mathbf{x}$ or $\mathbf{k}$ space, other than the scale defined by the given time t, and expressed by the dependence on z. We call this property of the dynamical system *"sliding-scale invariance"*.

In certain conditions, instabilities of a solution of Eq. (7) or (5) may generate chaos, or turbulence. In a sufficiently large system described by the local dynamical equation (7) or (5), in which the boundary conditions become immaterial, homogeneous, isotropic turbulence, (chaos) can be obtained, with a spectral density determined only by Eq. (7) or (5). The stationary autocorrelation function $A(\tau)$ is defined as an average scalar product, the average being over the turbulent ensemble

$$A(\tau) = \langle \mathbf{Y}(\mathbf{x},t)\mathbf{Y}(\mathbf{x},t+\tau)\rangle = \int \langle y(\mathbf{k},t)y(\mathbf{k},t+\tau)\rangle d^n\mathbf{k} = \int u(k,z)d^n\mathbf{k}. \quad (12)$$

Here we have introduced the scalar

$$u(\mathbf{k},z) = \langle y(\mathbf{k},t)y(\mathbf{k},t+\tau)\rangle \qquad (13)$$

of homogeneous, isotropic chaos (turbulence), which depends only on $|\mathbf{k}|$ and $z=k^p\tau$. All integrals are from minus infinity to plus infinity. The chain of integro-differential equations for the correlation functions of any order obeys the same sliding-scale invariance which we have noticed in the fundamental dynamical equation above. *Therefore, in isotropic, homogeneous, conditions, u can only depend on k and z.* Furthermore, the direct dependence on k must reflect this sliding-scale invariance, and is therefore of the form

$$u(\mathbf{k},z) = k^{-n}v(z). \qquad (14)$$

Indeed, only this form insures that $u(k,z)d^n\mathbf{k}$ and therefore also the corresponding integrals and multiple convolutions in k space have the necessary sliding-scale invariance.

According to the Wiener-Khintchine theorem, the spectral density is the Fourier-transform of A(t),

$$S_y(f) = \int e^{2\pi i f\tau} A(\tau)d\tau = (1/f) \int e^{2\pi i t'} \int k'^{-n} v(z) d^n k' dt' = C/f, \quad (15)$$

where we have set $f\tau=t'$, $k^n=fk'^n$, $z=k^n\tau=k'^n t'$, and the integral

$$C = \int e^{2\pi i t'} \int k'^{-n} v(z) d^n k' dt' = \int e^{2\pi i t'} \int k''^{-n} v(k''^n) d^n k'' dt' \quad (16)$$

is independent of f. We have defined the vector $\mathbf{k}''=t'^{1/n}\,\mathbf{k}$.

Eq. (15) proves the criterion as stated in Eq. (8) The extension to the form (5-6) is trivial. In conclusion, nonlinearity + homogeneity = 1/f noise if the laminar (nonchaotic) solution is unstable. The ultimate cause of the ubiquitous 1/f noise in nature is the omnipresence of nonlinearities (no matter how we and homogeneity. The latter is finally related to rotational invariance and to the isotropy of space. All our four specific theories of 1/f chaos in nonlinear systems are just special cases to which our criterion is applicable. They include our magneto-plasma theory of turbulence in intrinsic symmetric semiconductors (1966), our similar theory for metals (1971), the quantum 1/f theory (pure quantum electrodynamics, 1975), and the theory of Musha's traffic turbulence (1989). A fifth application concerns a one-dimensional crystal, i.e., a chain of atoms with slightly anharmonic interaction potentials, which is presented next.

4. Application of the sufficient criterion to a chain of atoms with a harmonic coupling

Consider a chain of atoms in the x direction, with a lattice constant b and displacements q_i from the equilibrium position. The equations of motion

$$m d^2q_n/dt^2 = A[(q_{n+1}-q_n)-(q_n-q_{n-1})] + B[(q_{n+1}-q_n)^2-(q_n-q_{n-1})^2] + C[(q_{n+1}-q_n)^3-(q_n-q_{n-1})^3] \quad (17)$$

contain anharmonic terms as long as B and C are different from zero. With $\alpha_n=q_{n+1}-q_n$ and $\beta_n=q_n-q_{n-1}$, neglecting the second-order term, we obtain

$$md^2q_n/dt^2 = [(q_{n+1}-q_n)-(q_n-q_{n-1})][A + B(q_{n+1}+q_{n-1}) + C(\alpha_n^2+\alpha_n\beta_n+\beta_n^2)]. \quad (18)$$

Going over from finite differences to a continuum description, we obtain a differential equation for $q(x,t)$

$$m\partial^2q/\partial t^2 = b^2\partial^2q/\partial x^2[A + 2Bq + 3Cb^2(\partial q/\partial x)^2]. \quad (19)$$

Performing a fourier transform with respect to x,

$$m\partial^2q_k/\partial t^2 = -Ab^2k^2q_k - 2b^2B\int k'^2q_{k'}q_{k-k'}dk' + 3Cb^4\int dk'\int dk''k'k''(k-k'-k'')^2q_{k'}q_{k''}q_{k-k'-k''}. \quad (20)$$

All integrals are from minus infinity to infinity. Substituting $q_k=u(k,t)\exp[ikbt(A/m)^{1/2}]$,

$$m\partial^2u/\partial t^2 + 2ikb(A/m)^{1/2}\partial u/\partial t = -2b^2B\int k'^2u_{k'}u_{k-k'}dk' + 3Cb^4\int dk'\int dk''k'k''(k-k'-k'')^2u_{k'}u_{k''}u_{k-k'-k''}. \quad (21)$$

Our 1/f noise criterion requires both nonlinearity and homogeneity, as well as the presence of chaos or of a quasichaotic state. The nonlinearity condition is satisfied unless B=0 and C=0, while homogeneity requires the existence of two numbers p and θ such that replacing k by λk everywhere except in the integration differentials, and replacing t by $\lambda^\theta t$ leaves the equation multiplied by a general factor λ^p, i.e., formally invariant. In our case we note that this criterion is satisfied with p=2 and θ=-1 if we neglect the third-order term by setting C=0. On the other hand, both in the general case and in the B=0 case the criterion is not satisfied, except for some low-frequency limiting case in which all k values and frequencies are so small, that we can neglect the term with B and one of the left hand side terms.

To see how the criterion works for C=0, we set $\lambda=1/|k|$ and call $|k|t=z$

$$m\partial^2u/\partial z^2 + 2ib(A/m)^{1/2}\partial u/\partial z = -2b^2B\int(k'/k)^2u_{k'}u_{k-k'}dk' \quad (22)$$

Substituting $u(k,t)=k^{-1}v(k,t)$ we get for v

$$m\partial^2 v/\partial z^2 + 2ib(A/m)^{1/2}\partial v/\partial z = -2b^2B\int(k'/k)v(k',z)v(k-k',z)dk'/(k-k')$$
$$= -2b^2B\int k"v(kk",z)v(k-kk",z)dk"/(1-k") \qquad (23)$$

We note that k has disappeared from the equation and is present only as a scale factor in the arguments of v on the rhs. Therefore we can expect the existence of solutions v(k,z) of this equation which do not depend on the first argument. Such solutions exhibit "sliding scale invariance", because t and k or t and x provide a scale for each other, with no other scale present.

In certain conditions, instabilities of a solution of Eq. (20) may generate chaos, or turbulence. In a sufficiently large system described by the local dynamical equation (6), in which the boundary conditions become immaterial, homogeneous, isotropic turbulence, (chaos) can be obtained, with a spectral density determined only by Eq. (20). In the absence of instability and chaos, a certain type of random stirring forces can generate a quasichaotic stochastic state which can also be described with our methods familiar from turbulence theory. The stationary autocorrelation function $A(\tau)$ is defined as an average scalar product, the average being over the turbulent ensemble

$$A(\tau) = \langle u(x,t)u(x,t+\tau)\rangle = \int\langle u_k(t)u_k(t+\tau)\rangle dk = \int U(k,z)dk. \qquad (24)$$

Here we have introduced the scalar

$$U(k,z) = \langle u_k(t)u_k(t+\tau)\rangle \qquad (25)$$

of homogeneous, isotropic chaos (turbulence), which depends only on $|k|$ and $z=|k|^P\tau$, because there is nothing else in Eqs. (20) and (21). All integrals are from minus infinity to plus infinity. The chain of integro-differential equations for the correlation functions of any order obeys the same sliding-scale invariance which we have noticed in the fundamental dynamical equation (21) above. *Therefore, in isotropic, homogeneous, conditions, $u_k(t)$ can only depend on k and z.* Furthermore, the direct dependence on k must reflect this sliding-scale invariance, and is therefore of the form

$$u_k(z) = |k|^{-1}v(z). \qquad (26)$$

Indeed, only this form insures that $u_k(z)dk$ and therefore also the corresponding integrals and multiple convolutions in k space have the necessary sliding-scale invariance.

According to the Wiener-Khintchine theorem, the spectral density is the Fourier-transform of A(t),

$$S_u(f) = \int e^{2\pi i f\tau} A(\tau)d\tau = (1/f) \int dk' \int dt' e^{2\pi i t' k'^{-1}} v(z) = C/f, \qquad (27)$$

where we have set $f\tau=t'$, $k=fk'$, $z=k\tau=k't'$, and the integral

$$C = \int dk' \int dt' e^{2\pi i t' k'^{-1}} v(z) = \int dk'' \int dt' e^{2\pi i t' k''^{-1}} v(k'') \qquad (28)$$

is independent of f. We have defined the vector $k''=t' k$.

The 1/f spectrum obtained by us for the amplitude u(t) carries over also for the squared amplitude $u^2(t)$. Indeed, the autocorrelation $A'(\tau)=\langle u^2(x,t)u^2(x,t+\tau)\rangle$ is given by $2A^2(\tau)+A^2(0)$ if we assume the amplitude u(t) to be well approximated by a Gaussian process. The Fourier transform of $A^2(\tau)$ is the autoconvolution of C/f, which is C^2/f, if we interpret all 1/f spectra as the limit of $f^{\varepsilon-1}$ spectra for arbitrarily small ε. Therefore, $S_{u2}(f) = 2C^2/f + A^2(0)\delta(f)$, where $\delta(f)$ is the delta function. The energy density and the phonon number density are both proportional to u^2. This proves that in this case the energy density and the phonon number density are both fluctuating with a 1/f spectral density if they fluctuate at all, i.e., if the system is either chaotic, or in a quasichaotic state caused by a suitable system of random stirring forces. This confirms for the one-dimensional case the prediction of T. Musha. In three-dimensional piezoelectric crystals similar 1/f fluctuations of the phonon number are predicted by the quantum 1/f theory as we show next, and have been observed experimentally in the Brillouin scattering of light by T. Musha[13].

5. Quantum 1/f effect in quartz resonators

According to the general quantum 1/f formula, $\Gamma^{-2}S_\Gamma(f)=2\alpha A/f$ with $\alpha=e^2/hc=1/137$ and $A=2(\Delta j/ec)^2/3\pi$ is the quantum 1/f effect in any physical process rate Γ. Setting $j=dP/dt=\dot{P}$, where P is the vector of the dipole moment of the quartz crystal, we obtain for the rate Γ of phonon removal from the main resonator oscillation mode by scattering on a phonon from any other mode of the crystal the spectral density

$$S_\Gamma(f) = \Gamma^2 4\alpha(\Delta P)^2/3\pi e^2 c^2, \qquad (29)$$

where $(\Delta P)^2$ is the square of the polarization rate change associated with the removal of one of the N phonons present in the main resonator mode. To calculate it, we write the energy W of the resonator and its change in the form

$$W = (N+1/2)\hbar\omega = P^2/2V\chi\omega^2; \quad \Delta W = \hbar\omega = P\Delta P/V\chi\omega^2. \qquad (30)$$

Her χ is the susceptibility and V the volume of the quartz crystal. Solving the last equation for ΔP, squaring, and multiplying with the first, we get

$$(\Delta P)^2 = \hbar\omega^3 V\chi/(2N+1), \qquad (31)$$

and

$$S_\Gamma(f) = \Gamma^2 4\alpha\hbar\omega V\chi/3\pi e^2 c^2(2N+1)f = \Gamma^2(2\omega^3\chi/3\pi c^3 f)(\hbar\omega V/W) \qquad (32)$$

The corresponding frequency fluctuations are given by

$$\omega^{-2}S_\omega(f) = (2\omega^3\chi/3\pi c^3 f)(\hbar\omega V/W). \qquad (33)$$

6. Quantum 1/f mobility fluctuations in semiconductors

A first principles calculation of quantum 1/f cross correlations performed[9] for the first time in 1987 has yielded a slightly different result compared to earlier expectations. This same new form of the quantum 1/f cross correlations was derived again with a different method by Van Vliet in 1989. It differs from the old form used in the 1985 calculation of Kousik et. al. by a correction which is zero when the momentum changes of the two current carriers involved in the cross correlation are identical, but increases to finite values when the momentum differences caused by the scattering process are different. The correction is proportional to the squared difference of the two momentum changes. We have repeated all calculations in the original paper by Kousik et.al[10]., obtaining both for impurity scattering and for the various types of phonon scattering new analytical expressions which show a

considerable increase of the final quantum 1/f noise. The results obtained are applicable both to direct and indirect bandgap semiconductors.

6.1 Introduction

We have performed an analytical calculation of mobility fluctuations in silicon and gallium arsenide, using the new quantum 1/f cross-correlations formula. This calculation is of major importance for the 1/f noise-related optimization of the two types of materials, and of the many devices constructed with them for military and civilian applications in the electronic and opto-electronic industry.

The new cross-correlation formula gives the cross-spectral density which describes the way in which simultaneous quantum 1/f scattering rate fluctuations ΔW observed in the direction of the outgoing scattered wave-vector $\mathbf{K}'$ are correlated with those in the $\mathbf{K}''$ direction, when the two corresponding incoming current carriers have the wave vectors $\mathbf{K}_1$ and $\mathbf{K}_2$:

$$S_{\Delta W}(\mathbf{K}_1,\mathbf{K}';\mathbf{K}_2,\mathbf{K}'';f) = (2\alpha/3\pi f)(\hbar/m^*c)^2 W_{\mathbf{K}_1,\mathbf{K}'} W_{\mathbf{K}_2,\mathbf{K}''}[(\mathbf{K}'-\mathbf{K}_1)^2+(\mathbf{K}''-\mathbf{K}_2)^2]\delta_{\mathbf{K}_1,\mathbf{K}_2}. \qquad (34)$$

The form conjectured by us earlier had $2(\mathbf{K}'-\mathbf{K}_1)(\mathbf{K}''-\mathbf{K}_2)$ in place of the rectangular bracket.

6.2 Impurity Scattering

For impurity scattering of electrons in solids, fluctuations $\Delta\tau$ of the collision times τ will cause mobility fluctuations

$$\Delta\mu_{band}(t) = [e/m^*\langle\langle v^2\rangle\rangle]\Sigma_{\mathbf{K}} v_{\mathbf{K}}^2 \Delta\tau(t) n_{\mathbf{K}}. \qquad (35)$$

where $\langle\langle v^2\rangle\rangle$ is both the average over all states of wave-vectors $\mathbf{K}$, with occupation numbers $n_{\mathbf{K}}$, in the conduction band, and the thermal equilibrium average of the quadratic carrier velocities. With the help of the relation

$$1/\tau(\mathbf{K}) = (V/8\pi^3)\int(1 - \cos\theta'/\cos\theta) W_{\mathbf{K},\mathbf{K}'} d^3K', \qquad (36)$$

the mobility fluctuations are reduced to fluctuations of the elementary scattering rates $W_{\mathbf{K},\mathbf{K}'}$, governed by Eq. (34). Here V is the volume of the normalization box which disappears in the final result, θ and θ' respectively the angles $\mathbf{K}$ and $\mathbf{K}'$ form

with the direction of the applied field. One finally obtains after tedious multiple integrations

$$\mu^{-2}S_{\Delta\mu}(f) = [256\pi\alpha\kappa^2\varepsilon^4\hbar^{12}/3m^{*8}Z^4e^8N_i^2](1/f)\Sigma_K K^{10}[\ln(1+a^2)-a^2/(1+a^2)]^{-3}$$
$$[(2a^2+a^4)/(1+a^2)-2\ln(1+a^2)]F(E_K)[\Sigma_K v_K^2\tau(K)F(E_K)]^{-2}, \quad (37)$$

where $a=2K/\kappa$, $\kappa^2=e^2n(T)/\varepsilon k_BT$, $n(T)$ is the electron concentration, $F(E_K)=\exp(E_F-E_K)$ for non-degenerate semiconductors, N_i the concentration of impurities of charge Ze and ε the dielectric constant. The corresponding partial Hooge parameter for impurity scattering is thus

$$\alpha_i = [4\sqrt{2}\pi\alpha\kappa\hbar^5N_c/3m^{*7/2}(k_BT)^{3/2}c^2]\int_0^\infty dx\, x^{11/2}e^{-x}$$
$$[\ln(bx+1)-bx/(bx+1)]^{-3}[(2bx+b^2x^2)/(bx+1)^2-2\ln(bx+1)]$$
$$\{\int_0^\infty dx\, x^3e^{-x}[\ln(bx+1)-bx/(bx+1)]^{-1}\}^{-2}. \quad (38)$$

6.3 Acoustic Electron-Phonon Scattering

In this case the calculation is similar, and leads to the result

$$\alpha_{ac} = [32\pi\alpha N_c m^* C^7\hbar^3/3c^2k_BT)^4]\{(1/R^2)\int_1^\infty dx\, x^{-4}$$
$$[(x-1)^7/7+(R+1)(x-1)^6/6+R(x-1)^5/5]$$
$$[(x-1)^5/5+(R+1)(x-1)^4/4+R(x-1)^3/3]\exp(-x^2/4R)$$
$$+\int_0^1 dx\, x^{-4}[(x+1)^5/5-(x+1)^6/6+(x-1)^5/5+(x-1)^6/6]$$
$$[(x+1)^3/3+(x-1)^4/4+(x-1)^3/3-(x+1)^4/4]\exp(-x^2/4R)$$
$$+\int_1^\infty dx\, x^{-4}[(x+1)^5/5-(x+1)^6/6][(x+1)^3/3-(x+1)^4/4]\exp(-x^2/4R)\}, \quad (39)$$

where $R=k_BT/2m^*C_l^2$, C_l is the deformation potential, and N_c is the effective density of states for the conduction band.

6.4 Non-Polar Optical Phonon Scattering

This time one obtains

$$\alpha_{n.o.ph} = [8\pi\sqrt{2\,\hbar\omega_o}\alpha N_c\hbar^2/3m^{*5/2}c^2\omega_o]\{\int_0^\infty dx\, x^{5/2}$$

$$[(F+1)(x-1)^{1/2}\theta(x-1)+F(x+1)^{1/2}]^{-4}$$

$$[(F+1)^2(x-1)(2x-1)\theta(x-1)+F^2(x+1)(2x+1)]\exp(-\hbar\omega_o x/k_B T)\}$$

$$\{\int_0^\infty dx\, x^{3/2}[(F+1)(x-1)^{1/2}\theta(x-1)+F(x+1)^{1/2}]^{-1}\exp(-\hbar\omega_o x/k_B T)\}^{-2}, \qquad (40)$$

where $F=[\exp(\hbar\omega_o/k_B T)-1]^{-1}$, and ω_o is the optical phonon frequency.

6.5 Polar Optical Phonon Scattering

Proceeding as in Secs. 2 and 4, we obtain

$$\alpha_{p.o.ph} = [8\pi\sqrt{2\,\hbar\omega_l}\alpha N_c\hbar^2/3m^{*5/2}c^2\omega_l]\{\int_0^\infty dx\, x^4$$

$$[F^2(x+1)^{1/2}\ln(2x^{1/2}+2(x+1)^{1/2})$$

$$+(F+1)^2(x-1)^{1/2}\ln(2x^{1/2}+(x-1)^{1/2})\theta(x-1)]\exp(-\hbar\omega_l x/k_B T)$$

$$[(F+1)\operatorname{arcsinh}(x-1)^{1/2}\theta(x-1)+F\operatorname{arcsinh}(x^{1/2})]^{-4}\}. \qquad (41)$$

Here ω_l is the longitudinal phonon frequency.

6.6 Intervalley Scattering

This type of scattering, present in indirect bandgap semiconductors, transfers electrons from one of the six minima (or valleys) of the conduction band energy in k-space to one of the other five minima. Transitions between a valley and the nearest valley, which is along the same k-space direction in the next copy of the first Brilloin zone in the periodic zone scheme, are of the Umklapp type, and are called g-processes. Transitions to the four valleys present in the same zone along the other two k-space directions are called f-processes. Repeating a previous calculation[10] on the basis of the new cross-correlation formula[9, 11] (34), we obtain for g-processes

$$\alpha_g = [8\pi\sqrt{2\,\hbar\omega_{ij}}\alpha N_c\hbar^2/3m^{*5/2}c^2\omega_{ij}]\{\int_0^\infty dx\, x^{5/2}$$

$$[(F+1)(x-1)^{1/2}\theta(x-1)+F(x+1)^{1/2}]^{-4}$$

$$[(F+1)^2(x-1)(2x-1)\theta(x-1)+F^2(x+1)(2x+1)]\exp(-\hbar\omega_{ij} x/k_B T)\}$$

$$\{\int_0^\infty dx\, x^{3/2}[(F+1)(x-1)^{1/2}\theta(x-1)+F(x+1)^{1/2}]^{-1}\exp(-\hbar\omega_{ij}x/k_BT)\}^{-2}, \qquad (42)$$

where $\hbar\omega_{ij}$ is the phonon energy corresponding to the momentum difference required by the intervalley transition. For the corresponding f-process we obtain[12]

$$\alpha_f = (k_o/q_o)^2\alpha_g, \qquad (43)$$

where k_o/q_o is the ratio between the position vector of a conduction band energy minimum in k space, and twice the distance of the minimum from the Brillouin zone boundary, 0.85/0.3 for silicon. There are three g-type (from LA, TA and LO phonons) and three f-type contributions (from TA, LA and TO phonons).

The various quantum 1/f contributions derived here can be approximately superposed to yield the resultant quantum 1/f coefficient according to the rule

$$\alpha_H = \Sigma_i(\mu/\mu_i)^2\,\alpha_i \qquad (44)$$

The support of the Army Research Office is thankfully acknnowledged.

References

1. A. van der Ziel, Solid St. Electron. **25**, 141 (1982).
2. A. van der Ziel, *Noise in Solid State Devices and Circuits*. New York, NY: Wiley, 1986.
3. A. van der Ziel, Proc. IEEE **76**, 233 (1988).
4. T. G. M. Kleinpenning, Physica **98B**, 289 (1980).
5. P. H. Handel, Phys. Rev. Lett. **34**, 1492 (1975).
6. P. H. Handel, Phys. Rev. **A22**, 745 (1980).
7. P. H. Handel, Archiv für Elektronik u. Übertr. **43**, 261 (1989).
8. R. M. Warner, Jr., and B. L. Grung: *Transistors/Fundamentals for the Integrated-Circuit Engineer*, New York, NY: Wiley, 1983, Eq. (7-6).
9. P. H. Handel: " Quantum 1/f Cross-Correlations and Spectra", pp. 167-170., Proc. of the X. Int. Conf. on Noise in Physical Systems, Budapest, Aug. 20-25, 1989, A. Ambrozy, Ed., Akademiai Kiado, Budapest 1990, pp. 155-158.
10. G. S. Kousik, C. M. van Vliet, G. Bosman and P. H. Handel: "Quantum 1/f Noise Associated with Ionized Impurity Scattering and Electron-phonon Scattering in Condensed Matter", Advances in Physics 34, 663-702 (1985).
11. P. H. Handel: "Starting Points of the Quantum 1/f Noise Approach", p. 1-26, Subm. to Phys. Rev. B, February 1988.
12. G. S. Kousik, C. M. Van Vliet, G. Bosman, and Horng-Jye Luo, Phys. stat. sol. **154**, 713-726 (1989).
13. T. Musha, B. Crabor, and S. Minorn, Phys. Rev. Lett. 64, 2394-2397, 1990.
14. Proceedings on 4th Symposium on Quantum 1/f Noise, Minneapolis, May 1990, University of Missouri Publ. Office.

APPENDIX D

EXAMPLES

The general criterion developed in the main text will now be illustrated on the basis of more examples.

D.1 Classical Turbulence Theory for the Current Carriers in Semiconductors

In the case of homogeneous, isotropic turbulence[1-3] caused in the electron-hole plasma of an infinite sample of a symmetric intrinsic semiconductor by dynamical instabilities of any kind, we start from the equations

$$\nu \mathbf{v}^{+} = (e/2c)\mathbf{v}^{-}\times\mathbf{B} - (1/n)\nabla P, \tag{D1}$$

$$\nu \mathbf{v}^{-} = 2e[\mathbf{E} + \mathbf{v}^{+}\times\mathbf{B}/c] - (2/n)\nabla(P_p - P_n), \tag{D2}$$

$$\nabla\cdot\mathbf{v}^{+} = 0 \quad (n = \text{const}), \tag{D3}$$

$$\nabla\times\mathbf{E} = -(1/c)\partial\mathbf{B}/\partial t, \tag{D4}$$

$$\nabla\times\mathbf{B} = 2\pi e n\mathbf{v}^{-}/c, \tag{D5}$$

$$\nabla\cdot\mathbf{B} = 0. \tag{D6}$$

Here n is the total carrier concentration including an equal number of electrons and holes, ν/e their reciprocal mobility assumed to be the same for electrons and holes, P_n and P_p the partial pressures of electrons and holes, P the total carrier pressure, $2\mathbf{v}^{+}$, $\mathbf{v}^{-}$ the sum and the difference of the carrier drift velocities. Inertial terms proportional to the effective masses of the carriers, as well as electrostatic terms and compressibility terms have been neglected here in a consistent way[4-7], because we are interested in the low-

frequency domain only. Although we do not work this out here, this system of equations can be shown to admit an energy theorem. Performing a Fourier expansion, we obtain

$$\nu v^{+}(\mathbf{k}) = (e/2c)\Sigma_{\mathbf{k}'} v^{-}(\mathbf{k}')\times \mathbf{B}(\mathbf{k}-\mathbf{k}') - (i/n)\mathbf{k}\cdot P(\mathbf{k}), \tag{D7}$$

$$\nu v^{-}(\mathbf{k}) = 2e[\mathbf{E}(\mathbf{k}) + \Sigma_{\mathbf{k}'} v^{+}(\mathbf{k}')\times \mathbf{B}(\mathbf{k}-\mathbf{k}')/c] - (2i/n)\mathbf{k}(P_p - P_n), \tag{D8}$$

$$\mathbf{k}\cdot v^{+}(\mathbf{k}) = 0. \tag{D9}$$

$$i\mathbf{k}\times \mathbf{E}(\mathbf{k}) = -(1/c)\partial \mathbf{B}(\mathbf{k})/\partial t, \tag{D10}$$

$$i\mathbf{k}\times \mathbf{B}(\mathbf{k}) = 2\pi e n v^{-}(\mathbf{k})/c, \tag{D11}$$

$$\mathbf{k}\cdot \mathbf{B}(\mathbf{k}) = 0, \tag{D12}$$

Substituting $\mathbf{E}$ from Eq. (D8) into Eq. (D10), we obtain with Eq. (D11)

$$\partial \mathbf{B}(\mathbf{k})/\partial t + \mu k^2 \mathbf{B}(\mathbf{k}) = i\mathbf{k}\times \Sigma_{\mathbf{k}'} v^{+}(\mathbf{k}')\times \mathbf{B}(\mathbf{k}-\mathbf{k}'), \tag{D13}$$

where $\mu = c^2\nu/4\pi n e^2$. Eqs. (D7) and (D11) yield

$$v^{+}(\mathbf{k}) = (i/4\pi\nu n)\,\Sigma_{\mathbf{k}''}\{\mathbf{B}(\mathbf{k}'')[\mathbf{k}''\cdot\mathbf{B}(\mathbf{k}-\mathbf{k}'')] - \mathbf{k}''[\mathbf{B}(\mathbf{k}'')\cdot\mathbf{B}(\mathbf{k}-\mathbf{k}'')] - (\mathbf{k}/k^2)(1-\delta_{\mathbf{k},0})[\mathbf{k}''\cdot\mathbf{B}(\mathbf{k}-\mathbf{k}'')\,\mathbf{k}\cdot\mathbf{B}(\mathbf{k}'') - \mathbf{B}(\mathbf{k}'')\cdot\mathbf{B}(\mathbf{k}-\mathbf{k}'')\,(\mathbf{k}\cdot\mathbf{k}'')]\}. \tag{D14}$$

Substituting this into Eq. (D13), we obtain the fundamental dynamical field-equation of turbulence in the electron-hole plasma of a symmetric intrinsic semiconductor

$$\partial b_\beta(\mathbf{k},t)/\partial t + \mu k^2 b_\beta(\mathbf{k},t) = \Sigma_{\mathbf{k}'\mathbf{k}''} b_j(\mathbf{k}-\mathbf{k}',t)\, b_l(\mathbf{k}'',t)\, b_m(\mathbf{k}'-\mathbf{k}'',t) \cdot (k_j\delta_{\beta s} - k_s\delta_{\beta j})[k_s\delta_{lm} - k_m''\delta_{ls} + (k_s'/k'^2)(1-\delta_{\mathbf{k}',0})(k_m''k_l' - \mathbf{k}'\cdot\mathbf{k}''\delta_{lm})], \tag{D15}$$

in terms of $\mathbf{b} \equiv \mathbf{B}/(2\pi\nu n)^{1/2}$. This dynamical equation has the form of Eq. (3), with p=2 in Eq. (4), and with G defined as the r.h.s. minus the term in k^2 on the l.h.s.. Our sufficient criterion thus tells us that this nonlinear system will yield a 1/f spectrum. We present below the direct derivation for this example.

Multiplying Eq. (D15) with $b_\alpha^*(\mathbf{k},t-\tau)$ and taking the average over a statistical ensemble which represents our notion of stationary turbulence, we obtain in quasi-stationary conditions

$$\partial w_{\alpha\beta}(\mathbf{k},\tau)/\partial\tau + \mu k^2 w_{\alpha\beta}(\mathbf{k},\tau) = \Sigma_{\mathbf{k}'\mathbf{k}''} \langle b_\alpha^*(\mathbf{k},t-\tau) b_j(\mathbf{k}-\mathbf{k}',t) b_l(\mathbf{k}'',t) b_m(\mathbf{k}'-\mathbf{k}'',t)\rangle R_{jml\beta}, \quad \text{(D16)}$$

with $w_{\alpha\beta}(\mathbf{k},\tau) \equiv (L/2\pi)^3 \langle b_\alpha^*(\mathbf{k},t-\tau) b_\beta(\mathbf{k},t)\rangle$, where L is the edge of the cubic normalization box, and

$$R_{jml\beta} \equiv (k_j\delta_{\beta s} - k_s\delta_{\beta j})[k_s\delta_{lm} - k_m''\delta_{ls} + (k_s'/k'^2)(1-\delta_{\mathbf{k}',0})(k_m''k_l' - \mathbf{k}'\cdot\mathbf{k}''\delta_{lm})]. \quad \text{(D17)}$$

Multiplying Eq. (D15) with more magnetic field components and averaging, we obtain equations connecting the fourth-order correlation tensor to the sixth-order tensor, and so on[4-7]. To end this infinite chain of equations for the correlation functions, we make a quasinormality assumption which expresses the fourth-order moment appearing in Eq. (D16) according to the scheme

$$\langle ABCD\rangle = \langle AB\rangle\langle CD\rangle + \langle AC\rangle\langle BD\rangle + \langle AD\rangle\langle BC\rangle, \quad \text{(D18)}$$

valid if the four field components would approximate a joint normal distribution. This approximation does not alter the homogeneity of the system, which ultimately causes the 1/f spectrum. This approximation yields the closed equation

$$\partial w_{\alpha\beta}(\mathbf{k},\tau)/\partial\tau + \mu k^2 w_{\alpha\beta}(\mathbf{k},\tau) = (2\pi/L)^3 w_{\alpha j}(\mathbf{k},\tau)\Sigma_{\mathbf{k}'} w_{lm}(\mathbf{k}',0) R_{jml\beta}(\mathbf{k},\mathbf{k}'). \quad \text{(D19)}$$

Isotropic turbulence requires $w_{\alpha\beta} = A_1(k)\delta_{\alpha\beta} + A_2(k)k_\alpha k_\beta$, with coefficients A_1 and A_2 related through Eq. (D12), yielding

$$w_{\alpha\beta}(\mathbf{k},\tau) = (1/2)[\delta_{\alpha\beta} - k_\alpha k_\beta/k^2]u(k,\tau), \qquad (D20)$$

where $u(k,\tau) = \Sigma_\alpha w_{\alpha\alpha}(\mathbf{k},\tau)$. Therefore, the scalar correlation function $u(k,\tau)$ satisfies the dynamical equation of homogeneous, isotropic, stationary turbulence

$$\frac{\partial v(k,x)}{\partial |x|} + v(k,x) = -\frac{1}{2}v(k,x)\int\frac{d^3k'}{k'^3}\frac{k^2+\mathbf{k}\cdot\mathbf{k}'}{(\mathbf{k}+\mathbf{k}')^2}[1-(\frac{\mathbf{k}\cdot\mathbf{k}'}{kk'})^2]v(k',0), \qquad (D21)$$

where $v(k,x)\equiv k^{-3}u(k,\tau)$, and $x = \mu\tau k^2$ is a dimensionless variable replacing τ. We convince ourselves that the integral is independent of k, provided $v(k,x)$ does not depend on its first argument, by setting $\mathbf{k}'/k\equiv\kappa$. This yields a solution. However, with $v=e^{-m|x|}$ we get a logarithmic divergence at $\kappa=0$. We look for an exact solution of the form[4-7]

$$v(k,x) = hk^\varepsilon e^{-|x|m(k)}, \quad \text{or} \quad u(k,x) = (h/k^{3-\varepsilon})\, e^{-|x|m(k)}, \qquad (D22)$$

where $m(k)$ is very close to a constant, almost independent of k, and h is a constant proportional to the intensity of the turbulence, or the turbulence level. Substituting this into Eq. (D21) and performing the integration, we obtain a finite result only for $0<\varepsilon<2$:

$$m(k) = 1 + h\, r(\varepsilon)k^\varepsilon, \text{ with } r(\varepsilon)=[2\pi^2\cot an(\varepsilon\pi/2)]/[(1-\varepsilon^2)(3-\varepsilon^2)]. \qquad (D23)$$

We notice that $m(k)$ is indeed practically constant when $0<\varepsilon<<1$ is very small, arbitrarily small. The value $\varepsilon=0$ leads to a logarithmic divergence, but we can set $\varepsilon=0$ for practical purposes.

The spectral density corresponding to Eq. (D22) with $\varepsilon=0$ is

$$w_{\alpha\beta}(\omega) = (1/\pi)\int_0^\infty \cos\omega\tau d\tau \int w_{\alpha\beta}(k,\tau)d^3k$$

$$= \tfrac{4}{3}\delta_{\alpha\beta}\int_0^\infty k^2 dk \int_0^\infty d\tau\, u(k,\tau)\cos\omega\tau = \tfrac{4}{3}h\delta_{\alpha\beta}\int_0^\infty \frac{mk\,dk}{\omega^2+m^2k^2} = \tfrac{\pi}{3}\frac{h}{\omega}\delta_{\alpha\beta}. \qquad \text{(D24)}$$

This is a 1/f spectrum. At the low frequency end we do not get a divergent spectral integral, because the more exact form of the spectrum with a finite small $\varepsilon<<1$ is[4-7]

$$\int_0^\infty \frac{mk^{1+\varepsilon}dk}{\omega^2+m^2k^4} = \frac{1}{\omega^{1-\varepsilon/2}m^{\varepsilon/2}}\int_0^\infty \frac{x^{1+\varepsilon}dx}{1+x^4}, \qquad \text{(D25)}$$

which is proportional to $f^{\varepsilon/2-1}$. It is interesting to note that for $\varepsilon<<1$ cotan $\varepsilon\pi/2 \approx 2/\varepsilon\pi$ in Eq. (23), and that the value of ε calculated from Eq. (23) is therefore proportional to h, or to the intensity of the turbulence. This feature of the classical theory[8-11] is expressed with fascinating clarity in the quantum form of the theory, where ε is replaced by $2\alpha A$ which also appears as an intensity factor multiplying the quantum 1/f noise.

The essential element which led to the 1/f spectrum in the classical turbulence theory is the *nonlinearity* of the equations of motion, caused by the reaction of the electric currents back on themselves via the generated electromagnetic field. The same feedback reaction, via the electromagnetic field, also caused the nonlinearity in the quantum 1/f theory, and in QED in general, leading in the same way to an identical 1/f spectrum, this time with a physically more meaningful $\varepsilon=2\alpha A$. This *nonlinearity* induces the coupling between various scales of turbulence and leads to the dynamical equilibrium between eddies of all sizes, expressed by the 1/f spectrum. In the $\varepsilon=0$, or $\alpha A=0$, limit, this dynamical equilibrium assumes both for the quantum case and for homogeneous, isotropic, turbulence in the unbounded semiconductor sample the simplest form, characterized by

scale-homogeneity, or scale invariance. Indeed, replacing for $\varepsilon=0$ in Eqs. (D21) and (D22) k and k' by λk and $\lambda k'$, while also replacing τ by τ/λ^2, (or ω by $\lambda^2\omega$), Eq. (D21) is not affected, and λ drops out. We conclude that *in the weak turbulence limit ($\varepsilon=0$) we obtain perfect self-similarity of the turbulence process at all scales in space and time, classically and quantum-mechanically*. The implied scale invariance is caused by the absence of any characteristic length or time scale, or by the presence of a sliding scale. Indeed, the frequency scale μk^2 is a function of the size of the eddies, given by the wave number k which can have any value. The actual frequency and wave-number spectra are closely related fractals, but in the weak-turbulence limit they approach an exact 1/f and $1/k^3$ spectrum respectively. In fact, we are here understanding the nonlinear dynamics which shapes this fractal for the first time.

D.2 Turbulence Theory for Drude Electrons in Metals

Our classical turbulence theory can be extended to the case of metals or degenerate extrinsic semiconductors[7] in the Drude model. The system of integro-differential equations is quite different,

$$\nu \mathbf{v}^+ = -e\mathbf{E} - (e/c)\mathbf{v}\times\mathbf{B} - (1/n)\nabla P \qquad \text{(D26)}$$

$$\nabla\times\mathbf{E} = -(1/c)\partial\mathbf{B}/\partial t \qquad \text{(D27)}$$

$$\nabla\times\mathbf{B} = -(4\pi en/c)\mathbf{v} \qquad \text{(D28)}$$

$$\nabla\cdot\mathbf{B} = 0, \qquad \text{(D29)}$$

and leads to a third-order nonlinearity[7] in the resulting closed equation of motion, or nonlinear field-equation, which replaces Eq. (D14):

$$\partial\mathbf{B}(\mathbf{k},t)/\partial t + \nu k^2\mathbf{B}(\mathbf{k},t) = -(c/4\pi ne)\mathbf{k}\times\int d^3k'\mathbf{B}(\mathbf{k}-\mathbf{k}',t)\times[\mathbf{k}'\times\mathbf{B}(\mathbf{k}',t)]. \qquad \text{(D30)}$$

This is again in the form of Eq. (3), with p=2 in Eq. (4). We thus expect a 1/f spectrum in this system as well. This time we only sketch the derivation. The corresponding infinite chain of equations for the correlation tensors now goes in steps of one. As was shown above, it went in steps of two for semiconductors. The third-order correlation can be eliminated between the first and second equations in the chain. The resulting dynamical equation[7] for homogeneous, isotropic, stationary turbulence, which replaces Eq. (D21), with the same notations, using $\mathbf{e}_3$ as the unit vector of the third axis, is

$$-\frac{\partial^2 v(k,x)}{\partial x^2} + v(k,x) = -\frac{1}{2}\int \frac{d^3\kappa}{\kappa^3} \frac{1+\kappa\cdot e_3}{|e_3+\kappa|^3}\left[1-\frac{(\kappa\cdot e_3)^2}{\kappa^2}\right] v(\kappa k,\kappa^2 x)\, v(k|e_3+\kappa|,x|e_3+\kappa|^2). \quad \text{(D31)}$$

This also admits, in the $\varepsilon=0$ limit of weak turbulence, a solution $v(k,x)$ which does not depend on the first argument, and $u(k,x) = k^{-3}e^{-xm(x)}$, this time with an x-dependent m. With the change of variables $t=\omega\tau$ and $k'=k/\sqrt{\omega}$ in the second (middle, involving u) form of Eq. (D24), x remains invariant, and a factor $1/\omega$ will appear in front of the integrals which themselves will just yield a constant factor independent of ω, τ or k. We thus obtain again a universal 1/f spectrum. As is shown in detail elsewhere[7], this 1/f spectrum is expressed in the corresponding current and voltage fluctuations which can be observed in the semiconductor or metallic medium. We conclude that the 1/f spectrum is a general property of electrically conducting systems in interaction with the electromagnetic field, a property which is caused by the nonlinearity of the system of carriers and field in mutual interaction due to the absence of a characteristic scale in the nonlinear equation of motion, and which finds its clearest expression in the Quantum 1/f Effect.

APPENDIX REFERENCES

1. W. Heisenberg, Z. Physik **124**, 628 (1948); Proc. Roy. Soc. London **A 195**, 1042 (1948).
2. M.S. Uberoi, J. Aeronaut. Sci. **20**, 197 (1953).
3. G.K. Batchelor, *The Theory of Homogeneous Turbulence*, Cambridge Univ. Press, New York, 1953.
4. P.H. Handel: "Instabilitäten, Turbulenz und Funkelrauschen in Halbleitern III; Turbulenz in Halbleiterplasma und Funkelrauschen", Z. Naturforschg. **21a**, 579-93 (1966).
5. P.H. Handel: "Instabilities and Turbulence in Semiconductors", Phys. Stat. Sol. **29**, 299-306 (1968).
6. P.H. Handel: " Turbulence Theory for Solid State Plasmas", Proc. XVIII. P.I.B.-M.R.I. *Int. Symp. on Turbulence of Fluids and Plasmas*, New York (1968), Brooklyn Polytechnic Press, New York, p. 381-95 (1969).
7. P.H. Handel: "Turbulence Theory for the Current Carriers in Solids and a Theory of 1/f Noise", Phys. Rev. **A3**, 2066-73 (1971).
8. A. van der Ziel, Proc. IEEE **76**, 233 (1988).
9. A. van der Ziel, *Noise in Solid State Devices and Circuits*. New York, NY: Wiley, 1986.
10. X.L. Wu, J.B. Anderson and A. van der Ziel: "Diffusion and Recombination 1/f Noise in Long n+ -p $Hg_{1-x}Cd_xTe$ Diodes", IEEE Transactions on Electron Devices ED-**34**, 1971-77 (1987).
11. A. van der Ziel, P. Fang, L. He, X.L. Wu, A.D. van Rheenen and P.H. Handel: "1/f Noise Characterization of n^+-p and n-i-p $Hg_{1-x}Cd_xTe$ Detectors", J. Vac. Sci. Technol. **A7**, 550-554 (1989).

APPENDIX E

PAPERS PUBLISHED DURING THE GRANT PERIOD

(i) Journal Papers

1. P.H. Handel: "The Quantum 1/f Effect and the General Nature of 1/f Noise", Archiv für Elektronik und Übertragungstechnik (AEÜ) 43, 261-270 (1989); invited paper.

2. A. van der Ziel, P. Fang, L. He, X.L. Wu, A.D. van Rheenen and P.H. Handel: "1/f Noise Characterization of n^+-p and n-i-p $Hg_{1-x}Cd_xTe$ Detectors" J. Vac. Sci. Technol. A 7, 550-554 (1989).

(ii) Conference Contributions

1. P. H. Handel: "General Derivation of the Quantum 1/f Noise Effect in Physical Cross Sections and the 1/N Factor", Proc. of the X. Int. Conf. on Noise in Physical Systems, Budapest, Aug. 20-25, 1989, A. Ambrozy, Ed., Akademiai Kiado, Budapest 1990, pp. 155-158.

2. P. H. Handel: " Quantum 1/f Cross-Correlations and Spectra", Ibid., pp. 167-170.

3. D. Wolf, P. H. Handel and M. Sekine: "Characteristic Functional of Physical Thermal Noise which includes Equilibrium 1/f Noise", Ibid., pp. 365-368.

4. P. H. Handel: "1/f Noise and Quantum 1/f Approach in Ferroelectrics and Ferromagnetics", Ibid., pp. 433-435.

5. B. Weber, D. Wolf and P. H. Handel: "Analytical and Numerical Study of Fluctuations in Active Nonlinear Systems", Ibid., pp. 351-355.

6. P. H. Handel: "The Nonlinearity causing Quantum 1/f Noise; Sliding Scale Invariance and Quantum Chaos Definition", Ibid.,pp. 179-186.

7. P. H. Handel: "Quantum 1/f Effect - The Most Important Radiative Correction, and Quantum Chaos", Proc. IV. Symposium on Quantum 1/f Noise and Other Low Frequency Fluctuations in Electronic Devices, Minneapolis, Minnesota, May 10-11, 1990, p 55-63; University of Missouri Publication Office, St. Louis, MO 63121, Dec. 1990.

8. T. H. Chung and P. H. Handel: "Mobility Fluctuations in Semiconductors Based on the New Quantum 1/f Cross Correlation Formula", Ibid, p. 81-86.

9. T. H. Chung and P. H. Handel: "Initial Monte Carlo Calculation For Quantum 1/f Noise in HgCdTe", Ibid, p. 105-106.

10. P. H. Handel: "General Quantum 1/f Principle", Ibid, p. 107-108.